

# Towards determining the presence of barren plateaus in some chemically inspired variational quantum algorithms

Mao Rui<sup>1,2</sup>, Tian Guojing<sup>1,2</sup>, Sun Xiaoming<sup>1,2\*</sup>

<sup>1</sup>State Key Laboratory of Processors, Institute of Computing Technology, Chinese Academy of Sciences, Beijing, 100190, China.

<sup>2</sup>School of Computer Science and Technology, University of Chinese Academy of Sciences, Beijing, 100049, China.

\*Corresponding author(s). E-mail(s): [sunxiaoming@ict.ac.cn](mailto:sunxiaoming@ict.ac.cn);  
Contributing authors: [maorui21b@ict.ac.cn](mailto:maorui21b@ict.ac.cn); [tianguojing@ict.ac.cn](mailto:tianguojing@ict.ac.cn);

## Abstract

In quantum chemistry, the variational quantum eigensolver (VQE) is a promising algorithm for molecular simulations on near-term quantum computers. However, VQEs using hardware-efficient circuits face scaling challenges due to the barren plateau problem. This raises the question of whether chemically inspired circuits from unitary coupled cluster (UCC) methods can avoid this issue. Here we provide theoretical evidence indicating they may not. By examining alternated dUCC ansätze and relaxed Trotterized UCC ansätze, we find that in the infinite depth limit, a separation occurs between particle-hole one- and two-body unitary operators. While one-body terms yield a polynomially concentrated energy landscape, adding two-body terms leads to exponential concentration. Numerical simulations support these findings, suggesting that popular 1-step Trotterized unitary coupled-cluster with singles and doubles (UCCSD) ansätze may not scale. Our results emphasize the link between trainability and circuit expressiveness, raising doubts about VQEs' ability to surpass classical methods.

## 1 Introduction

In recent years, there has been significant interest in developing quantum algorithms to harness the capabilities of noisy intermediate-scale quantum (NISQ) devices [1], hoping to solve classically intractable computational problems in the near term. Computational chemistry is anticipated to be one of the first domains that benefit from such progress [2]. A promising NISQ algorithm for molecular simulation in chemistry is the variational quantum eigensolver (VQE), aiming to find the ground energy of a given Hamiltonian. VQE is a hybrid quantum-classical algorithm — a quantum computer is used to prepare a parameterized trial state, an ansätze, and perform measurements to get the expectation value of the given Hamiltonian, the cost function. A classical computer is then used to iteratively train the parameters such that the cost function is minimized, according to the Rayleigh-Ritz variational principle.

While VQE has been successfully demonstrated for various small molecules [3–7], it faces several challenges. From a practical point of view, the number of measurements required can be too large to afford, and the circuit depth is limited due to hardware noise. More critically, the theoretical understanding of VQE is lacking, as it is a heuristic algorithm with no guarantee of producing a more accurate solution than classical methods. Moreover, it has been found that for variational quantum algorithms, the ability to produce a better solution often comes at the cost of the barren plateau (BP) problem [8], i.e., the gradients vanish exponentially concerning system size. This means even if the global minimum is better than classical methods, VQE may fail to find it [9, 10], despite the

efforts devoted to mitigating BP [11–19]. It is unclear whether there exists VQE that are both more accurate than classical methods, or at least cannot be classically simulated, and trainable.

The ansätze employed in VQEs can be broadly categorized into three types [20, 21]: chemically inspired ansätze [3], hardware-efficient ansätze (HEA [4]), and Hamiltonian variational ansätze (HVA [22]). The first category originates from well-established classical quantum chemistry methods [23], thereby offering higher accuracy. The unitary coupled cluster (UCC) ansätze are a leading class of chemically inspired ansätze [3, 24, 25]. The second category is designed to be more compatible with NISQ devices, while the third category lies somewhere in between. It is known that HEA [26] and HVA [27] in general suffer from BP. There remains hope that chemically inspired ansätze can avoid BP, based on the intuition that the space explored by chemically inspired ansätze is restricted [28].

Among chemically inspired ansätze, the alternated disentangled UCC (dUCC) offers the advantage over UCC of being provably able to express the exact FCI state using only single and double excitations as  $k \rightarrow \infty$  [29]. Several commonly discussed ansätze can be considered as examples of alternated dUCC ansätze, including  $k$  products of unitary pair coupled cluster with generalized singles and doubles ( $k$ -UpCCGSD) ansätze [25], basis rotation ansätze (BRA [30], since the Givens rotations are equivalent to single excitation rotations when acting on neighboring qubits), and the 1-step Trotterized unitary coupled-cluster with singles and doubles (UCCSD) ansätze.

In this work, we contribute to the theoretical understanding of VQE by studying the trainability of a class of chemically inspired VQEs. We focus on a common setting in VQE, where the Hamiltonian is chosen to be an electronic structure Hamiltonian, and the initial guess is chosen to be the uncorrelated Hartree-Fock state [21]. The ansätze we study is a relaxed version of  $k$ -step Trotterized UCC ansätze, which we refer to as the alternated disentangled UCC (dUCC) ansätze. By “relaxed” we mean that the parameters across the  $k$  alternations in the  $k$ -steps Trotterized UCC ansätze become independent. We proved, under the assumption of  $k \rightarrow \infty$  and the presence of sufficient single excitation rotations connecting all the qubits, the following results:

1. If the ansätze comprises solely single excitation rotations, the cost function concentrates around its mean polynomially concerning the qubit number  $n$ .
2. If the ansätze incorporates additional double excitation rotations, the concentration of the cost function scales inversely with  $\binom{n}{n_e}$ , where  $n_e$  represents the number of electrons.

Here, the mean and variance are defined in the sense of random parameter initialization. It is well known that BP has a close relationship with cost concentration [31]. For our specific setting, we also prove a quantitative relationship between them, which indicates that cost concentration implies BP. Furthermore, we conducted numerical simulations to explore the scenario where  $k$  is small, which is more practical. The findings indicate that the relative error between the cost variance for finite  $k$  and its asymptotic value decreases exponentially as  $k$  increases, suggesting that the assumption  $k \rightarrow \infty$  can be significantly relaxed. For  $k$  products of UCCSD ( $k$ -UCCSD), our predictions are quite accurate even at  $k = 2$  for qubit numbers ranging from 4 to 24. When  $k = 1$ , the variance of the cost function also exhibits an exponential decrease as the number of qubits grows. These numerical results show that our results are instructive for practical applications. We also study the “qubit” version of alternated dUCC ansätze in Supplementary Information, where all Pauli Z terms are trimmed after the Jordan-Wigner transformation of excitation operators [32]. Remark that the Givens rotations can be viewed as qubit single excitation rotations [30]. The most important finding is that the qubit version of  $k$  products of unitary coupled cluster with singles ( $k$ -UCCS) ansätze is exactly the same as  $k$ -UCCSD in terms of cost variance, which may indicate the connection between qubit UCCS and standard UCCSD. Our results can be interpreted in two aspects. Firstly, it is known that ansätze composed of single excitation rotations only can be simulated classically [33] while ansätze composed of single and double excitation rotations cannot [34]. Hence, our results question the hope that VQE may surpass classical methods. Secondly, our results show the trade-off between trainability and expressibility for VQE, aligning with the findings that expressibility can induce BP [8, 27, 35–37], since single excitation rotations only explore a polynomial space while single and double excitations together explore a  $\binom{n}{n_e}$  one.

## 2 Results

### 2.1 Notations

In this work, we study the scalability of alternated disentangled UCC (dUCC) ansätze, which can be viewed as a relaxed version of Trotterized UCC. Recall that in UCC theory [3, 24, 25], the

trial wave function is parameterized as the unitary exponentiation of excitation operators  $\hat{T}(\boldsymbol{\theta}) = \sum_{ia} \theta_{ia} \hat{a}_a^\dagger \hat{a}_i + \sum_{ijab} \theta_{ijab} \hat{a}_a^\dagger \hat{a}_b^\dagger \hat{a}_i \hat{a}_j + \dots$  acting upon a reference state  $|\psi_0\rangle$ :

$$|\psi_{\text{UCC}}(\boldsymbol{\theta})\rangle = e^{\hat{T}(\boldsymbol{\theta}) - \hat{T}^\dagger(\boldsymbol{\theta})} |\psi_0\rangle. \quad (1)$$

Here,  $\hat{a}$  ( $\hat{a}^\dagger$ ) represents the annihilation (creation) operator [23], and we use the convention that  $i, j, \dots$  ( $a, b, \dots$ ) label the occupied (virtual) orbitals. Generalized excitations without the occupation constraint are also allowed, and we will use  $p, q, r, s, \dots$  to label any orbital to emphasize the difference. The widely used UCCSD variant [3, 21] corresponds to truncated  $\hat{T}$  up to second excitations. For circuit implementation, it is unclear how to exactly implement the large exponentiation in Equation (1) efficiently (i.e., to a polynomial number of one and two-qubit gates), except for the case when there are only single excitations. The canonical approach is to take a  $k$ -steps Trotter approximation, with systematic error up to  $O(k^{-1})$ . In contrast, for the ease of our analysis, we will incorporate an additional relaxation step after Trotterization, as described below:

$$e^{\sum_{j=1}^m \theta_j (\hat{\tau}_j - \hat{\tau}_j^\dagger)} \xrightarrow{\text{Trotter}} \prod_{i=1}^k \prod_{j=1}^m e^{\frac{\theta_j}{k} (\hat{\tau}_j - \hat{\tau}_j^\dagger)} \xrightarrow{\text{Relax}} \prod_{i=1}^k \prod_{j=1}^m e^{\theta_j^{(i)} (\hat{\tau}_j - \hat{\tau}_j^\dagger)}, \quad (2)$$

where  $\hat{\tau}_j \in \{\hat{a}_p^\dagger \hat{a}_q, \hat{a}_p^\dagger \hat{a}_q^\dagger \hat{a}_r \hat{a}_s, \dots\}$ . Remark that  $\theta_j$  and  $\theta_j^{(i)}$  are different sets of parameters, and we implicitly make the assumption that all parameters are real (this is valid if we only care about real wave functions). Obviously, such relaxation can offer higher variational accuracy, at the cost of higher training overhead. We refer to the last unitary in Equation (2) as alternated dUCC ansätze, which is formally defined below. The term ‘‘dUCC’’ [29] was used to refer to any sequence of excitation rotations (similar to a 1-step Trotterization but conceptually different), and was proved to be able to express the exact FCI state in the limit  $k \rightarrow \infty$  even when only single and double excitations are involved. We add the ‘‘alternated’’ prefix to emphasize the alternative structure. To avoid bothering with the fermionic ladder operators  $\hat{a}, \hat{a}^\dagger$ , we will identify  $\hat{a}_p, \hat{a}_p^\dagger$  with  $Q_p \prod_{a < p} Z_a, Q_p^\dagger \prod_{a < p} Z_a$  respectively, by the Jordan-Wigner transformation. The Jordan-Wigner transformation is also employed in the canonical implementation. Other transformations such as the Bravyi-Kitaev’s may be investigated in future work. Here, we define  $Q = |0\rangle\langle 1|$ . A ‘‘qubit’’ version of UCC theory, where the  $Z$ -string is eliminated after the Jordan-Wigner transformation, is also considered in this work.

**Definition 1** (Alternated (qubit) dUCC ansätze). *Call the unitary  $U_k^{\mathbf{R}}(\boldsymbol{\theta})$  ( $k \in \mathbb{N}_+$ ) an alternated (qubit) dUCC ansätze, if it can be written as*

$$U_k^{\mathbf{R}}(\boldsymbol{\theta}) = \prod_{i=1}^k \prod_{j=1}^m R_j(\theta_j^{(i)}), \quad (3)$$

where  $\mathbf{R} = (R_1, \dots, R_m)$  is a sequence of (qubit) excitation rotations,  $R_j(\theta) = \exp(\theta(\hat{\tau}_j - \hat{\tau}_j^\dagger))$  and  $\hat{\tau}_j \in \{\hat{a}_p^\dagger \hat{a}_q, \hat{a}_p^\dagger \hat{a}_q^\dagger \hat{a}_r \hat{a}_s, \dots\}$  (or  $\hat{\tau}_j \in \{Q_p^\dagger Q_q, Q_p^\dagger Q_q^\dagger Q_r Q_s, \dots\}$  in qubit version).

While Definition 1 encompasses any (qubit) excitations, our primary focus lies on single and double (qubit) excitations. This is particularly relevant in scenarios like UCCSD. To this end, we will introduce dedicated notation for single and double (qubit) excitation rotations, as follows.

$$A_{pq}(\theta) = \exp\left(\theta(Q_p^\dagger Q_q - h.c.) \prod_{a=q+1}^{p-1} Z_a\right), \quad (4)$$

$$B_{pqrs}(\theta) = \exp\left(\theta(Q_p^\dagger Q_q^\dagger Q_r Q_s - h.c.) \prod_{b=s+1}^{r-1} Z_b \prod_{a=q+1}^{p-1} Z_a\right), \quad (5)$$

$$A_{pq}^{\text{qubit}}(\theta) = \exp(\theta(Q_p^\dagger Q_q - h.c.)), \quad (6)$$

$$B_{pqrs}^{\text{qubit}}(\theta) = \exp(\theta(Q_p^\dagger Q_q^\dagger Q_r Q_s - h.c.)), \quad (7)$$

where ‘‘h.c.’’ stands for Hermitian conjugation, and  $p > q > r > s$ . Examples of alternated (qubit) dUCC ansätze (including at most double (qubit) excitations) are

$$k\text{-UCCS}(\boldsymbol{\theta}) = \prod_{i=1}^k \prod_{p>n_e \geq q} A_{pq} \left( \theta_{pq}^{(i)} \right), \quad (8)$$

$$k\text{-UCCGS}(\boldsymbol{\theta}) = \prod_{i=1}^k \prod_{p>q} A_{pq} \left( \theta_{pq}^{(i)} \right), \quad (9)$$

$$k\text{-UCCSD}(\boldsymbol{\theta}) = \prod_{i=1}^k \prod_{p>n_e \geq q} A_{pq} \left( \theta_{pq}^{(i)} \right) \prod_{p>q>n_e \geq r>s} B_{pqrs} \left( \theta_{pqrs}^{(i)} \right), \quad (10)$$

$$k\text{-UCCGSD}(\boldsymbol{\theta}) = \prod_{i=1}^k \prod_{p>q} A_{pq} \left( \theta_{pq}^{(i)} \right) \prod_{p>q>r>s} B_{pqrs} \left( \theta_{pqrs}^{(i)} \right), \quad (11)$$

$$k\text{-qubit-UCCS}(\boldsymbol{\theta}) = \prod_{i=1}^k \prod_{p>n_e \geq q} A_{pq}^{\text{qubit}} \left( \theta_{pq}^{(i)} \right), \quad (12)$$

$$k\text{-qubit-UCCGS}(\boldsymbol{\theta}) = \prod_{i=1}^k \prod_{p>q} A_{pq}^{\text{qubit}} \left( \theta_{pq}^{(i)} \right), \quad (13)$$

$$k\text{-qubit-UCCSD}(\boldsymbol{\theta}) = \prod_{i=1}^k \prod_{p>n_e \geq q} A_{pq}^{\text{qubit}} \left( \theta_{pq}^{(i)} \right) \prod_{p>q>n_e \geq r>s} B_{pqrs}^{\text{qubit}} \left( \theta_{pqrs}^{(i)} \right), \quad (14)$$

$$k\text{-qubit-UCCGSD}(\boldsymbol{\theta}) = \prod_{i=1}^k \prod_{p>q} A_{pq}^{\text{qubit}} \left( \theta_{pq}^{(i)} \right) \prod_{p>q>r>s} B_{pqrs}^{\text{qubit}} \left( \theta_{pqrs}^{(i)} \right), \quad (15)$$

$$k\text{-BRA}(\boldsymbol{\theta}) = \prod_{i=1}^k \prod_{p=1}^{n-1} A_{p,p+1} \left( \theta_{p,p+1}^{(i)} \right), \quad (16)$$

$$k\text{-UpCCGSD}(\boldsymbol{\theta}) = \prod_{i=1}^k \prod_{p>q} A_{pq} \left( \theta_{pq}^{(i)} \right) \prod_{a>b} B_{2a,2a-1,2b,2b-1} \left( \theta_{ab}^{(i)} \right). \quad (17)$$

Here the ‘G’ in the name of ansätze stands for “generalized”. Notice that in Equations (8) to (17), the ordering of products of excitations within each block  $k$  is not specified. The reason is two-fold. Firstly, there exists no established convention regarding the ordering of these products, and their optimality has only been investigated numerically [38]. Secondly, our results, focusing on the  $k \rightarrow \infty$  regime, remain unaffected by the specific ordering of excitations.

In VQE, the cost function to be optimized is naturally chosen to be the energy of the molecule system:

$$C(\boldsymbol{\theta}; \rho, U, O) = \text{tr}(OU(\boldsymbol{\theta})\rho U(\boldsymbol{\theta})^\dagger). \quad (18)$$

Here,

- $\rho$  is an easy-to-prepare reference state. In this work,  $\rho$  is fixed to be  $|\psi_0\rangle\langle\psi_0|$ , where  $|\psi_0\rangle$  is a Hartree-Fock state [39],

$$|\psi_0\rangle := |\underbrace{1 \dots 1}_{n_e} \underbrace{0 \dots 0}_{n-n_e}\rangle. \quad (19)$$

- $U(\boldsymbol{\theta})$  is the ansätze, such that  $U(\boldsymbol{\theta})|\psi_0\rangle$  produces a trial state.
- $O$  is the observable, usually the electronic structure Hamiltonian  $H_{\text{el}} = \sum_{pq} h_{pq} \hat{a}_p^\dagger \hat{a}_q + \sum_{pqrs} g_{pqrs} \hat{a}_p^\dagger \hat{a}_q^\dagger \hat{a}_r \hat{a}_s$ . In our study, we focus on the real case, where the one- and two-electron integrals  $h_{pq}$  and  $g_{pqrs}$  are assumed to be both real and symmetric ( $h_{pq} = h_{qp} \in \mathbb{R}$  and  $g_{pqrs} = g_{srqp} \in \mathbb{R}$ ). Moreover, we assume that  $g_{pqrs} \neq 0$  only if  $p > q > r > s$  or  $p < q < r < s$ . In other words, terms such as  $\hat{a}_1^\dagger \hat{a}_3^\dagger \hat{a}_2 \hat{a}_4$  are forbidden. It is important to note that this assumption is made for ease of analysis, rather than due to the drawback of our proof techniques. In fact, our results can be generalized to any observables, although the progress of extending the analysis could be tedious. Remark that under the aforementioned assumptions,  $H_{\text{el}}$  can be written as:

$$H_{\text{el}} = \sum_{p>q} h_{pq} (\hat{a}_p^\dagger \hat{a}_q + h.c.) + \sum_{p>q>r>s} g_{pqrs} (\hat{a}_p^\dagger \hat{a}_q^\dagger \hat{a}_r \hat{a}_s + h.c.). \quad (20)$$

The cost function we study may take various forms, with  $\rho = |\psi_0\rangle\langle\psi_0|$  fixed, and  $U(\boldsymbol{\theta})$ ,  $O$  potentially varying in different instances. For simplicity, we will slightly abuse the notation and use  $C(\boldsymbol{\theta}; U, O)$ ,  $C(\boldsymbol{\theta}; U)$ ,  $C(\boldsymbol{\theta}; O)$ , or even  $C(\boldsymbol{\theta})$  instead of  $C(\boldsymbol{\theta}; \rho, U, O)$  whenever the context is clear.

## 2.2 Cost concentration and barren plateau

While VQA and VQE are promising in the NISQ era, there are several unresolved obstacles, among which the Barren Plateaus (BP) phenomenon poses a major concern [28]. Analogous to the gradient vanishing problem in training classical neural networks, BP refers to the exponential concentration of gradients (of the cost function in VQA) around 0 over random parameters, thus ruling out any gradient-based optimization method with a random starting point. Another related concept is the concentration of the cost function, which also characterizes the flatness of the cost landscape. For example, the exponential concentration of the cost function around its mean would rule out any gradient-free optimization method with a random starting point. The two types of concentration are strictly defined as follows. Let  $\{C_n\}_{n \in \mathbb{N}_+}$  be a family of cost functions indexed by qubit number  $n$  such that  $\mathbb{E}_{\boldsymbol{\theta}} [\partial_{\theta_j} C(\boldsymbol{\theta})] = 0$  for all  $\theta_j \in \Theta$ .

**Definition 2** (Gradient concentration and BP). *Let  $G(n) = \max_{\theta_j \in \Theta} \text{Var}_{\boldsymbol{\theta}} (\partial_{\theta_j} C_n(\boldsymbol{\theta}))$ . We say the gradients of  $\{C_n\}_{n \in \mathbb{N}_+}$  concentrate polynomially if  $G(n) = 1/\text{poly}(n)$ , and concentrate exponentially if  $G(n) = 1/\exp(\Omega(n))$ . Specifically,  $\{C_n\}_{n \in \mathbb{N}_+}$  exhibits BP if the gradients concentrate exponentially.*

**Definition 3** (Cost concentration). *Let  $F(n) = \text{Var}_{\boldsymbol{\theta}} (C_n(\boldsymbol{\theta}))$ . We say  $\{C_n\}_{n \in \mathbb{N}_+}$  concentrates polynomially if  $F(n) = 1/\text{poly}(n)$ , and concentrates exponentially if  $F(n) = 1/\exp(\Omega(n))$ .*

Intuitively, both gradient concentration and cost concentration describe the flatness of the landscape. The equivalence between exponential cost concentration and exponential gradient concentration (i.e., BP) was established for ansätze comprising a polynomial number of independent rotations whose generator is Hermitian with eigenvalue  $\pm 1$ , using integral arguments and the parameter shift rule [31]. Another recent work [40] also proves such equivalence using an elementary derivation by considering the Riemannian gradient instead of the Euclidean gradient. They also assume each parameterized gate to explore a whole unitary group.

Since these results are not directly applicable in our setting, in the following lemma we derive a quantitative relationship between cost variance and gradient variances, using the fact that the cost function of alternated dUCC ansätze is periodic and has no rapid oscillations. The proof of this lemma is postponed to Supplementary Note 2, and is largely inspired by another work [41].

**Lemma 1** (Relationship between variances of cost and gradients). *Let  $U_k^{\mathbf{R}}(\boldsymbol{\theta})$  be an alternated (qubit) dUCC ansätze defined in Equation (3), and  $C(\boldsymbol{\theta}; U_k^{\mathbf{R}})$  defined in Equation (20), then*

$$(k|\mathbf{R}|)^{-1} \cdot \text{Var}_{\boldsymbol{\theta}} (C) \leq \max_{\theta_j \in \Theta} \text{Var}_{\boldsymbol{\theta}} (\partial_{\theta_j} C) \leq \text{Var}_{\boldsymbol{\theta}} (C). \quad (21)$$

Consequently, for alternated dUCC ansätze, the exponential decay of cost variance implies exponential decay of gradient variance by second inequality of Equation (21), while the reverse holds only when  $k|\mathbf{R}|$  is sub-exponential by the first inequality. Our main focus will be determining the scaling of variance of cost, and bound the variance of gradients by Lemma 1.

## 2.3 Separation between single and double excitation rotations

In this section, we lay out our main result, proving the scaling of cost concentration for alternated dUCC ansätze composed of (qubit) single and double excitation rotations. The detailed proofs can be found in Supplementary Information.

**Theorem 2** (Main result). *Let  $U_k^{\mathbf{R}}(\boldsymbol{\theta})$  be an alternated (qubit) dUCC ansätze defined in Equation (3), and  $C(\boldsymbol{\theta}; U_k^{\mathbf{R}}, H_{\text{el}})$  defined in Equation (18), where the qubit number is  $n$ , and  $H_{\text{el}}$  is defined in Equation (20), with one- and two-electron integrals  $h_{pq}, g_{pqrs}$ . Denote the simple undirected graph formed by index pairs of (qubit) single excitations in  $\mathbf{R}$  by  $G$ , i.e.,*

$$G := (V = [n], E = \{(u, v) | A_{uv} \text{ or } A_{uv}^{\text{qubit}} \in \mathbf{R}\}). \quad (22)$$

*Suppose  $G$  is connected. The limit  $\lim_{k \rightarrow \infty} \text{Var} (C(\boldsymbol{\theta}; U_k^{\mathbf{R}}, H_{\text{el}})) =: V(n)$  exists, and*

- 1. If  $\mathbf{R}$  contains only single excitation rotations, then  $V(n) \sim \text{poly}(n^{-1}, n_e, \|\mathbf{h}\|, \|\mathbf{g}\|)$ .*
- 2. If  $\mathbf{R}$  contains both single and double excitation rotations, then  $V(n) \sim \text{poly}(\|\mathbf{h}\|, \|\mathbf{g}\|) / \binom{n}{n_e}$ .*

3. If  $\mathbf{R}$  contains only single qubit excitation rotations, then  $V(n) \sim \text{poly}(n^{-1}, n_e, \|\mathbf{h}\|, \|\mathbf{g}\|)$  if the maximum degree of  $G$  is 2, and  $V(n) \sim \text{poly}(\|\mathbf{h}\|, \|\mathbf{g}\|) / \binom{n}{n_e}$  otherwise.
4. If  $\mathbf{R}$  contains both single and double qubit excitation rotations (and satisfies the condition in Supplementary Theorem 37), then  $V(n) \sim \text{poly}(\|\mathbf{h}\|, \|\mathbf{g}\|) / \binom{n}{n_e}$ .

Combining Lemma 1 and Theorem 2, we have the following corollary.

**Corollary 3.** *There exists finite function  $K(n)$ , such that the following alternated (qubit) dUCC ansätze suffer from BP when the number of alternations  $k > K(n)$ :  $k$ -UCC( $G$ )SD,  $k$ -UpCCGSD,  $k$ -qubit-UCC( $G$ )S,  $k$ -qubit-UCC( $G$ )SD.*

We make three remarks regarding the main result.

Firstly, the separation between cost concentration can be understood as the result of a difference in expressiveness. By Thouless theorem [33], an alternated dUCC ansätze composed of single excitation rotations can be identified with a single  $2^n \times 2^n$  unitary

$$\exp\left(\sum_{i,j=1}^n h_{ij}(\hat{a}_p^\dagger \hat{a}_q - h.c.)\right), \quad \text{with } h \in O(n). \quad (23)$$

Hence, if there are only single excitation rotations, the ansätze will only explore an  $O(n^2)$ -dimensional subspace. On the other hand, if there are both single and double excitation rotations, the ansätze will explore the real invariant space of dimension  $\binom{n}{n_e}$ , spanned by all computational basis states with Hamming weight  $n_e$  [29]. The cost concentration of the alternated qubit dUCC ansätze composed of single qubit excitation rotations can be linked with the classical simulatability of matchgates on different topologies. Observe that qubit excitation rotations, or equivalently the Grover rotations, are matchgates. It is well-known [42] that circuits composed of matchgates acting on nearest neighbors can be classically efficiently simulated, in a way similar to Equation (23), and circuits composed of matchgates that act on nearest neighbors and next-nearest neighbors can perform universal quantum computation. This fact corresponds to Item 3 of Theorem 2. A recent work [43] discussed the seemingly deep connection between BP and classical simulatability, by examining existing BP results. Our results provide another example supporting their arguments.

Secondly, our results can be partly explained by the dynamic Lie algebra (DLA), which is used in recent works [27, 35–37] to establish a unified theory of the barren plateau of deep periodic ansätze. Notice that the alternated dUCC ansätze can also be seen as periodic ansätze. When there are both single and double (qubit) excitations, as in Item 2 of Theorem 2, the DLA is  $\mathfrak{g} = \mathfrak{so}\left(\binom{n}{n_e}\right)$  when restricted to the invariant subspace. Hence, the cost variance can also be obtained by integrating over  $e^{\mathfrak{g}} = \text{SO}\left(\binom{n}{n_e}\right)$  [44]. However, other cases are more involved. It is important to note that these results [27, 35–37] cannot be directly applied in our setting for different reasons, such as  $\mathfrak{g}$  being real,  $i\rho, iO \notin \mathfrak{g}$ , or the ansätze considered is a specific one that differs from ours. Moreover, our method is different from theirs, relying more on symmetries and taking a combinatorial approach. Another work [45], although their techniques do not fall into the DLA category, also studies the ansätze composed of single excitations. Their results differ from ours into they assumed that the input or output of the ansätze are Haar distributed. In contrast, our results are predicated on a fixed input state, the Hartree-Fock state, with assumptions made regarding the structure of the ansätze rather than focusing on the output.

Finally, to obtain the main results, we made three assumptions: (1) the number of alternations  $k \rightarrow \infty$ ; (2) independence of parameters between different Trotter steps (cf. Equation (2)); and (3) random initialization of parameters. These assumptions greatly simplify the analysis but at the same time deviate from practical applications. In Trotterized UCCSD, parameters between different Trotter steps are coupled, while in  $k$ -UpCCGSD the parameters are independent. In both cases, the number of Trotter steps or alternations  $k$  is finite. Additionally, the parameters in VQE are almost always initialized in all-zero. Regrettably, our techniques currently face challenges in fully addressing the limitations associated with these three assumptions. Nevertheless, we hope that our results are also instructive for practical applications. In fact, the convergence of cost variance towards its asymptotic value is equivalent to the convergence of alternating projections [46], which is exponential in  $k$ . Such exponential convergence is also verified through numerical experiments in the ‘‘Simulations’’ subsection in the Results. In that sense, the assumption that  $k \rightarrow \infty$  can be greatly relaxed, except that we failed to find a way to determine the exact convergence rate, for example the  $K(n)$  in Corollary 3, through our current techniques. Recently, a step was made in calculating the mixing time

to  $t$ -designs, which is analogous to  $k$ , determining that the time is  $\text{poly}(n)$  rather than some finite value [36]. Their techniques may prove helpful in improving our results. In our work, the convergence rate is numerically studied in the ‘‘Simulations’’ subsection in the Results, where the results hint that the  $K(n)$  in Corollary 3 could even be a constant as small as 1 for the case of  $k$ -UCCSD. This finding further mitigates the gap between our theoretical results and practical applications. The implications and caveats of assumptions (2) and (3) will be discussed in ‘‘Discussion’’ subsection.

## 2.4 Simulations

We conduct numerical experiments to validate our theoretical results and explore the more practical scenarios where  $k$  is finite.

First, we verify the prediction in Theorem 2 that the variance of the cost function converges as  $k$  increases and investigate its convergence rate. In Figure 1, we present experimental data for 4 alternated dUCC ansätze:  $k$ -BRA,  $k$ -UCCS,  $k$ -UCCSD and  $k$ -UpCCGSD. For each ansätze, we plot the scaling of the following distances concerning  $k \in \{1, 2, \dots, 100\}$  for different values of  $n \in \{4, 6, 8, 10\}$ : (1) The  $\ell^1, \ell^2, \ell^\infty$  distance between  $\left(\prod_{j=1}^m \mathbb{E} \left[ R_j^{\otimes 2, 2} \right] \right)^k |\psi_0\rangle^{\otimes 2}$  and  $P_M |\psi_0\rangle^{\otimes 2}$ . (2) The distances (relative errors) between cost variance at  $k$  and the asymptotic variance  $\lim_{k \rightarrow \infty} \text{Var}(C)$ , with respect to monomial observables  $\hat{a}_p^\dagger \hat{a}_q + h.c.$  ( $p > q$ ) and  $\hat{a}_p^\dagger \hat{a}_q^\dagger \hat{a}_r \hat{a}_s + h.c.$  ( $p > q > r > s$ ). In all cases, we set  $n_e = n/2$ . This choice is reasonable since in practice  $n_e = \Theta(n)$  [47]. In each alternation of these ansätze, the excitation rotations are arranged in lexicographical order according to their position, and when there are both single and double excitation rotations, the single excitation rotations are placed before the double ones. It is noted that all data are accurate within machine precision, as all calculations are based on the formulas derived in the Supplementary Note 6 and 8. Due to the complexity of computations, the maximum value for  $n$  is limited to 10. The results indicate that all distances decay to zero as  $k$  increases, until exhausting machine precision, which confirms the correctness of our theoretical results. Moreover, all distances converge exponentially concerning  $k$ , and for increasing  $n$ , it appears that the convergence rates decrease moderately for  $k$ -BRA and  $k$ -UCCS, and slightly increase for  $k$ -UCCSD and  $k$ -UpCCGSD.

Based on the results in Figure 1, it is appealing to conjecture that  $k$ -UCCSD and  $k$ -UpCCGSD exhibit BP even for constant  $k$ . To support this conjecture, we further investigate how the variance of the cost function for  $k$ -UCCSD changes with increasing  $n$  when  $k$  is small. In Figure 2, we plot the scaling of the cost variance concerning  $n \in \{4, 6, \dots, 24\}$  when  $k \in \{1, 2, 3, \infty\}$ . We only display the results for two fixed observables  $\hat{a}_2^\dagger \hat{a}_1 + h.c.$  and  $\hat{a}_4^\dagger \hat{a}_3^\dagger \hat{a}_2 \hat{a}_1 + h.c.$  because, according to previous numerical and theoretical results, the cost variances corresponding to different one- (or two-) body operators are similar. Additionally, the number of electrons is still set to  $n_e = n/2$ . Unlike Figure 1, the cost variances for  $k = 1, 2, 3$  are estimated by randomly sampling 6000 times for each different  $n$ . The asymptotic variance of the cost function is calculated using the formulas derived in the Supplementary Note 8. We also fit the estimated data points with an exponential function  $a \exp(b \cdot n)$ , where  $a$  and  $b$  are fitting parameters. The data points and the fitted curves match well, justifying our conjecture. Moreover, the variances converge to their asymptotic values quickly. A very small value of  $k = 2$  or  $3$  seems to be enough for the relative error between finite- $k$  variance and asymptotic variance to be bounded by a constant. In Supplementary Note 9, we present numerical results for  $n_e = n/4$ , which is similar to the case of  $n_e = n/2$ . This shows that our conclusion on  $k$ -UCCSD is not affected by the number of electrons.

In summary, these numerical results reduce the distance between our theoretical results and reality. Specifically:

1. The unrealistic assumption of  $k \rightarrow \infty$  can be greatly relaxed. Figure 1 shows that the relative error between the variance of the cost function with finite  $k$  and the asymptotic value decays exponentially with  $k$ , and the convergence rate does not degrade much with increasing qubit count.
2. Our theoretical results regarding  $k$ -UCCSD seem to extend to cases when  $k$  is constant. Figure 2 shows that for  $k$ -UCCSD, our predictions are already accurate enough when  $k = 2$ , and when  $k = 1$ , the variance of the cost function also exhibits exponential decay with qubit count. This implies that our theory is also instructive for ansätze like 1-step Trotterized UCCSD that are used in practice.

It should be noted that these conclusions are merely observations derived from numerical results and are limited by the scale of these numerical experiments due to computational resources. Unfortunately, our current technology cannot provide more theoretical evidence to support our views. We leave more theoretical analysis for future work.

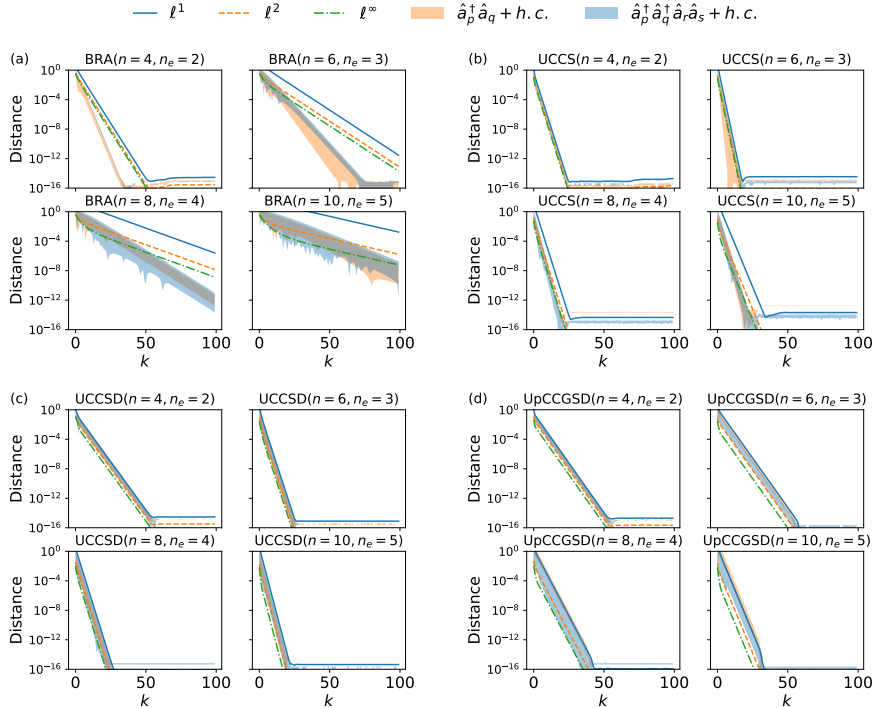


**Fig. 1** Convergence of the projected state and cost variance for four alternated dUCC ansätze. The four panels correspond to four ansätze: (a) basis rotation ansätze (BRA), (b) unitary coupled cluster with singles (UCCS), (c) unitary coupled cluster with singles and doubles (UCCSD), and (d) unitary pair coupled cluster with generalized singles and doubles (UpCCGSD). For each ansätze, we provide four plots corresponding to number of orbitals  $n = 4, 6, 8, 10$  and number of electrons  $n_e = n/2$ . The number of alternations  $k$  takes value in  $\{1, 2, \dots, 100\}$ . The y-axes are the dimensionless distances between the finite-alternations quantities and the infinite-alternations quantities ( $k \rightarrow \infty$ ). The blue solid, orange dashed, and green dash-dotted curves represent the  $\ell^1, \ell^2, \ell^\infty$  distance, respectively. The shaded areas in orange and blue encompass all single and double excitation monomials. The abbreviation “h.c.” stands for “Hermitian conjugate”.

### 3 Discussion

In this work, we conducted a rigorous analysis of cost concentration for the alternated dUCC ansätze at infinite depth. Contrary to previous belief [28], we showed that the chemically inspired ansätze can also suffer from BP. Specifically, our findings indicate that while double excitations are essential for accuracy [23], they can significantly increase the training cost. Numerical results suggest that our results can be extended to the finite-depth cases, and potentially even a constant number of alternations for interesting ansätze such as  $k$ -UCCSD.

While we made specific assumptions regarding the domain of parameters and the form of the electronic structure Hamiltonian to derive our main results, our proof techniques can be adapted to a more general scenario without these assumptions, albeit with increased complexity. In fact, we anticipate the applicability of our proof techniques to analyze the concentration and BP of other periodic cost functions. Furthermore, our analysis of cost concentration involves characterizations of the  $t^{\text{th}}$  moment of any excitation rotations for any  $t$ , which may be of independent interest.

We acknowledge that our work is at a distance from ruling out the practicality of chemically inspired ansätze, in the following aspects.

Firstly, our study focused on alternated dUCC ansätze, incorporating a large number of independent parameters. The Trotterized UCCSD may be free of BP because its correlated parameters are limited in a smaller range with increasing Trotter steps (cf. Equation (2)) [48]. That said, such



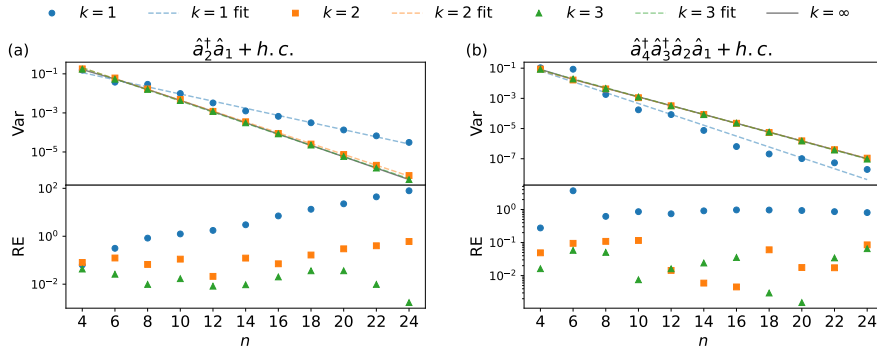


**Fig. 2** Scaling of the cost variance and relative error to asymptotic variance for  $k$ -UCCSD when  $n_e = n/2$ . Here we present the cost variance (Var) and the relative error to asymptotic variance (RE) for the  $k$  alternations of unitary coupled cluster with singles and doubles ( $k$ -UCCSD) ansätze measured by (a)  $\hat{a}_2^\dagger \hat{a}_1 + h.c.$  and (b)  $\hat{a}_4^\dagger \hat{a}_3^\dagger \hat{a}_2 \hat{a}_1 + h.c.$ . The abbreviation “h.c.” stands for “Hermitian conjugate”. The number of qubit is  $n \in \{4, 6, \dots, 24\}$ , with the number of electrons given by  $n_e = n/2$ . For each observable, the illustrated variances for  $k = 1, 2, 3$  are estimated from 6000 random samples at each  $n$  value, and are represented by blue circles, orange squares, and green triangles, respectively. The variances for  $k = 1, 2, 3$  are fitted using the function  $a \exp(b \cdot n)$ , with the resulting fitting curves shown as blue, orange, and green dashed lines. The computed asymptotic variances ( $k \rightarrow \infty$ ) are depicted as gray solid curves. In the lower half of each panel, we display the relative error of the variances at  $k = 1, 2, 3$  compared to the asymptotic variances, also represented by blue circles, orange squares, and green triangles. The error bars, estimated as  $\sqrt{2/(6000 - 1)} \cdot \text{Var}$ , are not shown as they are smaller than the data points.

an argument essentially builds upon the assumption that the circuit can be approximated by a local Hamiltonian evolution, which is unlikely reasonable for an ansätze such as UCCSD.

Secondly, the BP phenomenon is considered under random parameter initialization, whereas VQE often benefits from reasonable heuristics for choosing an initial guess. For example, the all-zero initialization is commonly used in the UCC ansätze. If the initial guess happens to be inside the same local trap as the optimal solution, the optimizer may effortlessly find the optimal solution, even if the landscape is a plateau elsewhere. Otherwise, BP prevents the optimizer from escaping the narrow gorge, resulting in a sub-optimal solution. One possible solution to this is to use adaptive ansätze, which have been reported to be able to “burrow” out of local traps [49].

Lastly, we exclusively considered the Jordan-Wigner transformation, as employed in the canonical implementation of UCCSD. However, the Bravyi-Kitaev transformation might be a better choice due to its locality [50].

In recent years, there has been significant progress in the study of BP for periodic ansätze of the form  $U(\boldsymbol{\theta}) = \prod_{i=1}^k U_i(\boldsymbol{\theta}_i)$ , where  $U_i(\boldsymbol{\theta}_i) = \prod_{j=1}^m e^{-iH_j \theta_{ij}}$ . This class of ansätze includes the quantum approximate optimization algorithm (QAOA) [51], HVA, and the alternated dUCC ansätze that we investigate. Specifically, the pioneering work [27] points out that the dynamic Lie algebra (DLA), defined by the real span of the Lie closure of the generators  $\mathfrak{g} := \text{span}_{\mathbb{R}} \langle iH_1, \dots, iH_m \rangle_{\text{Lie}}$ , could be a powerful tool for diagnosing BP of periodic ansätze. This is because when  $k$  is large enough, the set of unitaries that can be generated by the periodic ansätze is precisely  $e^{\mathfrak{g}} := \{e^V : V \in \mathfrak{g}\}$ . When  $\mathfrak{g} = \mathfrak{su}(2^n)$ ,  $\mathfrak{so}(2^n)$ , or is effectively full-rank within an invariant subspace containing the initial state, the distribution over  $e^{\mathfrak{g}}$  converges to a 2-design as  $k \rightarrow \infty$  [27]. This allows the variance of gradients to be calculated via integration over the special unitary (or orthogonal) group. Despite the elegance and intuition of their methods, several limitations exist. Firstly, the characterization of the generated unitary set and its distribution relies on the assumption that  $k$  is sufficiently large, with the specific scaling of  $k$  remaining unknown. Secondly, they assume the parameters to be independently and fully tunable. But there are other parameter initialization strategies, such as constraining the parameters to be small or correlated, that are used in practice and may avoid BP [16, 48]. Thirdly, their results for the full-rank subspace case rely on the initial state being in that subspace. Lastly, their analysis was limited to full-rank DLA due to the intricacy of integrating over a proper subgroup of the unitary group. Recent works [35, 36] have resolved this last limitation, providing a finer analysis of how large  $k$  must be for the distribution to approximate a 2-design [36]. Nonetheless, their theories still depend on either the initial state  $\rho$  or the observable  $O \in i\mathfrak{g}$ , which does not apply in our settings. These constraints can be removed for specific ansätze, but only for a certain ansätze [37]. Our work differs from these works in two aspects. Secondly, we address a problem where existing methods are not fully applicable. However, our results share similar limitations concerning  $k$  and parameter assumptions.

## 4 Methods

### 4.1 Sketch of the proof of the main theorem

We analyze cost concentration for the alternated dUCC in the infinite depth limit by providing an explicit formula for the cost variance. In a unified manner, we will analyze the  $t^{\text{th}}$  moment of the cost function,  $\mathbb{E}[C^t]$ , with a focus on  $t = 1, 2$ . The calculation of  $\mathbb{E}[C^t]$  involves two key steps:

1. Through tensor network contraction [52–55],  $\mathbb{E}[C^t]$  can be represented as product of enlarged tensors corresponding to the reference state, gates, and the observable:

$$\mathbb{E}[C^t] = \langle H_{\text{el}} |^{\otimes t} \left( \prod_{j=1}^m \mathbb{E}[R_j^{\otimes t, t}] \right)^k | \psi_0 \rangle^{\otimes 2t}. \quad (24)$$

Here,  $M^{\otimes t, t} := M^{\otimes t} \otimes (M^*)^{\otimes t}$ . This representation allows for the separation of different parameters, resolving non-linearity by incorporating an enlarged Hilbert space with dimension  $2^{2tn}$ .

2. The periodicity of excitation rotations implies that each  $\mathbb{E}[R_j^{\otimes t, t}]$  is an orthogonal projection, denoted as  $P_{M_j}$ . Let  $M := \bigcap_j M_j$  represent the intersection space. Through the convergence of alternating projections [46], we obtain:

$$\lim_{k \rightarrow \infty} \mathbb{E}[C^t] = \langle H_{\text{el}} |^{\otimes t} P_M | \psi_0 \rangle^{\otimes 2t}. \quad (25)$$

This approach circumvents the challenge of tracking the evolution of  $|\psi_0\rangle^{\otimes 2t}$  or  $|H_{\text{el}}\rangle^{\otimes t}$  at finite  $k$ . Instead, it suffices to determine the intersection space  $M$ , which turns out to be tractable.

Let us elaborate a bit more on the two key steps. Firstly, to facilitate a more straightforward description of the elevated tensors, the  $2tn$  qubits are rearranged so that the enlarged Hilbert space can be conceptualized as a tensor product of  $n$  subsystems. Each subsystem, which we refer to as a site, comprises  $2t$  qubits. As an illustrative example,  $|\psi_0\rangle^{\otimes 2t}$  is identified with

$$|\psi_0\rangle^{\otimes 2t} = \underbrace{|1 \dots 1\rangle}_{2t}^{\otimes n_e} \underbrace{|0 \dots 0\rangle}_{2t}^{\otimes (n - n_e)}. \quad (26)$$

Secondly, in BP studies, it is common that the  $t^{\text{th}}$  moment superoperators of parameterized gates, such as  $\mathbb{E}[R_j^{\otimes t, t}]$  in our case, are orthogonal projections. For instance, the circuit or block of gates is often assumed to be Haar random up to the 2<sup>nd</sup> moment [26, 50, 54]. Under such an assumption one can verify that the 2<sup>nd</sup> moment superoperator of the circuit or block of gates is an orthogonal projection of rank 2. However, the projections encountered in our analysis are notably more intricate. Specifically, the  $t^{\text{th}}$  moment of qubit single excitation rotations forms a projection of rank 70 within the subsystem it acts on, let alone normal excitation rotations that are highly non-local. Consequently, while the evolution of the reference state can be successfully tracked under the Haar random assumption [50], achieving a similar goal may not be possible in the present setting. Instead, we turn to studying the infinite case. It is worth noting that the phenomenon where the infinite case is easier than the finite one also arises in the theoretical analysis of classical neural networks [56].

Thirdly, we ascertain the intersection space  $M$  by leveraging the following identity:

$$M^\perp = M_1^\perp + M_2^\perp + \dots + M_m^\perp. \quad (27)$$

In other words, it suffices to determine the spanning set of  $M_j^\perp$ , and then take the union to obtain the spanning set of  $M^\perp$ . To further simplify the analysis, we utilize the symmetries of  $P_{M_j} = \mathbb{E}[R_j^{\otimes t, t}]$  and identify the spanning set of  $M_j^\perp$  within the invariant spaces induced by these symmetries. To be specific, the symmetries and their corresponding invariant spaces that contain  $|\psi_0\rangle^{\otimes 2t}$  are listed below.

- The  $Z_p^{\otimes 2t}$ -symmetry induces an invariant space  $\mathcal{H}_t^{\text{even}} = \text{span } \mathcal{S}_t^{\text{even}}$ , where

$$\mathcal{S}_t^{\text{even}} := \left\{ |b_1 b_2 \dots b_{2t}\rangle \left| \sum_i b_i \equiv 0 \right. \right\}^{\otimes n}. \quad (28)$$

- The particle number symmetry further induces an invariant space  $\mathcal{H}_2^{\text{paired}} = \text{span } \mathcal{S}_2^{\text{paired}}$  at  $t = 2$ . Here, we define  $\mathcal{S}_2^{\text{paired}} \subseteq \mathcal{S}_2^{\text{even}}$  to be the set of paired states and a vector  $|\Phi\rangle \in \mathcal{S}_2^{\text{even}}$  is called a paired state, if

$$\# |0000\rangle = \# |1111\rangle + n - 2n_e, \quad (29)$$

$$\# |0011\rangle = \# |1100\rangle, \quad (30)$$

$$\# |0101\rangle = \# |1010\rangle, \quad (31)$$

$$\# |0110\rangle = \# |1001\rangle, \quad (32)$$

where  $\# |b_1 b_2 b_3 b_4\rangle$  counts the number of sites in  $|\Phi\rangle$  that are in state  $|b_1 b_2 b_3 b_4\rangle$ .

- The  $(S_\tau^b)^{\otimes n}$ -symmetry induces an invariant space  $\mathcal{H}_t^\tau$ . Here, the operator  $S_\tau^b$  defines a permutation of qubits in one site by  $\tau \in \mathfrak{S}_{2t}$ , and  $\mathcal{H}_t^\tau$  is the +1 eigenspace of  $(S_\tau^b)^{\otimes n}$ .

In Supplementary Note 4, the spanning set of  $M_j^\perp \cap \mathcal{H}_2^{\text{paired}}$  and  $M_j^\perp \cap \mathcal{H}_2^{\text{paired}} \cap \bigcap_{\tau \in \mathfrak{S}_4} \mathcal{H}_2^\tau$  is characterized at  $t = 2$ . With these spanning sets in hand, we can then characterize the intersection space  $M$  inside these invariant spaces, according to Equation (27). Surprisingly, as shown in Supplementary Note 4, while the dimension of each  $M_j$  is exponentially large, the dimension of the intersection  $M \cap \mathcal{H}_2^{\text{paired}}$  is at most  $\text{poly}(n)$  at  $t = 2$ , under a mild assumption.

## 4.2 Simulation details

The code used in this study is available [57]. The implementation is designed to run with Python version 3.10.12 and Rust version 1.72.1. The computations were performed on a system equipped with an NVIDIA GeForce RTX 3090 (24 GB) GPU and an Intel(R) Xeon(R) Gold 5222 CPU running at 3.80 GHz.

## Data availability

The data generated in this study along with the accession codes are available at <https://doi.org/10.5281/zenodo.13359192>.

## Code availability

The code used in this study is available at <https://doi.org/10.5281/zenodo.13359192>.

## Acknowledgements

We would like to thank Reviewers for taking the time and effort necessary to review the manuscript. This work was supported in part by the National Natural Science Foundation of China Grants No. 62325210 and the Strategic Priority Research Program of Chinese Academy of Sciences Grant No. XDB28000000.

## Author contributions

The project was conceived by all authors. R.M. developed the methodology, conducted the simulations, and analyzed the results with inputs from G.T. and X.S. The manuscript was written by R.M. and G.T. All authors contributed to the manuscript review.

## Competing interests

The authors declare no competing interests.

# Supplementary Methods: Notations

Throughout the text, we will use  $X, Y, Z$  for Pauli matrices,  $I$  for  $2 \times 2$  identity matrix, and  $\mathbb{1}_N$  for  $N \times N$  identity matrix. Two additional  $2 \times 2$  matrices are used: qubit annihilation operator  $Q = |0\rangle\langle 1|$ , and occupation number operator  $N = |1\rangle\langle 1|$ . The symbol  $n$  is reserved for the number of orbitals (qubits), and  $n_e$  for the number of occupied orbitals. For any  $2 \times 2$  matrix  $M$  (for example  $X, Y, Z, I$ ), we define  $M_i := I^{\otimes i-1} \otimes M \otimes I^{\otimes n-i}$ , where  $i \in [n]$  and  $[n] := \{1, \dots, n\}$ .

We use  $z^*$  to denote the complex conjugate of  $z$ , and  $M^\dagger$  to denote the conjugate transpose of matrix  $M$ .  $i$  represents the imaginary unit. Denote  $\mathfrak{S}_m$  as the symmetric group on a set of size  $m$ . The set of bit strings of length  $m$  is denoted by  $\mathbb{F}_2^m$ . For a bit string  $\mathbf{b} \in \mathbb{F}_2^m$ ,  $\bar{\mathbf{b}}$  denotes the flip of  $\mathbf{b}$ , i.e.,  $\bar{\mathbf{b}} = b_1 b_2 \dots b_m \in \mathbb{F}_2^m$  and  $\bar{b}_i = 1 - b_i, \forall i$ . For two bit strings  $\mathbf{b}, \mathbf{b}' \in \mathbb{F}_2^m$ ,  $\mathbf{b} \odot \mathbf{b}'$  denotes the bitwise dot, defined by  $\sum_{i=1}^m b_i \cdot b'_i$ .

We first recall some notations, definitions, and theorems from the main text.

Cost function

$$C(\boldsymbol{\theta}; \rho, U, O) = \text{tr}(OU(\boldsymbol{\theta})\rho U(\boldsymbol{\theta})^\dagger). \quad (33)$$

Reference state

$$|\psi_0\rangle := |\underbrace{1 \dots 1}_{n_e} \underbrace{0 \dots 0}_{n-n_e}\rangle. \quad (34)$$

Electronic structure Hamiltonian

$$H_{\text{el}} = \sum_{p>q} h_{pq} (\hat{a}_p^\dagger \hat{a}_q + h.c.) + \sum_{p>q>r>s} g_{pqrs} (\hat{a}_p^\dagger \hat{a}_q^\dagger \hat{a}_r \hat{a}_s + h.c.). \quad (35)$$

**Definition 4** (Alternated (qubit) dUCC ansätze). *Call the unitary  $U_k^{\mathbf{R}}(\boldsymbol{\theta})$  ( $k \in \mathbb{N}_+$ ) an alternated (qubit) dUCC ansätze, if it can be written as*

$$U_k^{\mathbf{R}}(\boldsymbol{\theta}) = \prod_{i=1}^k \prod_{j=1}^m R_j(\theta_j^{(i)}), \quad (36)$$

where  $\mathbf{R} = (R_1, \dots, R_m)$  is a sequence of (qubit) excitation rotations,  $R_j(\theta) = \exp(\theta(\hat{\tau}_j - \hat{\tau}_j^\dagger))$  and  $\hat{\tau}_j \in \{\hat{a}_p^\dagger \hat{a}_q, \hat{a}_p^\dagger \hat{a}_q^\dagger \hat{a}_r \hat{a}_s, \dots\}$  (or  $\hat{\tau}_j \in \{Q_p^\dagger Q_q, Q_p^\dagger Q_q^\dagger Q_r Q_s, \dots\}$  in qubit version).

**Lemma 4** (Relationship between variances of cost and gradients). *Let  $U_k^{\mathbf{R}}(\boldsymbol{\theta})$  be an alternated (qubit) dUCC ansätze defined in Supplementary Equation (36), and  $C(\boldsymbol{\theta}; U_k^{\mathbf{R}})$  defined in Supplementary Equation (35), then*

$$(k|\mathbf{R}|)^{-1} \cdot \text{Var}_{\boldsymbol{\theta}}(C) \leq \max_{\theta_j \in \boldsymbol{\theta}} \text{Var}_{\boldsymbol{\theta}}(\partial_{\theta_j} C) \leq \text{Var}_{\boldsymbol{\theta}}(C). \quad (37)$$

**Theorem 5** (Main result). *Let  $U_k^{\mathbf{R}}(\boldsymbol{\theta})$  be an alternated (qubit) dUCC ansätze defined in Supplementary Equation (36), and  $C(\boldsymbol{\theta}; U_k^{\mathbf{R}}, H_{\text{el}})$  defined in Supplementary Equation (33), where the qubit number is  $n$ , and  $H_{\text{el}}$  is defined in Supplementary Equation (35), with one- and two-electron integrals  $h_{pq}, g_{pqrs}$ . Denote the simple undirected graph formed by index pairs of (qubit) single excitations in  $\mathbf{R}$  by  $G$ , i.e.,*

$$G := (V = [n], E = \{(u, v) | A_{uv} \text{ or } A_{uv}^{\text{qubit}} \in \mathbf{R}\}). \quad (38)$$

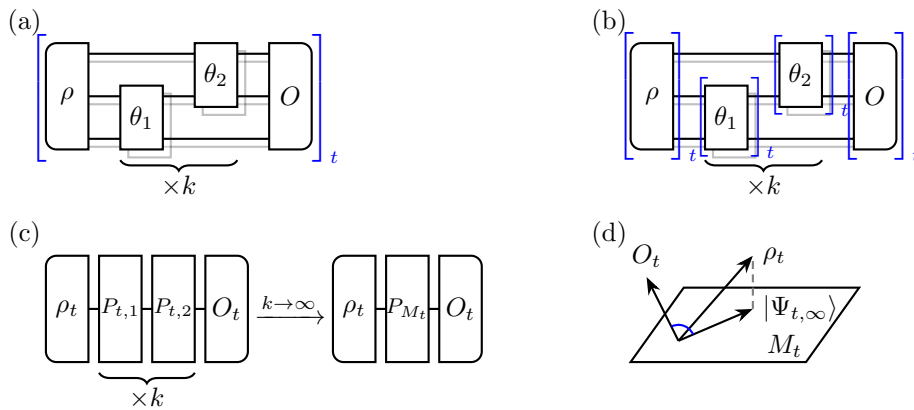
Suppose  $G$  is connected. The limit  $\lim_{k \rightarrow \infty} \text{Var}(C(\boldsymbol{\theta}; U_k^{\mathbf{R}}, H_{\text{el}})) =: V(n)$  exists, and

1. If  $\mathbf{R}$  contains only single excitation rotations, then  $V(n) \sim \text{poly}(n^{-1}, n_e, \|\mathbf{h}\|, \|\mathbf{g}\|)$ .
2. If  $\mathbf{R}$  contains both single and double excitation rotations, then  $V(n) \sim \text{poly}(\|\mathbf{h}\|, \|\mathbf{g}\|) / \binom{n}{n_e}$ .
3. If  $\mathbf{R}$  contains only single qubit excitation rotations, then  $V(n) \sim \text{poly}(n^{-1}, n_e, \|\mathbf{h}\|, \|\mathbf{g}\|)$  if the maximum degree of  $G$  is 2, and  $V(n) \sim \text{poly}(\|\mathbf{h}\|, \|\mathbf{g}\|) / \binom{n}{n_e}$  otherwise.
4. If  $\mathbf{R}$  contains both single and double qubit excitation rotations (and satisfies the condition in Supplementary Theorem 44), then  $V(n) \sim \text{poly}(\|\mathbf{h}\|, \|\mathbf{g}\|) / \binom{n}{n_e}$ .

## Supplementary Note 5: Summary of proof

Supplementary Notes 7 to 12 are devoted to the proof of Theorem 5, which is, in fact, the calculation of the cost variance  $\text{Var}(C)$ . The proof is divided into the following parts (illustrated in Supplementary Figure 3):

- In Supplementary Note 7, we give a high-level description of how we calculate the  $t^{\text{th}}$  moment of the cost function.
  - We represent the  $t^{\text{th}}$  moment of cost function as a circuit-like tensor network (Lemma 9), by contracting the initial state, gates, and observable into larger tensors:  $\mathbb{E}[C^t] = \langle H_{\text{el}} \rangle^{\otimes t} \left( \prod_{j=1}^{|\mathbf{R}|} \mathbb{E}[R_j^{\otimes t, t}] \right)^k |\psi_0\rangle^{\otimes 2t}$ . Since the  $t^{\text{th}}$  moment of cost is essentially captured by the vector  $|\Psi_{t,k}^{\mathbf{R}}\rangle := \left( \prod_{j=1}^{|\mathbf{R}|} \mathbb{E}[R_j^{\otimes t, t}] \right)^k |\psi_0\rangle^{\otimes 2t}$ , we refer to such vector as  $(\mathbf{R}, t, k)$ -moment vector (Definition 6).
  - We introduce site decomposition (Definition 7), so that the enlarged space  $\mathbb{C}^{2^{2tn}}$  involved in calculating  $\mathbb{E}[C^t]$  can be still viewed as tensor product of  $n$  subsystems. These subsystems are referred to as sites, each containing  $2t$  qubits. Under site decomposition, tensor like  $\mathbb{E}[R_j^{\otimes t, t}]$  can be viewed as an operator acting on sites.
  - We show that each  $\mathbb{E}[R_j^{\otimes t, t}]$  is an orthogonal projection (Lemma 11), denoted by  $P_{M_j}$ .
  - The convergence of alternating projections hence assures that  $|\Psi_{t,\infty}^{\mathbf{R}}\rangle = P_M |\psi_0\rangle^{\otimes 2t}$ , where  $M = \bigcap_{j=1}^{|\mathbf{R}|} M_j$  (Corollary 13). While it is not obvious how to find the intersection space  $M$ , it is easy to find its orthogonal complement  $M^\perp$ , since  $M^\perp = \sum_{j=1}^{|\mathbf{R}|} M_j^\perp$  (Lemma 14).
- In Supplementary Note 8, we characterize the spanning set of  $M_j^\perp$  (Lemma 20). Symmetries of  $\mathbb{E}[R_j^{\otimes t, t}]$  are used to reduce the space.
  - The  $Z_p^{\otimes 2t}$ -symmetry helps to reduce to the invariant space  $\mathcal{H}_2^{\text{even}}$  (Corollary 16).
  - The particle number symmetry helps to further reduce to the invariant space  $\mathcal{H}_2^{\text{paired}}$  (Lemma 19) when  $t = 2$ .
  - The  $(S_\tau^b)^{\otimes n}$ -symmetry helps to reduce to the invariant space  $\mathcal{H}_t^\tau$  (Corollary 23).
- In Supplementary Note 9, we prove that the cost function is unbiased, i.e., the first moment is zero. We also illustrate how to calculate the second moment by an example.
- In Supplementary Notes 10 to 12, we prove our main result in Theorem 5, by calculating  $|\Psi_{2,\infty}^{\mathbf{R}}\rangle$ , and taking the inner product between  $|\Psi_{2,\infty}^{\mathbf{R}}\rangle$  and  $|H_{\text{el}}\rangle^{\otimes 2}$  which evaluates to  $\mathbb{E}[C^2]$ .
  - The proof of case 1 and part of case 2 is constructive: we give an explicit vector  $|\Psi^*\rangle$ , and prove  $|\Psi_{t,\infty}^{\mathbf{R}}\rangle = |\Psi^*\rangle$  by showing that  $|\Psi^*\rangle \in M$  and  $|\Psi^*\rangle - |\psi_0\rangle^{\otimes 4} \in M^\perp$ . In this proof, we use the spanning set of the orthogonal complement  $M$  inside  $\mathcal{H}_2^{\text{paired}} - (M \cap \mathcal{H}_2^{\text{paired}})^\perp \cap \mathcal{H}_2^{\text{paired}}$ .
  - We prove the rest of the theorem by showing that  $\dim(M \cap \mathcal{H}_2^{\text{paired}} \cap \bigcap_\tau \mathcal{H}_2^\tau) = 1$ . In such a case,  $|\Psi_{t,\infty}^{\mathbf{R}}\rangle$  is obvious.



**Supplementary Figure 3** Illustration of how we calculate the  $t^{\text{th}}$  moment of the cost function. (a) Tensor network representation of the  $t^{\text{th}}$  moment. Here the square bracket represents taking the  $t^{\text{th}}$  moment. (b) Use the independence of parameters to contract the tensor network into a circuit-like one. (c) The  $t^{\text{th}}$  moment of each excitation rotation is an orthogonal projection. In the infinite depth limit, these projections contract into an orthogonal projection onto the intersection space  $M_t$ . (d) The  $t^{\text{th}}$  moment in the infinite depth limit can be recovered as the inner product between vector  $O_t$  and moment vector  $|\Psi_{t,\infty}\rangle$  (projected  $\rho_t$ ).

## Supplementary Note 6: Proof of Lemma 4

In this section, we prove the equivalence between the variances of the cost and gradients for alternated (qubit) dUCC ansätze (Lemma 4). In fact, we prove a more generalized version in Lemma 6 for any bounded frequency periodic function (defined below). Intuitively, such a function does not have rapid oscillation.

**Definition 5** (Bounded frequency periodic function). *A function  $f : \mathbb{R}^L \rightarrow \mathbb{R}$  is called bounded frequency periodic if it is periodic with the following Fourier expansion*

$$f(\boldsymbol{\theta}) = \sum_{\mathbf{n} \in \mathbb{Z}^L} c_{\mathbf{n}} \exp(i\mathbf{n} \cdot \boldsymbol{\theta}), \quad \text{where } c_{\mathbf{n}} \in \mathbb{C}. \quad (39)$$

Moreover, there exists a constant  $B > 0$  independent of  $L$ , s.t.

$$c_{\mathbf{n}} = 0 \quad \text{if } \|\mathbf{n}\|_{\infty} > B. \quad (40)$$

Notice that we implicitly assumed the bounded frequency periodic function to have a period of  $2\pi$ , but it can be generalized to any periodic function by rescaling. The following proof is similar to Lemma 1 of [41]. We include the proof for completeness.

**Lemma 6** (Relationship between variances of cost and gradients, generalized). *For bounded frequency periodic function  $f : \mathbb{R}^L \rightarrow \mathbb{R}$  where the frequencies are bounded by  $B$  as in Supplementary Equation (40),*

$$L^{-1} \cdot \text{Var}_{\boldsymbol{\theta}}(f(\boldsymbol{\theta})) \leq \max_{1 \leq j \leq L} \text{Var}_{\boldsymbol{\theta}}(\partial_{\theta_j} f(\boldsymbol{\theta})) \leq B^2 \cdot \text{Var}_{\boldsymbol{\theta}}(f(\boldsymbol{\theta})). \quad (41)$$

*Proof.* Expand  $f$  in Fourier basis as in Supplementary Equation (39). Since  $f$  is real-valued,  $c_{\mathbf{n}} = c_{-\mathbf{n}}^*$  for any  $\mathbf{n} \in \mathbb{Z}^L$ . Since  $\mathbb{E}_{\boldsymbol{\theta} \in \mathbb{R}}[e^{im\boldsymbol{\theta}}] = \delta(m)$  for any integer  $m$ , we have

$$\text{Var}(f) = \mathbb{E}[f^2] - \mathbb{E}[f]^2 = \sum_{\mathbf{n}} |c_{\mathbf{n}}|^2 - |c_{\mathbf{0}}|^2 = \sum_{\mathbf{n} \neq \mathbf{0}} |c_{\mathbf{n}}|^2, \quad (42)$$

$$\text{Var}(\partial_{\theta_j} f) = \mathbb{E}[(\partial_{\theta_j} f)^2] - \mathbb{E}[\partial_{\theta_j} f]^2 = \sum_{\mathbf{n}} |c_{\mathbf{n}}|^2 n_j^2 - 0 = \sum_{\mathbf{n}} |c_{\mathbf{n}}|^2 n_j^2. \quad (43)$$

By the fact that  $|n_j| \leq B$ ,

$$\text{Var}(f) \leq \sum_{\mathbf{n}} |c_{\mathbf{n}}|^2 \|\mathbf{n}\|_2^2 = \sum_j \text{Var}(\partial_{\theta_j} f) \leq L \max_j (\partial_{\theta_j} f) \leq LB^2 \cdot \text{Var}(f). \quad (44)$$

□

The following two lemmas show that the cost function of alternated (qubit) dUCC ansätze is bounded frequency periodic, completing the proof of Lemma 4.

**Lemma 7** (Periodicity of (qubit) excitation rotations). *Let  $R(\theta)$  be a (qubit) excitation rotation (Definition 4).  $R(\theta)$  is periodic with a period of  $2\pi$ . Moreover, there exists constant matrices  $M_R^+, M_R^-, M_R^0$ , such that*

$$R(\theta) = e^{i\theta} M_R^+ + e^{-i\theta} M_R^- + M_R^0. \quad (45)$$

*Proof.* Recall  $R(\theta) = \exp(\theta(\hat{\tau} - \hat{\tau}^\dagger))$ , where  $\hat{\tau} \in \{\hat{a}_p^\dagger \hat{a}_q, \hat{a}_p^\dagger \hat{a}_q^\dagger \hat{a}_r \hat{a}_s, \dots\} \cup \{Q_p^\dagger Q_q, Q_p^\dagger Q_q^\dagger Q_r Q_s, \dots\}$ . Notice that  $\hat{\tau} - \hat{\tau}^\dagger$  is anti-Hermitian. It suffices to show that the eigenvalues of  $\hat{\tau} - \hat{\tau}^\dagger$  are  $0, \pm i$ . In fact,

$$\begin{aligned} (\hat{\tau} - \hat{\tau}^\dagger)^2 &= (Q_p^\dagger Q_q^\dagger \dots Q_r Q_s \dots - Q_r^\dagger Q_s^\dagger \dots Q_p Q_q \dots)^2 \\ &= -(N_p N_q \dots + N_r N_s \dots - N_p N_q \dots N_r N_s \dots). \end{aligned} \quad (46)$$

Hence,  $(\hat{\tau} - \hat{\tau}^\dagger)^2$  is a diagonal matrix, and each element on the diagonal is either 0 or -1. □

**Lemma 8.** *Let  $U_k^{\mathbf{R}}(\boldsymbol{\theta})$  be an alternated (qubit) dUCC ansätze defined in Supplementary Equation (36). The cost function  $C(\boldsymbol{\theta}; U_k^{\mathbf{R}})$  defined in Supplementary Equation (33) is bounded frequency periodic.*

*Proof.* By Lemma 7,

$$C(\boldsymbol{\theta}; U_k^{\mathbf{R}}) = \text{tr}(OU_k^{\mathbf{R}}(\boldsymbol{\theta})|\psi_0\rangle\langle\psi_0|U_k^{\mathbf{R}}(\boldsymbol{\theta})^\dagger) \quad (47)$$

$$= \text{tr}\left(O\left(\prod_{ij} R_j(\theta_i^{(j)})\right)|\psi_0\rangle\langle\psi_0|\left(\prod_{ij} R_j(\theta_i^{(j)})\right)^\dagger\right) \quad (48)$$

$$= \sum_{\mathbf{c}, \mathbf{c}' \in \{0, \pm 1\}^m} e^{i(\mathbf{c} - \mathbf{c}') \cdot \boldsymbol{\theta}} \text{tr}\left(O\left(\prod_{ij} M_{R_j}^{c_{ij}}\right)|\psi_0\rangle\langle\psi_0|\left(\prod_{ij} M_{R_j}^{c'_{ij}}\right)^\dagger\right). \quad (49)$$

Since  $\|\mathbf{c} - \mathbf{c}'\|_\infty \leq 2$ ,  $C(\boldsymbol{\theta}; U_k^{\mathbf{R}})$  is bounded frequency periodic.  $\square$

To conclude this section, we make two remarks. First, the lower bound in Lemma 6 can be saturated, for example by the function  $f(\boldsymbol{\theta}) = \sum_j \cos^2 \frac{\theta_j}{2}$ . Notice that  $f(\boldsymbol{\theta})$  emerges as the global cost function  $C(\boldsymbol{\theta}) = \text{tr}(OU(\boldsymbol{\theta})|\mathbf{0}\rangle\langle\mathbf{0}|U^\dagger(\boldsymbol{\theta}))$ , where  $U(\boldsymbol{\theta}) = \prod_{j=1}^n \exp(i\theta_j X_j)$  and  $O = \sum_{j=1}^n |0\rangle\langle 0|_j$ . Second, we only utilize the periodicity of alternated (qubit) dUCC ansätze (Lemma 7) when proving the equivalence between cost variance and gradient variance. Such an argument could possibly be strengthened using other properties such as non-locality.

## Supplementary Note 7: Moments of cost function

In the last section, we showed that for alternated dUCC ansätze, the variance of the gradient can be bounded by the variance of the cost itself in both directions (Lemmas 6 and 8). From now on, we turn to calculating the variance of the cost function. To start with, we employ the common trick in the study of BP [52–55] to express the  $t^{\text{th}}$  moment of the cost function as a circuit-like tensor network. The motivation is to separate the initial state, gates, and observables apart, and to resolve the non-linearity in high-order moment.

### 7.1 Circuit-like tensor network representation of $\mathbb{E}[C^t]$ and moment vector

In this section, we express the  $t^{\text{th}}$  moment of the cost function as a circuit-like tensor network. All quantum gates related to the same parameter are contracted into one “elevated” tensor which has a larger dimension, namely, the  $t^{\text{th}}$  moment superoperator. The (matrix form of)  $t^{\text{th}}$  moment superoperator of an operator  $T(\theta)$  with a real parameter  $\theta$  is defined as

$$\mathbb{E}_{\theta \in \mathbb{R}} [T(\theta)^{\otimes t, t}] = \int_{\mathbb{R}} T(\theta)^{\otimes t} \otimes T^*(\theta)^{\otimes t} d\theta. \quad (50)$$

To simplify the notations, we will use the shorthand  $\mathbb{E}[T^{\otimes t, t}] := \mathbb{E}_{\theta \in \mathbb{R}} [T(\theta)^{\otimes t, t}]$  whenever the context is clear. Moreover, we introduce dedicated notation  $\bar{T}, \tilde{T}$  for the 1<sup>st</sup> and 2<sup>nd</sup> moments of  $T(\theta)$ , as they will be used frequently:

$$\bar{T} := \mathbb{E}[T^{\otimes 1, 1}], \quad \tilde{T} := \mathbb{E}[T^{\otimes 2, 2}]. \quad (51)$$

The vectorization of an operator  $U \in \mathbb{C}^{2^m \times 2^m}$  is defined as  $|U\rangle := (U \otimes \mathbb{1}_{2^m}) \sum_{i \in \mathbb{F}_2^m} |i, i\rangle$ .

Using the fact that  $\mathbb{E}[XY] = \mathbb{E}[X]\mathbb{E}[Y]$  for independent random variables  $X, Y$ , we can express the  $t^{\text{th}}$  moment of the cost function of alternated (qubit) dUCC ansätze as the product of the  $t^{\text{th}}$  moment of excitation operators.

**Lemma 9** ( $t^{\text{th}}$  moment of cost function). *Let  $U_k^{\mathbf{R}}(\boldsymbol{\theta})$  be an alternated (qubit) dUCC ansätze defined in Definition 4,  $C(\boldsymbol{\theta}; U_k^{\mathbf{R}}, O)$  be the cost function defined in Supplementary Equation (33) where  $O$  is any observable. For any  $t \in \mathbb{N}_+$  and observables  $O_1, \dots, O_t \in \mathbb{C}^{2^m \times 2^m}$ ,*

$$\mathbb{E}\left[\prod_{l=1}^t C(\boldsymbol{\theta}; U_k^{\mathbf{R}}, O_l)\right] = \left(\bigotimes_{l=1}^t \langle O_l | \right) \left(\prod_{j=1}^{|\mathbf{R}|} \mathbb{E}[R_j^{\otimes t, t}]\right)^k |\psi_0\rangle^{\otimes 2t}. \quad (52)$$

In particular, the  $t^{\text{th}}$  moment of the cost function  $C(\boldsymbol{\theta}; U_k^{\mathbf{R}}, O)$  for some observable  $O$  is

$$\mathbb{E} [C^t(\boldsymbol{\theta}; U_k^{\mathbf{R}}, O)] = \langle O |^{\otimes t} \left( \prod_{j=1}^{|\mathbf{R}|} \mathbb{E} [R_j^{\otimes t, t}] \right)^k | \psi_0 \rangle^{\otimes 2t}. \quad (53)$$

*Proof.* Observe that  $C(\boldsymbol{\theta}; U, O) = \text{tr}(OU(\boldsymbol{\theta})|\psi_0\rangle\langle\psi_0|U(\boldsymbol{\theta})^\dagger) = \langle O|U(\boldsymbol{\theta})^{\otimes 1,1}|\psi_0\rangle^{\otimes 2}$ , and use the independence of parameters.  $\square$

We make two remarks regarding Lemma 9.

1. Supplementary Equation (52) is useful in calculating covariance, or other quantities alike.
2. The expectations in Lemma 9 are taken over random parameters  $\boldsymbol{\theta}$  sampled from  $\mathbb{R}^{k|\mathbf{R}|}$ , or equivalently from  $[0, 2\pi)^{k|\mathbf{R}|}$  by the periodicity of (qubit) excitation rotations (Lemma 7).

Lemma 9 indicates that the  $t^{\text{th}}$  moment of cost function for different observables are essentially captured by a vector, which is the product of  $t^{\text{th}}$  moment superoperators of excitation rotations and initial state. In other words, one can in principle calculate  $\mathbb{E}[C(\boldsymbol{\theta}; O)^t]$  for any observable  $O$  if such vector is known — just take an inner product of the vectorization of  $O$  and the vector. Hence, we refer to such a vector as a moment vector, as defined below.

**Definition 6** ( $(\mathbf{R}, t, k)$ -moment vector). *Let  $\mathbf{R}$  be a sequence of excitation rotations defined in Definition 4, and  $|\psi_0\rangle$  be the Hartree-Fock state defined in Supplementary Equation (34). For  $t, k \in \mathbb{N}_+$ , the  $(\mathbf{R}, t, k)$ -moment vector is defined to be*

$$|\Psi_{t,k}^{\mathbf{R}}\rangle = \left( \prod_{j=1}^{|\mathbf{R}|} \mathbb{E} [T_j^{\otimes t, t}] \right)^k |\psi_0\rangle^{\otimes 2t}. \quad (54)$$

In particular, the moment vector of  $k$ -UCCSD,  $k$ -BRA etc. is denoted by  $|\Psi_{t,k}^{\text{UCCSD}}\rangle, |\Psi_{t,k}^{\text{BRA}}\rangle$  etc.

And the moment vector of  $k$ -qubit-UCCSD etc. is denoted by  $|\Psi_{t,k}^{\text{qUCCSD}}\rangle$  etc.

Supplementary Equation (53) can be rewritten as  $\mathbb{E}[C^t] = \langle O |^{\otimes t} |\Psi_{t,k}^{\mathbf{R}}\rangle$ . As an example,  $\langle \mathbb{1}^{\otimes t} | \Psi_{t,k}^{\mathbf{R}} \rangle = \langle \mathbb{1} |^{\otimes t} |\Psi_{t,k}^{\mathbf{R}}\rangle = \mathbb{E}[C^t(\boldsymbol{\theta}; U_k^{\mathbf{R}}, \mathbb{1})] = 1$ .

## 7.2 Site decomposition: a straightforward way to describe the elevated tensors

So far, we have addressed the non-linearity in calculating the  $t^{\text{th}}$  moment of cost by considering  $2t$  replicas of the original system. Moreover,  $\mathbb{E}[C^t]$  turns out to be the inner product of the vectorization of  $O$  and the  $(\mathbf{R}, t, k)$ -moment vector  $|\Psi_{t,k}^{\mathbf{R}}\rangle$ . Before delving into the calculation of  $|\Psi_{t,k}^{\mathbf{R}}\rangle$ , it is worthwhile to reorder the qubits in the enlarged Hilbert space so that the elevated tensor can be described naturally. Such reordering, which we refer to as site decomposition, is formally defined below.

**Definition 7** (Site decomposition). *The isomorphism between Hilbert spaces  $\mathcal{H}^{\otimes 2t} \cong \bigotimes_{i=1}^n \mathcal{H}_i$  with  $\mathcal{H} = \mathbb{C}^{2^n}$ ,  $\mathcal{H}_i = \mathbb{C}^{2^{2t}}$ , defined by*

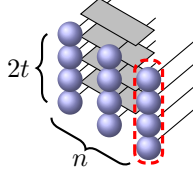
$$\bigotimes_{j=1}^{2t} |b_1^{(j)} \dots b_n^{(j)}\rangle \rightarrow \bigotimes_{i=1}^n |b_i^{(1)} \dots b_i^{(2t)}\rangle, \quad (55)$$

is called a site decomposition. Each  $\mathcal{H}_i = \mathbb{C}^{2^{2t}}$  is called a site of length  $2t$ . Moreover, we will use  $|\Psi\rangle$  to denote any state in the enlarged space  $\mathbb{C}^{2^{2tn}}$ , while  $|\Phi\rangle$  is reserved for computational basis states.  $\Phi$  is interpreted as a bit string in  $\mathbb{F}_2^{2tn}$ . For  $i \in [n]$ ,  $j \in [2t]$ ,  $\Phi_i$  denotes the bit string of the  $i^{\text{th}}$  site, and  $\Phi_{ij}$  denotes the  $j^{\text{th}}$  bit of  $i^{\text{th}}$  site.

This procedure described in Definition 7 can be understood as reordering and splitting the  $2tn$  qubits into  $n$  equally-sized subsystems, with each subsystem forming a site. As an example, the  $t^{\text{th}}$  moment of a qubit single excitation rotation acting on qubits 1 and 2 can be viewed as a tensor acting on sites 1 and 2, as illustrated in Supplementary Figure 4. Without site decomposition, it is



less straightforward to describe such a tensor. The reader should be aware that we will implicitly



**Supplementary Figure 4** Illustration of the  $t^{\text{th}}$  moment of a double qubit gate acting on qubits 1 and 2, which can be viewed as a larger tensor acting on sites 1 and 2. Here  $t = 2$  and  $n = 3$ . Each ball represents a qubit, the gray boxes together represent the  $t^{\text{th}}$  moment of the double qubit gate, and the balls in the red dashed cycle form the  $3^{\text{rd}}$  site of length  $2t$ .

assume site decomposition in the subsequent text.

The following proposition reexpresses the initial state and vectorization of the observable  $\hat{a}_p^\dagger \hat{a}_q + h.c.$  and  $\hat{a}_p^\dagger \hat{a}_q^\dagger \hat{a}_r \hat{a}_s + h.c.$  under site decomposition.

**Proposition 10** (Initial state and observable under site decomposition). *Let  $t \in \mathbb{N}_+$ , and  $|\psi_0\rangle$  as defined in Supplementary Equation (34). Under site decomposition,*

$$|\psi_0\rangle^{\otimes 2t} = \underbrace{|1\dots 1\rangle}_{2t}^{\otimes n_e} \underbrace{|0\dots 0\rangle}_{2t}^{\otimes (n-n_e)}. \quad (56)$$

After Jordan-Wigner transformation, when  $O = \hat{a}_p^\dagger \hat{a}_q + h.c.$  ( $p > q$ ),

$$|O\rangle^{\otimes t} = \left( |01\rangle_q |10\rangle_p + |10\rangle_q |01\rangle_p \right)^{\otimes t} \otimes \bigotimes_{a \in [1, q \cup (p, n)]} (|00\rangle_a + |11\rangle_a)^{\otimes t} \otimes \bigotimes_{b \in (p, q)} (|00\rangle_b - |11\rangle_b)^{\otimes t}. \quad (57)$$

And when  $O = \hat{a}_p^\dagger \hat{a}_q^\dagger \hat{a}_r \hat{a}_s + h.c.$  ( $p > q > r > s$ ),

$$|O\rangle^{\otimes t} = \left( |01\rangle_s |01\rangle_r |10\rangle_q |10\rangle_p + |10\rangle_s |10\rangle_r |01\rangle_q |01\rangle_p \right)^{\otimes t} \otimes \bigotimes_{a \in [1, s] \cup (r, q) \cup (p, n)} (|00\rangle_a + |11\rangle_a)^{\otimes t} \otimes \bigotimes_{b \in (s, r) \cup (q, p)} (|00\rangle_b - |11\rangle_b)^{\otimes t}. \quad (58)$$

*Proof.* Notice that after Jordan-Wigner transformation  $\hat{a}_p = Q_p \prod_{a < p} Z_a$ , and the vectorization of  $Q, I, Z$  is  $|Q\rangle = |01\rangle, |I\rangle = |00\rangle + |11\rangle, |Z\rangle = |00\rangle - |11\rangle$ , respectively.  $\square$

The following operators related to sites will be useful.

**Definition 8** ( $S_\pi, S_{pq}, S_\tau^b, F_V^W$ ). *Let  $\pi \in \mathfrak{S}_n, \tau \in \mathfrak{S}_{2t}, V \subseteq [n],$  and  $W \subseteq [2t]$ .*

1. Define  $S_\pi \in \mathbb{C}^{2tn \times 2tn}$  as the permutation of sites by  $\pi$ :

$$S_\pi |\Phi_1 \Phi_2 \dots \Phi_n\rangle = |\Phi_{\pi^{-1}(1)} \Phi_{\pi^{-1}(2)} \dots \Phi_{\pi^{-1}(n)}\rangle, \quad \forall \Phi_i \in \mathbb{F}_2^{2t}. \quad (59)$$

In particular, denote  $S_{pq} := S_{(pq)}$  the swap of site  $p$  and  $q$ .

2. Define  $S_\tau^b \in \mathbb{C}^{2t \times 2t}$  as the permutation of qubits in one site by  $\tau$ :

$$S_\tau^b |b_1 b_2 \dots b_{2t}\rangle = |b_{\tau^{-1}(1)} b_{\tau^{-1}(2)} \dots b_{\tau^{-1}(2t)}\rangle, \quad \forall b_i \in \mathbb{F}_2. \quad (60)$$

3. Define  $F_V^W \in \mathbb{C}^{2tn \times 2tn}$  as the flip of the  $j^{\text{th}}$  bit in the  $i^{\text{th}}$  site for all  $i \in V, j \in W$ :

$$F_V^W = \prod_{i=1}^n \bigotimes_{j=1}^{2t} X_i^{[i \in V \wedge j \in W]}. \quad (61)$$

In particular, denote  $F_{pq\dots}^{ab\dots} = F_{\{p, q, \dots\}}^{\{a, b, \dots\}}$ .

### 7.3 Moments of excitation rotations

After introducing site decomposition, we now return to the calculation of moment vector  $|\Psi_{t,k}^{\mathbf{R}}\rangle$ .

Recall the definition of  $|\Psi_{t,k}^{\mathbf{R}}\rangle$  in Definition 6. Since the initial state is fixed to be  $|\psi_0\rangle$ , it remains to determine each  $\mathbb{E}[R_j^{\otimes t,t}]$ , where  $R_j$  is some (qubit) excitation rotation. The following lemma gives some basic properties of  $\mathbb{E}[R_j^{\otimes t,t}]$ . More properties will be covered in later sections.

**Lemma 11** (Basic properties of  $\mathbb{E}[R^{\otimes t,t}]$ ). *Let  $R(\theta)$  be a (qubit) excitation rotation (Definition 4), and  $t \in \mathbb{N}_+$ .*

1.  $\mathbb{E}[R^{\otimes t,t}] = \mathbb{E}[R^{\otimes 2t}]$ .
2.  $\mathbb{E}[R^{\otimes t,t}]$  is an orthogonal projection.
3. Suppose  $R(\theta)$  is a qubit excitation rotation, i.e.,  $R(\theta) = \exp(\theta(\hat{\tau} - \hat{\tau}^\dagger))$  for some  $\hat{\tau} = Q_{p_1}^\dagger \dots Q_{p_r}^\dagger Q_{p_{r+1}} \dots Q_{p_{2r}}$ . Define  $\Phi_{p_1:p_{2r},j} := \Phi_{p_1,j} \dots \Phi_{p_{2r},j}$ ,  $\mathbf{b}_0 := 0^r 1^r$ ,  $\mathbf{b}_1 := 1^r 0^r$ , and

$$n_{ab} := \#\{j \in [2t] | \Phi_{p_1:p_{2r},j} = \mathbf{b}_a, \Phi'_{p_1:p_{2r},j} = \mathbf{b}_b\}, \quad \forall a, b \in \mathbb{F}_2. \quad (62)$$

Then

$$\langle \Phi | \mathbb{E}[R^{\otimes t,t}] | \Phi' \rangle = \begin{cases} 0, & (*) \\ (-1)^{n_{01}} \frac{(n_{00}+n_{11}-1)!!(n_{01}+n_{10}-1)!!}{(n_{00}+n_{11}+n_{01}+n_{10})!!}, & \text{otherwise.} \end{cases} \quad (63)$$

Here we use the convention that  $(-1)!! := 1$ , and  $(*)$  is the union of the following cases:

- $\Phi_i \neq \Phi'_i$  for some  $i \in [n] \setminus \{p_s | s \in [2r]\}$ .
  - $\Phi_{p_1:p_{2r},j} \neq \Phi'_{p_1:p_{2r},j}$  and  $\{\Phi_{p_1:p_{2r},j}, \Phi'_{p_1:p_{2r},j}\} \not\subseteq \{\mathbf{b}_0, \mathbf{b}_1\}$  for some  $j \in [2t]$ .
  - One of  $n_{00} + n_{11}$  and  $n_{01} + n_{10}$  is odd.
4. Suppose  $R(\theta)$  is an excitation rotation, i.e.,  $R(\theta) = \exp(\theta(\hat{\tau} - \hat{\tau}^\dagger))$  for some  $\hat{\tau} = \hat{a}_{p_1}^\dagger \dots \hat{a}_{p_r}^\dagger \hat{a}_{p_{r+1}} \dots \hat{a}_{p_{2r}}$ . Assume  $\hat{\tau} = \pm Q_{p_1}^\dagger \dots Q_{p_r}^\dagger Q_{p_{r+1}} \dots Q_{p_{2r}} \prod_{i \in V} Z_i$  for index set  $V \subset [n] \setminus \{p_s | s \in [2r]\}$ . Define  $\hat{\tau}' := Q_{p_1}^\dagger \dots Q_{p_r}^\dagger Q_{p_{r+1}} \dots Q_{p_{2r}}$ ,  $R'(\theta) := \exp(\theta(\hat{\tau}' - (\hat{\tau}')^\dagger))$ ,  $\mathbf{z} := \bigotimes_{a \in V} \Phi_a$  and  $X_i^{\mathbf{z}} := \bigotimes_{j=1}^{2t} X_i^{z_j}$ . The following conversion rule holds:

$$\mathbb{E}[R^{\otimes t,t}] |\Phi\rangle = \left( \prod_{i=1}^n X_i^{\mathbf{z}} \right) \mathbb{E}[(R')^{\otimes t,t}] \left( \prod_{i=1}^n X_i^{\mathbf{z}} \right) |\Phi\rangle. \quad (64)$$

*Proof.* Item 1. Notice that  $R(\theta)$  is real.

Item 2. Since  $R(\theta) = \exp(\theta(\hat{\tau} - \hat{\tau}^\dagger))$  for some constant operator  $\hat{\tau}$ ,

$$\mathbb{E}_{\theta_1} [R(\theta_1)^{\otimes t,t}] \mathbb{E}_{\theta_2} [R(\theta_2)^{\otimes t,t}] = \mathbb{E}_{\theta_1} [\mathbb{E}_{\theta_2} [R(\theta_1 + \theta_2)^{\otimes t,t}]]. \quad (65)$$

By Lemma 7,  $R(\theta)$  is periodic. Thus,

$$\mathbb{E}_{\theta_1} [\mathbb{E}_{\theta_2} [R(\theta_1 + \theta_2)^{\otimes t,t}]] = \mathbb{E}_{\theta_1} [\mathbb{E}_{\theta_2} [R(\theta_2)^{\otimes t,t}]] = \mathbb{E}_{\theta_2} [R(\theta_2)^{\otimes t,t}]. \quad (66)$$

Combining Supplementary Equation (65) and Supplementary Equation (66), we have  $\mathbb{E}[R^{\otimes t,t}]^2 = \mathbb{E}[R^{\otimes t,t}]$ .

Moreover,

$$\mathbb{E}[R(\theta)^{\otimes t,t}]^\dagger = \mathbb{E}[R(-\theta)^{\otimes t,t}] = \mathbb{E}[R(\theta)^{\otimes t,t}]. \quad (67)$$

Hence,  $\mathbb{E}[R^{\otimes t,t}]$  is an orthogonal projection.

Item 3. By taking the Taylor expansion of matrix exponential  $e^M = \sum_{m \geq 0} \frac{M^m}{m!}$ , it is easy to verify that

$$R(\theta) = \exp\left(\theta(|\mathbf{b}_1\rangle\langle\mathbf{b}_1| - |\mathbf{b}_0\rangle\langle\mathbf{b}_0|)_{p_1, \dots, p_{2r}}\right) \quad (68)$$

$$= \mathbb{1}_{2^n} + (\sin \theta (|\mathbf{b}_1\rangle\langle\mathbf{b}_0| - |\mathbf{b}_0\rangle\langle\mathbf{b}_1|) + (\cos \theta - 1) (|\mathbf{b}_0\rangle\langle\mathbf{b}_0| + |\mathbf{b}_1\rangle\langle\mathbf{b}_1|))_{p_1, \dots, p_{2r}}. \quad (69)$$

Consequently,  $\langle \Phi | \mathbb{E} [R^{\otimes t, t}] | \Phi' \rangle$  can only be non-zero if none of the first 2 cases of (\*) happens. If so,

$$\begin{aligned} & \langle \Phi | \mathbb{E} [R(\theta)^{\otimes t, t}] | \Phi' \rangle \\ &= \mathbb{E} \left[ (-1)^{n_{01}} \cos(\theta)^{n_{00}+n_{11}} \sin(\theta)^{n_{01}+n_{10}} \right] \\ &= \begin{cases} 0, & \text{if } n_{00} + n_{11} \text{ or } n_{01} + n_{10} \text{ is odd,} \\ (-1)^{n_{01}} \frac{(n_{00}+n_{11}-1)!!(n_{01}+n_{10}-1)!!}{(n_{00}+n_{11}+n_{01}+n_{10})!!}, & \text{otherwise.} \end{cases} \end{aligned} \quad (70)$$

Item 4. Since  $\hat{\tau}' - (\hat{\tau}')^\dagger$  anti-commutes with  $\prod_{i=1}^n X_i$ ,

$$\begin{aligned} \mathbb{E} [R(\theta)^{\otimes 2t}] | \Phi \rangle &= \mathbb{E} \left[ \bigotimes_{j=1}^{2t} R'((-1)^{z_j} \theta) \right] | \Phi \rangle \\ &= \left( \prod_{i=1}^n X_i^z \right) \mathbb{E} [R'(\theta)^{\otimes 2t}] \left( \prod_{i=1}^n X_i^z \right) | \Phi \rangle. \end{aligned} \quad (71)$$

□

## 7.4 Convergence of alternating projections

One of the most important findings in Lemma 11 is that the  $t^{\text{th}}$  moment superoperator of (qubit) excitation rotations  $\mathbb{E} [R^{\otimes t, t}]$  are orthogonal projections. This is not unusual in BP studies. For example, in [26, 50, 54] the circuit (or block of gates) is assumed to be Haar random up to  $2^{\text{nd}}$  moment. Under such an assumption one verifies that the  $2^{\text{nd}}$  moment superoperator of the circuit (or block of gates) is an orthogonal projector of rank 2. However, the projectors we encountered are significantly more complex compared to the Haar random case. In fact, the  $2^{\text{nd}}$  moment of qubit single excitation rotations is a projector of rank 70 in the subsystem it acts on, let alone normal excitation rotations which are highly non-local. Hence, we do not expect it to be easy to figure out or even bound  $|\Psi_{t,k}^{\mathbf{R}}\rangle$  for any finite  $k$ . Rather, we turn to study the infinite- $k$  case, which turns out to be tractable. The phenomenon that the infinite case is easier than the finite one is ubiquitous, for example, in the theoretical analysis of classical neural networks [56]. The following lemma will play a central role.

**Lemma 12** (Convergence of alternating projections [46]). *Let  $\mathcal{H}$  be a Hilbert space and denote  $P_M$  to be the orthogonal projection onto a subspace  $M \subseteq \mathcal{H}$ . Given  $N$  subspace  $M_1, \dots, M_N$  with intersection  $M = M_1 \cap \dots \cap M_N$ ,*

$$\lim_{k \rightarrow \infty} \|(P_{M_N} \cdots P_{M_1})^k(x) - P_M(x)\| = 0, \quad \forall x \in \mathcal{H}. \quad (72)$$

Remark that we are working in a finite Hilbert space, and in such a case uniform convergence  $\lim_{k \rightarrow \infty} (P_{M_N} \cdots P_{M_1})^k = P_M$  can be shown.

**Corollary 13.** *Let  $\mathbf{R}$  be a sequence of excitation rotations defined in Definition 4, and  $t \in \mathbb{N}_+$ . Denote the projection  $\mathbb{E} [R_j^{\otimes t, t}]$  by  $P_{M_j}$ , where  $M_j$  is the subspace that  $P_{M_j}$  projects onto. Define  $M := \bigcap_j M_j$ . We have*

$$\lim_{k \rightarrow \infty} \left( \prod_{j=1}^{|\mathbf{R}|} \mathbb{E} [R_j^{\otimes t, t}] \right)^k = P_M \quad \text{and} \quad |\Psi_{t,\infty}^{\mathbf{R}}\rangle = P_M |\psi_0\rangle^{\otimes 2t}. \quad (73)$$

We make two remarks regarding Corollary 13.

1. The reason why the infinite case is easier is that, by Corollary 13, it suffices to figure out the intersection  $M = \bigcap_j M_j$ , rather than tracking how  $|\psi_0\rangle^{\otimes 2t}$  evolves.
2. In the subsequent text, regardless of the form of  $\mathbf{R}$  and the order of moment  $t$ , we will denote the subspace that  $\mathbb{E} [R_j^{\otimes t, t}]$  projects onto by  $M_j$ , and the intersection space  $\bigcap_j M_j$  by  $M$ , as in Corollary 13. The reader should be cautious about which  $\mathbf{R}$  and  $t$  are used in context to define  $M$  and  $M_j$ .

While we may be able to characterize (albeit a bit complex) each  $M_j$ , since the matrix form of  $\mathbb{E}[R_j^{\otimes t, t}]$  has been explicitly written out in Lemma 11, it is not obvious how to calculate their intersection at first sight. On the other hand, it is straightforward to determine the spanning set of the orthogonal complement  $M^\perp$  if one has determined the spanning set of each  $M_j^\perp$  — just take the union of these spanning sets. The reason is explained in Lemma 14 (Item 2). Lemma 14 also includes other properties of the orthogonal complement which will be used in later sections. The proof of Lemma 14 is elementary and is omitted.

**Lemma 14.** *Let  $V_1, V_2, \dots, V_m$ , and  $V'$  be subspaces of finite dimensional vector space  $V$ .*

1.  $(V_1^\perp)^\perp = V_1$ .
  2.  $(V_1 \cap V_2 \cap \dots \cap V_m)^\perp = V_1^\perp + V_2^\perp + \dots + V_m^\perp$ .
  3.  $((V_1 \cap V')^\perp \cap V')^\perp \cap V' = V_1 \cap V'$ .
  4.  $((V_1 \cap V_2 \cap \dots \cap V_m) \cap V')^\perp \cap V' = (V_1 \cap V')^\perp \cap V' + (V_2 \cap V')^\perp \cap V' + \dots + (V_m \cap V')^\perp \cap V'$ .
- If, in addition,  $[P_{V'}, P_{V_i}] = 0$  for all  $i = 1, 2, \dots, m$ , then
5.  $(V_1 \cap V')^\perp \cap V' = V_1^\perp \cap V'$ .
  6.  $((V_1 \cap V_2 \cap \dots \cap V_m) \cap V')^\perp \cap V' = (V_1 \cap V_2 \cap \dots \cap V_m)^\perp \cap V'$

## Supplementary Note 8: Reduce the space by symmetries

In the last section, we have hinted at how we will calculate the  $t^{\text{th}}$  moment of cost function at  $k = \infty$  for alternated dUCC ansätze:

1. we find out the spanning set of each  $M_j^\perp$  (recall that  $P_{M_j} := \mathbb{E}[R_j^{\otimes t, t}]$ ),
2. take the union to get the spanning set of  $M^\perp$  (recall that  $M := \bigcap_j M_j$ ),
3. somehow calculate  $P_M |\psi_0\rangle^{\otimes 2t}$ , using the spanning set of  $M^\perp$ ,
4. finally, take the inner product between  $|H_{\text{el}}\rangle^{\otimes t}$  and  $|\Psi_{t, \infty}^{\mathbf{R}}\rangle = P_M |\psi_0\rangle^{\otimes 2t}$ , which evaluates to  $\mathbb{E}[C^t]$ .

Steps 2 and 4 have been explained in the last section. This section will be devoted to step 1 and will sketch the idea behind step 3. We do so by restricting ourselves into invariant subspaces using symmetries of  $\mathbb{E}[R_j^{\otimes t, t}]$ . The reduction of space is in sequence. It is worth noting that while these symmetries should apply for any (qubit) excitation rotations and any  $t \in \mathbb{N}_+$ , we primarily focus on the cases of (qubit) single/double excitation rotations and  $t = 1, 2$  since these are enough for proving Theorem 5.

### 8.1 $Z_p^{\otimes 2t}$ -symmetry

The  $Z_p^{\otimes 2t}$ -symmetry of  $\mathbb{E}[R_j^{\otimes t, t}]$  helps to reduce from the whole space  $\mathbb{C}^{2^{2tn}}$  to  $\mathcal{H}_t^{\text{even}}$ , the space spanned by states where each site has an even Hamming weight.

**Definition 9** ( $\mathcal{S}_t^{\text{even}}, \mathcal{H}_t^{\text{even}}$ ). *Define  $\mathcal{S}_t^{\text{even}}, \mathcal{H}_t^{\text{even}} \subset \mathbb{C}^{2^{2tn}}$  as follows:*

$$\mathcal{S}_t^{\text{even}} := \left\{ |b_1 b_2 \dots b_{2t}\rangle \left| \sum_{i=1}^{2t} b_i \equiv 0 \pmod{2}, b_i \in \mathbb{F}_2 \right. \right\}^{\otimes n}, \quad \mathcal{H}_t^{\text{even}} := \text{span } \mathcal{S}_t^{\text{even}}. \quad (74)$$

Let  $R(\theta)$  be a (qubit) excitation rotation, and  $\mathbf{R}$  be a sequence of (qubit) excitation rotations (Definition 4).

**Lemma 15** ( $Z_p^{\otimes 2t}$ -symmetry). *For any  $p \in [n]$ ,  $[\mathbb{E}[R^{\otimes t, t}], Z_p^{\otimes 2t}] = 0$ .*

*Proof.* Notice that  $R(\theta) = \exp(\theta(\hat{\tau} - \hat{\tau}^\dagger))$  for some (qubit) excitation  $\hat{\tau}$ , and  $Z_p$  either commutes or anti-commutes with  $\hat{\tau} - \hat{\tau}^\dagger$  (since  $Z$  commutes with  $I, Z$  and anti-commutes with  $Q, Q^\dagger$ ).

- If  $Z_p$  commutes with  $\hat{\tau} - \hat{\tau}^\dagger$ , then  $Z_p$  commutes with  $R(\theta)$ , and thus  $Z_p^{\otimes 2t}$  commutes with  $\mathbb{E}[R(\theta)^{\otimes 2t}]$ .
- If  $Z_p$  anti-commutes with  $\hat{\tau} - \hat{\tau}^\dagger$ , then  $Z_p^{\otimes 2t} \mathbb{E}[R(\theta)^{\otimes 2t}] Z_p^{\otimes 2t} = \mathbb{E}[R(-\theta)^{\otimes 2t}] = \mathbb{E}[R(\theta)^{\otimes 2t}]$ .  $\square$

**Corollary 16** (Invariance of  $\mathcal{H}_t^{\text{even}}$ ).  *$\mathcal{H}_t^{\text{even}}$  is an invariant subspace of  $\mathbb{E}[R^{\otimes t, t}]$ . Moreover,  $|\Psi_{t, k}^{\mathbf{R}}\rangle, |\Psi_{t, \infty}^{\mathbf{R}}\rangle \in \mathcal{H}_t^{\text{even}}$ .*

*Proof.* Notice that  $\mathcal{H}_t^{\text{even}}$  is the common +1 eigenspace of  $Z_1^{\otimes 2t}, Z_2^{\otimes 2t}, \dots, Z_n^{\otimes 2t}$ . Since  $Z_1^{\otimes 2t}, Z_2^{\otimes 2t}, \dots, Z_n^{\otimes 2t}$  and  $\mathbb{E}[R^{\otimes t, t}]$  commute mutually,  $\mathcal{H}_t^{\text{even}}$  is an invariant subspace of  $\mathbb{E}[R^{\otimes t, t}]$ . By Proposition 10,  $|\psi_0\rangle^{\otimes 2t} \in \mathcal{H}_t^{\text{even}}$ . Hence,  $|\Psi_{t,k}^{\mathbf{R}}\rangle = \left(\prod_j \mathbb{E}[R_j^{\otimes t, t}]\right)^k |\psi_0\rangle^{\otimes 2t} \in \mathcal{H}_t^{\text{even}}$ . Since  $\mathcal{H}_t^{\text{even}}$  is closed,  $|\Psi_{t,\infty}^{\mathbf{R}}\rangle = \lim_{k \rightarrow \infty} |\Psi_{t,k}^{\mathbf{R}}\rangle \in \mathcal{H}_t^{\text{even}}$ .  $\square$

The invariance of  $\mathcal{H}_t^{\text{even}}$  is enough to calculate the first moment of the cost function. The reader can refer to Supplementary Note 9 for more details. To calculate the second moments, however, we still need to find the spanning set of  $M_j^\perp$ , or equivalently, diagonalize  $\tilde{R}_j = \mathbb{E}[R_j^{\otimes 2, 2}]$ . Since  $\mathcal{H}_t^{\text{even}}$  is an invariant subspace that contains  $|\Psi_{t,\infty}^{\mathbf{R}}\rangle$ , we can diagonalize within  $\mathcal{H}_t^{\text{even}}$  to save some work. But before that, we first introduce special notations for sites with an even Hamming weight at  $t = 2$ , so that the notation for states in  $\mathcal{H}_2^{\text{even}}$  can be simpler. Recall that when  $t = 2$ , each site has a length of 4, indicating that the dimension of the Hilbert space for each site is  $2^4$ . Out of the 16 computational basis states of each site, there are 8 with an even Hamming weight, as follows.

**Definition 10** (8 special basis states of site at  $t = 2$ ). *Define 8 product state in  $\mathbb{C}^{2^4}$  as follows:*

$$|I_{ab}\rangle = |a, I(a), b, I(b)\rangle, \quad |X_{ab}\rangle = |a, X(a), b, X(b)\rangle, \quad a, b \in \mathbb{F}_2. \quad (75)$$

*Namely, they are*

$$|I_{00}\rangle = |0000\rangle, \quad |I_{11}\rangle = |1111\rangle, \quad |I_{01}\rangle = |0011\rangle, \quad |I_{10}\rangle = |1100\rangle, \quad (76)$$

$$|X_{00}\rangle = |0101\rangle, \quad |X_{11}\rangle = |1010\rangle, \quad |X_{01}\rangle = |0110\rangle, \quad |X_{10}\rangle = |1001\rangle. \quad (77)$$

Remark that  $\mathcal{S}_2^{\text{even}} = \{|I_{ab}\rangle, |X_{ab}\rangle | a, b \in \mathbb{F}_2\}^{\otimes n}$ . For example, the following state is a paired state at  $n = 8$ . Different ‘‘pair’’s are marked in different colors.

$$|I_{00}\rangle |X_{11}\rangle |I_{01}\rangle |X_{10}\rangle |X_{00}\rangle |I_{10}\rangle |I_{11}\rangle |X_{01}\rangle. \quad (78)$$

We can give a more succinct expression to the square of the vectorization of  $\hat{a}_p^\dagger \hat{a}_q + h.c.$  and  $\hat{a}_p^\dagger \hat{a}_q^\dagger \hat{a}_r \hat{a}_s + h.c.$  compared to that in Proposition 10, using the notations  $|I_{ab}\rangle, |X_{ab}\rangle$  as follows.

**Proposition 17** (Succinct expression of  $|O\rangle^{\otimes 2}$ ). *After Jordan-Wigner transformation, when  $O = \hat{a}_p^\dagger \hat{a}_q + h.c.$  ( $p > q$ ),*

$$|O\rangle^{\otimes 2} = \left( \sum_{c,d \in \mathbb{F}_2} |X_{cd}\rangle_q |X_{\bar{c}\bar{d}}\rangle_p \right) \otimes \bigotimes_{a \in [1,q] \cup (p,n)} \left( \sum_{c,d \in \mathbb{F}_2} |I_{cd}\rangle_a \right) \otimes \bigotimes_{b \in (p,q)} \left( \sum_{c,d \in \mathbb{F}_2} (-1)^{c+d} |I_{cd}\rangle_b \right). \quad (79)$$

*And when  $O = \hat{a}_p^\dagger \hat{a}_q^\dagger \hat{a}_r \hat{a}_s + h.c.$  ( $p > q > r > s$ ),*

$$|O\rangle^{\otimes 2} = \left( \sum_{c,d \in \mathbb{F}_2} |X_{cd}\rangle_s |X_{cd}\rangle_r |X_{\bar{c}\bar{d}}\rangle_q |X_{\bar{c}\bar{d}}\rangle_p \right) \otimes \bigotimes_{a \in [1,s] \cup (r,q) \cup (p,n)} \left( \sum_{c,d \in \mathbb{F}_2} |I_{cd}\rangle_a \right) \otimes \bigotimes_{b \in (s,r) \cup (q,p)} \left( \sum_{c,d \in \mathbb{F}_2} (-1)^{c+d} |I_{cd}\rangle_b \right). \quad (80)$$

Now that we have defined the notation  $|I_{ab}\rangle, |X_{ab}\rangle$ , we return to the diagonalization of  $\tilde{R}_j$  inside  $\mathcal{H}_t^{\text{even}}$ . The following lemma gives the diagonalization of  $\tilde{A}^{\text{qubit}}$  and the partial diagonalization of  $\tilde{B}^{\text{qubit}}$  inside  $\mathcal{H}_t^{\text{even}}$ . These will be used in the next section to derive the spanning set of  $M_j^\perp$  for  $R_j \in \{A, A^{\text{qubit}}, B, B^{\text{qubit}}\}$ .

**Lemma 18** (Diagonalization of  $\tilde{A}^{\text{qubit}}, \tilde{B}^{\text{qubit}}$  within  $\mathcal{H}_t^{\text{even}}$ ).

1. The subspace that  $\tilde{A}_{pq}^{\text{qubit}}|_{\mathcal{H}_2^{\text{even}}}$  projects onto is spanned by  $S_1 \cup S_2 \cup S_3$ , where

$$S_1 := \{|\Phi\rangle \mid |\Phi\rangle \in \mathcal{S}_2^{\text{even}}, \Phi_p = \Phi_q\}, \quad (81)$$

$$S_2 := \{|\Phi\rangle + (-1)^{\Phi_p \odot \Phi_q} S_{pq} |\Phi\rangle \mid |\Phi\rangle \in \mathcal{S}_2^{\text{even}}, \Phi_p \neq \Phi_q, \Phi_p \neq \bar{\Phi}_q\}, \quad (82)$$

$$S_3 := \left\{ |\Phi\rangle + S_{pq} |\Phi\rangle + F_{pq}^{st} |\Phi\rangle + S_{pq} F_{pq}^{st} |\Phi\rangle \mid \begin{array}{l} |\Phi\rangle \in \mathcal{S}_2^{\text{even}}, |\Phi_p\rangle = |I_{00}\rangle, \\ |\Phi_q\rangle = |I_{11}\rangle, 1 \leq s < t \leq 4 \end{array} \right\}. \quad (83)$$

2. The space spanned by  $S := \{|\Phi\rangle \in \mathcal{S}_2^{\text{even}} \mid \Phi_p \neq \Phi_q, \Phi_p \neq \bar{\Phi}_q, \Phi_p = \bar{\Phi}_r, \Phi_q = \bar{\Phi}_s\}$  is invariant under  $\tilde{B}_{pqrs}^{\text{qubit}}$ , and when restricted to such subspace,  $\tilde{B}_{pqrs}^{\text{qubit}}$  is an orthogonal projection onto the space spanned by  $S' := \{|\Phi\rangle + (-1)^{\Phi_p \odot \Phi_q} S_{ps} S_{qr} |\Phi\rangle \mid |\Phi\rangle \in S\}$ .

*Proof.* Item 1. — By Lemma 11 (Item 3),  $\hat{A}_{pq}^{\text{qubit}}$  stabilizes every vector in  $S_1 \cup S_2 \cup S_3$ , and

$$\begin{aligned} \text{tr}\left(\hat{A}_{pq}^{\text{qubit}}|_{\mathcal{H}_2^{\text{even}}}\right) &= \sum_{|\Phi\rangle \in \mathcal{S}_2^{\text{even}}} \langle \Phi | \hat{A}_{pq}^{\text{qubit}} | \Phi \rangle \\ &= \left(8 \times 1 + 48 \times \frac{1}{2} + 8 \times \frac{3}{8}\right) \times 8^{n-2} = \sum_{i=1}^3 \dim(\text{span } S_i). \end{aligned} \quad (84)$$

Finally, since  $S_1, S_2, S_3$  are mutually orthogonal,  $\hat{A}_{pq}^{\text{qubit}}|_{\mathcal{H}_2^{\text{even}}}$  is a projection onto  $\text{span}(S_1 \cup S_2 \cup S_3)$ .

Item 2. — By Lemma 11 (Item 3), for any  $|\Phi\rangle \in S$ ,

$$\tilde{B}_{pqrs}^{\text{qubit}} |\Phi\rangle = \frac{1}{2} |\Phi\rangle + \frac{(-1)^{\Phi_p \odot \Phi_q}}{2} S_{ps} S_{qr} |\Phi\rangle. \quad (85)$$

Thus,  $S$  is invariant under  $\tilde{B}_{pqrs}^{\text{qubit}}$ , and  $\tilde{B}_{pqrs}^{\text{qubit}}|_{\text{span } S}$  is indeed an orthogonal projection onto the space spanned by  $S' := \{|\Phi\rangle + (-1)^{\Phi_p \odot \Phi_q} S_{ps} S_{qr} |\Phi\rangle \mid |\Phi\rangle \in S\}$ .  $\square$

## 8.2 Particle number symmetry

The particle number symmetry of  $\tilde{R}_j = \mathbb{E}[R_j^{\otimes 2,2}]$  helps to reduce the space from  $\mathcal{H}_2^{\text{even}}$  to  $\mathcal{H}_2^{\text{paired}}$ , where certain constraints regarding the number of  $|I_{ab}\rangle, |X_{ab}\rangle$  must be satisfied. Notice that we exclusively focus on the  $t = 2$  case for particle number symmetry, but such symmetry should hold for general  $t$ .

**Definition 11** (Paired state and related notions). *Let  $|\Phi\rangle \in \mathcal{S}_2^{\text{even}}$  and  $V \subseteq [n]$ .*

1. For any  $a, b \in \mathbb{F}_2$ , define

$$n_{ab}^I(|\Phi\rangle; V) := \#\{i \in V \mid |\Phi_i\rangle = |I_{ab}\rangle\}, \quad n_{ab}^X(|\Phi\rangle; V) := \#\{i \in V \mid |\Phi_i\rangle = |X_{ab}\rangle\}. \quad (86)$$

If  $V$  is omitted, it is assumed that  $V = [n]$ , i.e.,  $n_{ab}^I(|\Phi\rangle) := n_{ab}^I(|\Phi\rangle; [n]), n_{ab}^X(|\Phi\rangle) := n_{ab}^X(|\Phi\rangle; [n])$ .

2. Call  $|\Phi\rangle$  a paired state, if

$$n_{01}^I(|\Phi\rangle) - n_{10}^I(|\Phi\rangle) = n_{00}^X(|\Phi\rangle) - n_{11}^X(|\Phi\rangle) = n_{01}^X(|\Phi\rangle) - n_{10}^X(|\Phi\rangle) = 0, \quad (87)$$

$$n_{00}^I(|\Phi\rangle) - n_{11}^I(|\Phi\rangle) = n - 2n_e. \quad (88)$$

3. Denote the set of all paired states by  $\mathcal{S}_2^{\text{paired}}$ , and the Hilbert space spanned by these states by  $\mathcal{H}_2^{\text{paired}}$ .

4. Define the configuration of a paired state  $|\Phi\rangle$  by

$$\text{conf}(|\Phi\rangle) = (n_{01}^I(|\Phi\rangle), n_{00}^X(|\Phi\rangle), n_{01}^X(|\Phi\rangle)). \quad (89)$$

5. Denote the set of all paired states with configuration  $(a, b, c)$  by  $\mathcal{S}_{2,(a,b,c)}^{\text{paired}}$ , and the Hilbert space spanned by these states by  $\mathcal{H}_{2,(a,b,c)}^{\text{paired}}$ .

Remark that the 8 numbers  $n_{ab}^I(|\Phi\rangle), n_{ab}^X(|\Phi\rangle)$  are uniquely determined by the configuration of a paired state  $|\Phi\rangle$ , and  $n_{01}^I(|\Phi\rangle) + n_{00}^X(|\Phi\rangle) + n_{01}^X(|\Phi\rangle) \leq \min\{n_e, n - n_e\}$ .

**Lemma 19** (Invariance of  $\mathcal{H}_2^{\text{paired}}$ ). *Let  $\mathbf{R}$  be a sequence of (qubit) excitation rotations, with  $R_j \in \{A, A^{\text{qubit}}, B, B^{\text{qubit}}\}$ .  $\mathcal{H}_2^{\text{paired}}$  is an invariant subspace of each  $\tilde{R}_j$ . Moreover,  $|\Psi_{2,k}^{\mathbf{R}}\rangle, |\Psi_{2,\infty}^{\mathbf{R}}\rangle \in \mathcal{H}_2^{\text{paired}}$ .*

*Proof.* In order to prove invariance of  $\mathcal{H}_2^{\text{paired}}$ , it suffices to show that  $|\Psi\rangle := \tilde{R}|\Phi\rangle \in \mathcal{H}_2^{\text{paired}}$ , for all  $|\Phi\rangle \in \mathcal{S}_2^{\text{paired}}$  and  $R \in \{A, A^{\text{qubit}}, B, B^{\text{qubit}}\}$ .

- We first prove the case when  $R \in \{A^{\text{qubit}}, B^{\text{qubit}}\}$ . Since  $\tilde{A}_{pq}^{\text{qubit}}$  (and  $\tilde{B}_{pqrs}^{\text{qubit}}$ ) acts non-trivially only on 2 (and 4) sites, one can enumerate  $8^2$  (and  $8^4$ ) states of these sites to verify that if  $|\Phi'\rangle \in \mathcal{S}_2^{\text{even}}$  has non-zero overlap with  $|\Psi\rangle$ , then for all  $a, b \in \mathbb{F}_2$  and  $S \in \{I, X\}$ ,

$$n_{ab}^S(|\Phi'\rangle) - n_{ab}^S(|\Phi\rangle) = n_{a\bar{b}}^S(|\Phi'\rangle) - n_{a\bar{b}}^S(|\Phi\rangle). \quad (90)$$

Thus,  $|\Psi\rangle \in \mathcal{H}_2^{\text{paired}}$ . In fact, Supplementary Equation (90) is obvious when  $R = \tilde{A}^{\text{qubit}}$  by the diagonalization given in Lemma 18 (Item 1).

- In order to prove the case when  $R \in \{A, B\}$ , we utilize the conversion rule in Lemma 11 (Item 4). Notice that for any  $a, b \in \mathbb{F}_2$  and  $S \in \{I, X\}$ , there exists  $a', b' \in \mathbb{F}_2$  and  $S' \in \{I, X\}$ , such that for any  $|\Phi'\rangle \in \mathcal{S}_2^{\text{even}}$ ,

$$n_{ab}^S(|\Phi'\rangle) = n_{a'b'}^{S'} \left( \left( \prod_{i=1}^n X_i^z \right) |\Phi'\rangle \right), \quad n_{a\bar{b}}^S(|\Phi'\rangle) = n_{a'\bar{b}'}^{S'} \left( \left( \prod_{i=1}^n X_i^z \right) |\Phi'\rangle \right). \quad (91)$$

Here  $\prod_{i=1}^n X_i^z$  is defined as in Lemma 11 (Item 4) with respect to  $|\Phi\rangle$ . Thus, if  $|\Phi'\rangle \in \mathcal{S}_2^{\text{paired}}$  has a non-zero overlap with  $|\Psi\rangle$ , then

$$n_{ab}^S(|\Phi'\rangle) - n_{ab}^S(|\Phi\rangle) = n_{a'b'}^{S'} \left( \left( \prod_{i=1}^n X_i^z \right) |\Phi'\rangle \right) - n_{a'b'}^{S'} \left( \left( \prod_{i=1}^n X_i^z \right) |\Phi\rangle \right) \quad (92)$$

$$= n_{a'\bar{b}'}^{S'} \left( \left( \prod_{i=1}^n X_i^z \right) |\Phi'\rangle \right) - n_{a'\bar{b}'}^{S'} \left( \left( \prod_{i=1}^n X_i^z \right) |\Phi\rangle \right) \quad (93)$$

$$= n_{a\bar{b}}^S(|\Phi'\rangle) - n_{a\bar{b}}^S(|\Phi\rangle). \quad (94)$$

Supplementary Equation (93) follows from Lemma 11 (Item 4) and Supplementary Equation (90).

Finally, by Proposition 10,  $|\psi_0\rangle^{\otimes 4} \in \mathcal{H}_2^{\text{paired}}$ . Hence,  $|\Psi_{2,k}^{\mathbf{R}}\rangle = \left( \prod_j \tilde{R}_j \right)^k |\psi_0\rangle^{\otimes 4} \in \mathcal{H}_2^{\text{paired}}$ . Since  $\mathcal{H}_2^{\text{paired}}$  is closed,  $|\Psi_{2,\infty}^{\mathbf{R}}\rangle = \lim_{k \rightarrow \infty} |\Psi_{2,k}^{\mathbf{R}}\rangle \in \mathcal{H}_2^{\text{paired}}$ .  $\square$

Lemma 19 indicates that we can restrict ourselves to  $\mathcal{H}_2^{\text{paired}}$  — instead of the spanning set of each  $M_j^\perp$ , it suffices to find the spanning set of the orthogonal complement of each  $M_j$  inside  $\mathcal{H}_2^{\text{paired}}$ :  $(M_j \cap \mathcal{H}_2^{\text{paired}})^\perp \cap \mathcal{H}_2^{\text{paired}}$ . As one may expect, the union of these spanning sets spans  $(M \cap \mathcal{H}_2^{\text{paired}})^\perp \cap \mathcal{H}_2^{\text{paired}}$ , according to Lemma 14 (Item 4). The following lemma characterizes the spanning set of  $(M_j \cap \mathcal{H}_2^{\text{paired}})^\perp \cap \mathcal{H}_2^{\text{paired}}$  for  $R_j \in \{A, A^{\text{qubit}}, B, B^{\text{qubit}}\}$ .

**Lemma 20** (Spanning set of  $(M_j \cap \mathcal{H}_2^{\text{paired}})^\perp \cap \mathcal{H}_2^{\text{paired}}$  for  $A, A^{\text{qubit}}, B, B^{\text{qubit}}$ ). *Denote by  $M_1, M_2, M_3, M_4$  the space that  $\tilde{A}_{pq}, \tilde{A}_{pq}^{\text{qubit}}, \tilde{B}_{pqrs}, \tilde{B}_{pqrs}^{\text{qubit}}$  projects onto. Suppose  $p > q$  for (qubit) single excitations and  $p > q > r > s$  for (qubit) double excitations.*

1.  $(M_1 \cap \mathcal{H}_2^{\text{paired}})^\perp \cap \mathcal{H}_2^{\text{paired}}$  is spanned by all the following vectors: for any  $|\Phi\rangle \in \mathcal{S}_2^{\text{paired}}$ , let

$$\mathbf{z} := \bigoplus_{a \in (q,p)} \Phi_a,$$

- $|\Phi\rangle - (-1)^{(\Phi_p \oplus \mathbf{z}) \odot (\Phi_q \oplus \mathbf{z})} S_{pq} |\Phi\rangle$ .
- $|\Phi\rangle - (-1)^{z_1 + z_2} F_{pq}^{12} |\Phi\rangle - (-1)^{z_1 + z_3} F_{pq}^{13} |\Phi\rangle - (-1)^{z_2 + z_3} F_{pq}^{23} |\Phi\rangle$  if  $|\Phi_p\rangle = |I_{00}\rangle, |\Phi_q\rangle = |I_{11}\rangle$ .

2.  $(M_2 \cap \mathcal{H}_2^{\text{paired}})^\perp \cap \mathcal{H}_2^{\text{paired}}$  is spanned by all the following vectors: for any  $|\Phi\rangle \in \mathcal{S}_2^{\text{paired}}$ ,
  - $|\Phi\rangle - (-1)^{\Phi_p \odot \Phi_q} S_{pq} |\Phi\rangle$ .
  - $|\Phi\rangle - F_{pq}^{12} |\Phi\rangle - F_{pq}^{13} |\Phi\rangle - F_{pq}^{23} |\Phi\rangle$  if  $|\Phi_p\rangle = |I_{00}\rangle, |\Phi_q\rangle = |I_{11}\rangle$ .
3.  $(M_3 \cap \mathcal{H}_2^{\text{paired}})^\perp \cap \mathcal{H}_2^{\text{paired}}$  contains  $|\Phi\rangle - (-1)^{(\Phi_p \oplus \mathbf{z}) \odot (\Phi_q \oplus \mathbf{z})} S_{ps} S_{qr} |\Phi\rangle$ , where  $|\Phi\rangle \in \mathcal{S}_2^{\text{paired}}$ ,  $\Phi_p \neq \Phi_q, \Phi_p \neq \bar{\Phi}_q, \Phi_p = \bar{\Phi}_r, \Phi_q = \bar{\Phi}_s$ , and  $\mathbf{z} := \bigoplus_{a \in (s,r) \cup (q,p)} \Phi_a$ .
4.  $(M_4 \cap \mathcal{H}_2^{\text{paired}})^\perp \cap \mathcal{H}_2^{\text{paired}}$  contains  $|\Phi\rangle - (-1)^{\Phi_p \odot \Phi_q} S_{ps} S_{qr} |\Phi\rangle$ , where  $|\Phi\rangle \in \mathcal{S}_2^{\text{paired}}$ , and  $\Phi_p \neq \Phi_q, \Phi_p \neq \bar{\Phi}_q, \Phi_p = \bar{\Phi}_r, \Phi_q = \bar{\Phi}_s$ .

*Proof.* We first prove Items 2 and 4 using the diagonalization of  $\tilde{A}_{pq}^{\text{qubit}}, \tilde{B}_{pqrs}^{\text{qubit}}$  in  $\mathcal{H}_2^{\text{even}}$  (Lemma 18), then prove Items 1 and 3 using the qubit to non-qubit conversion rule in Lemma 11 (Item 4).

Item 2. — Denote the set of specified vectors by  $S$ . Obviously,  $S \subseteq \mathcal{H}_2^{\text{paired}}$ . We need to prove

- (1)  $S \subseteq (M_2 \cap \mathcal{H}_2^{\text{paired}})^\perp$ , (2)  $S^\perp \cap \mathcal{H}_2^{\text{paired}} \subseteq M_2 \cap \mathcal{H}_2^{\text{paired}}$  (since that would imply  $\text{span } S \supseteq (M_2 \cap \mathcal{H}_2^{\text{paired}})^\perp \cap \mathcal{H}_2^{\text{paired}}$ ).

- (1)  $S \subseteq (M_2 \cap \mathcal{H}_2^{\text{paired}})^\perp$ : We show that every vector in  $S$  is orthogonal to  $S_1 \cup S_2 \cup S_3$  defined in

Lemma 18 (Item 1), hence  $S \subseteq (M_2 \cap \mathcal{H}_2^{\text{even}})^\perp \subseteq (M_2 \cap \mathcal{H}_2^{\text{paired}})^\perp$ . First, consider the vector

$$v_1 := |\Phi\rangle - (-1)^{\Phi_p \odot \Phi_q} S_{pq} |\Phi\rangle \in S.$$

- If  $\Phi_p = \Phi_q$ , then  $v_1 = 0$  and  $v_1$  is orthogonal to  $S_1 \cup S_2 \cup S_3$ .
- If  $\Phi_p = \bar{\Phi}_q$ , then  $v_1$  is orthogonal to  $S_1 \cup S_2$ .  $v_1$  is also orthogonal to  $S_3$  since  $v_1 = |\Phi\rangle - S_{pq} |\Phi\rangle$  while for vectors in  $S_3$  the overlaps with  $|\Phi\rangle$  and  $S_{pq} |\Phi\rangle$  are the same.
- Otherwise,  $v_1$  is orthogonal to  $S_1 \cup S_3$ .  $v_1$  is also orthogonal to  $S_2$  since for vectors in  $S_2$  the overlaps with  $|\Phi\rangle$  and  $S_{pq} |\Phi\rangle$  differ by  $(-1)^{\Phi_p \odot \Phi_q}$ .

Next, consider the vector  $v_2 := |\Phi\rangle - F_{pq}^{12} |\Phi\rangle - F_{pq}^{13} |\Phi\rangle - F_{pq}^{23} |\Phi\rangle$  with  $|\Phi_p\rangle = |I_{00}\rangle, |\Phi_q\rangle = |I_{11}\rangle$ .  $v_2$  is orthogonal to  $S_1 \cup S_2$ .  $v_2$  is also orthogonal to  $S_3$  since for vectors in  $S_3$  the overlap with  $|\Phi\rangle$  equals one of the overlaps with  $F_{pq}^{12} |\Phi\rangle, F_{pq}^{13} |\Phi\rangle, F_{pq}^{23} |\Phi\rangle$ , while the rest two are both zero.

- (2)  $S^\perp \cap \mathcal{H}_2^{\text{paired}} \subseteq M_2 \cap \mathcal{H}_2^{\text{paired}}$ : Suppose  $v \in S^\perp \cap \mathcal{H}_2^{\text{paired}}$ , we prove  $v \in M_2 \cap \mathcal{H}_2^{\text{paired}}$ . Write  $v = \sum_{|\Phi\rangle \in \mathcal{S}_2^{\text{paired}}} c_\Phi |\Phi\rangle$ , with  $c_\Phi \in \mathbb{C}$ . Since  $v$  is orthogonal to  $S$ , we have

- $c_\Phi = (-1)^{\Phi_p \odot \Phi_q} c_{\Phi'}$  if  $|\Phi'\rangle = S_{pq} |\Phi\rangle$ .
- $c_\Phi = c_{\Phi^{12}} + c_{\Phi^{13}} + c_{\Phi^{23}}$  if  $|\Phi_p\rangle = |I_{00}\rangle, |\Phi_q\rangle = |I_{11}\rangle$  and  $|\Phi^{ab}\rangle = F_{pq}^{ab} |\Phi\rangle$ .

Hence,

$$\begin{aligned} v = & \sum_{\Phi_p = \Phi_q} c_\Phi |\Phi\rangle + \sum_{\Phi_p \neq \Phi_q, \bar{\Phi}_q} c_\Phi (|\Phi\rangle + (-1)^{\Phi_p \odot \Phi_q} |\Phi\rangle) \\ & + \sum_{\substack{|\Phi_p\rangle = F_{pq}^{ab} |I_{00}\rangle, |\Phi_q\rangle = F_{pq}^{ab} |I_{11}\rangle, \\ 1 \leq a < b \leq 4}} c_{\Phi^{ab}} (F_{pq}^{ab} |\Phi\rangle + F_{pq}^{ab} S_{pq} |\Phi\rangle + |\Phi\rangle + S_{pq} |\Phi\rangle). \end{aligned} \quad (95)$$

It is straightforward to verify that  $v \in \mathcal{H}_2^{\text{paired}}$  and by Lemma 18 (Item 1)  $v \in M_2 \cap \mathcal{H}_2^{\text{even}}$ . Thus,  $v \in M_2 \cap \mathcal{H}_2^{\text{paired}}$ .

Item 4. — Obviously,  $v := |\Phi\rangle - (-1)^{\Phi_p \odot \Phi_q} S_{ps} S_{qr} |\Phi\rangle \in \mathcal{H}_2^{\text{paired}}$ . Use the notation  $S, S'$  from Lemma 18 (Item 2). Since  $\text{span } S$  is an invariant space of  $P_{M_4}$  and  $\text{span } S \cap M_4 = \text{span } S'$ , we have  $M_4 = \text{span } S' \oplus ((\text{span } S)^\perp \cap M_4)$ .  $v$  is orthogonal to  $(\text{span } S)^\perp \cap M_4$  since  $v \in \text{span } S$ .  $v$  is also orthogonal to  $\text{span } S'$ , since for vectors in  $S'$  the overlaps with  $|\Phi\rangle$  and  $S_{ps} S_{qr} |\Phi\rangle$  differ by  $(-1)^{\Phi_p \odot \Phi_q}$ . Hence,  $v \in M_4^\perp \cap \mathcal{H}_2^{\text{paired}} = (M_4 \cap \mathcal{H}_2^{\text{paired}})^\perp \cap \mathcal{H}_2^{\text{paired}}$  by Lemma 14 (Item 5).

Items 1 and 3. — Same as Items 2 and 4 but use the conversion rule.  $\square$

Lemma 20 has a simple yet interesting corollary — if  $\mathbf{R}$  contains enough (qubit) single excitations, the dimension of  $M \cap \mathcal{H}_2^{\text{paired}}$  is at most  $\text{poly}(n)$ . Moreover, vectors in  $M \cap \mathcal{H}_2^{\text{paired}}$  have a nice decomposition which we refer to as decomposition in configuration basis.

**Corollary 21** (Configuration basis decomposition). *Let  $\mathbf{R}$  be a sequence of (qubit) excitation rotations defined in Definition 4,  $M$  be the intersection space defined in Lemma 12. Denote the simple undirected graph formed by index pairs of (qubit) single excitations in  $\mathbf{R}$  by  $G$  as in Theorem 5. If  $G$*



is connected, then there exists a function  $\text{sign}(a, b, c) \in \pm 1$  which defines a set of configuration basis  $\left\{ |\Psi_{(a,b,c)}\rangle = \sum_{|\Phi\rangle \in \mathcal{S}_{2,(a,b,c)}^{\text{paired}}} \text{sign}(|\Phi\rangle) |\Phi\rangle \right\}_{a,b,c}$ , such that for any  $|\Psi\rangle \in M \cap \mathcal{H}_2^{\text{paired}}$ ,

$$|\Psi\rangle = \sum_{a+b+c=0}^{\min\{n_e, n-n_e\}} c(a, b, c) |\Psi_{(a,b,c)}\rangle, \quad c(a, b, c) \in \mathbb{C}. \quad (96)$$

*Proof.* By Lemma 20,  $|\Phi\rangle \pm S_{uv} |\Phi\rangle \in \left( M \cap \mathcal{H}_2^{\text{paired}} \right)^\perp \cap \mathcal{H}_2^{\text{paired}}$ , for any  $|\Phi\rangle \in \mathcal{H}_2^{\text{paired}}$  and  $(u, v) \in E$ . By Lemma 14,  $\left( M \cap \mathcal{H}_2^{\text{paired}} \right)^\perp \cap \mathcal{H}_2^{\text{paired}} \subseteq M^\perp$ . Hence, for any  $|\Psi\rangle \in M \cap \mathcal{H}_2^{\text{paired}}$ , we have  $\langle \Phi | \Psi \rangle = \pm \langle \Phi | S_{uv}^\dagger | \Psi \rangle$ . In other words, if two paired states differ only by a site swap on an edge, their overlaps with  $|\Psi\rangle$  differs by either  $+1$  or  $-1$ , and such a relative sign is independent of  $|\Psi\rangle$ . Since  $G$  is connected, one can argue that if two paired states  $|\Phi\rangle, |\Phi'\rangle$  have the same configuration  $(a, b, c)$ , their overlaps with  $|\Psi\rangle$  differs by at most  $\pm 1$  — two paired states with the same configuration differ by some site permutation, which can be decomposed into a product of swaps, and each swap can, in turn, be decomposed into a product of swaps on edges. The decomposition of a site permutation into swaps on edges may not be unique, and if the signs induced by two different decomposition conflict, it must be  $c(a, b, c) = 0$  for all  $|\Psi\rangle \in M \cap \mathcal{H}_2^{\text{paired}}$  (one can argue that  $|\Phi\rangle \in M^\perp$ , and thus  $\mathcal{S}_{2,(a,b,c)}^{\text{paired}} \subseteq M^\perp$ ). Otherwise, the relative signs for paired states in  $\mathcal{S}_{2,(a,b,c)}^{\text{paired}}$  must be unique, and are independent of  $|\Psi\rangle$ . Hence, one can pick a sign function that satisfies the requirements — on  $\mathcal{S}_{2,(a,b,c)}^{\text{paired}} \subseteq M^\perp$ , define sign arbitrarily, and otherwise define sign arbitrarily on some  $|\Phi\rangle \in \mathcal{S}_{2,(a,b,c)}^{\text{paired}}$ , and extend to other  $|\Phi'\rangle \in \mathcal{S}_{2,(a,b,c)}^{\text{paired}}$  according the unique relative sign.  $\square$

Now that we have characterized the spanning set of  $\left( M_j \cap \mathcal{H}_2^{\text{paired}} \right)^\perp \cap \mathcal{H}_2^{\text{paired}}$ , we are prepared to prove case 1 and part of case 2 of Theorem 5. Our proof for these parts is constructive — we will give an explicit vector  $|\Psi^*\rangle$ , and prove that  $|\Psi^*\rangle = |\Psi_{2,\infty}^{\mathbf{R}}\rangle = P_M |\psi_0\rangle^{\otimes 4}$ . To be precise, we show that the following two conditions hold:

- $|\Psi^*\rangle$  is orthogonal to  $\left( M \cap \mathcal{H}_2^{\text{paired}} \right)^\perp \cap \mathcal{H}_2^{\text{paired}}$ , and  $|\Psi^*\rangle \in \mathcal{H}_2^{\text{paired}}$ , hence  $|\Psi^*\rangle \in M$  (Lemma 14 (Item 3)).
- $|\Psi^*\rangle - |\psi_0\rangle^{\otimes 4} \in \left( M \cap \mathcal{H}_2^{\text{paired}} \right)^\perp \cap \mathcal{H}_2^{\text{paired}}$ , hence  $|\Psi^*\rangle - |\psi_0\rangle^{\otimes 4} \in M^\perp$  (Lemma 14 (Item 6)).

The reader can jump to Supplementary Notes 10 and 11 for more details. Remark that such proof relies on the complete spanning set of  $\left( M \cap \mathcal{H}_2^{\text{paired}} \right)^\perp \cap \mathcal{H}_2^{\text{paired}}$ . We have only given an incomplete spanning set for  $\left( M_j \cap \mathcal{H}_2^{\text{paired}} \right)^\perp \cap \mathcal{H}_2^{\text{paired}}$  of  $R_j \in \left\{ \tilde{B}, \tilde{B}^{\text{qubit}} \right\}$ , thus simply taking the union of these spanning set is not enough. In fact, to prove the rest of Theorem 5 we utilize another symmetry discussed in the next section to reduce the space down to one dimension. In such case  $|\Psi_{2,\infty}^{\mathbf{R}}\rangle$  is obvious.

### 8.3 $(S_\tau^{\text{b}})^{\otimes n}$ -symmetry

The  $(S_\tau^{\text{b}})^{\otimes n}$ -symmetry of  $\mathbb{E} [R_j^{\otimes t, t}]$  helps to further reduce the space  $\mathcal{H}_2^{\text{paired}}$ . We use this symmetry to find a one-dimensional subspace of  $M \cap \mathcal{H}_2^{\text{paired}}$ , which contains  $|\Psi_{2,\infty}^{\mathbf{R}}\rangle$ .

**Definition 12** ( $\mathcal{H}_t^\tau$ ). For any  $\tau \in \mathfrak{S}_{2t}$ ,  $\mathcal{H}_t^\tau$  is defined to be the  $+1$  eigenspace of  $(S_\tau^{\text{b}})^{\otimes n}$ .

Let  $R(\theta)$  be a (qubit) excitation rotation, and  $\mathbf{R}$  be a sequence of (qubit) excitation rotations (Definition 4).

**Lemma 22** ( $(S_\tau^{\text{b}})^{\otimes n}$ -symmetry). For any  $\tau \in \mathfrak{S}_{2t}$ ,  $[\mathbb{E} [R^{\otimes t, t}], (S_\tau^{\text{b}})^{\otimes n}] = 0$ .

*Proof.*  $(S_\tau^{\text{b}})^{\otimes n} \mathbb{E} [R(\theta)^{\otimes 2t}] \left( (S_\tau^{\text{b}})^{\otimes n} \right)^{-1} = \mathbb{E} [R(\theta)^{\otimes 2t}]$ , since the action of  $(S_\tau^{\text{b}})^{\otimes n}$  induces a permutation of  $2t$  replicas of  $R(\theta)$  by  $\tau$ , which does not change the result.  $\square$

**Corollary 23** (Invariance of  $\mathcal{H}_t^\tau$ ). For any  $\tau \in \mathfrak{S}_{2t}$ ,  $\mathcal{H}_t^\tau$  is an invariant subspace of  $\mathbb{E} [R^{\otimes t, t}]$ . Moreover,  $|\Psi_{t,k}^{\mathbf{R}}\rangle, |\Psi_{t,\infty}^{\mathbf{R}}\rangle \in \mathcal{H}_t^\tau$ .

*Proof.* By Definition 12 and lemma 22,  $\mathcal{H}_t^\tau$  is an invariant subspace of  $\mathbb{E}[R^{\otimes t, t}]$ . By Proposition 10,  $|\psi_0\rangle^{\otimes 2t} \in \mathcal{H}_t^\tau$ . Hence,  $|\Psi_{t,k}^{\mathbf{R}}\rangle = \left(\prod_j \mathbb{E}[R_j^{\otimes t, t}]\right)^k |\psi_0\rangle^{\otimes 2t} \in \mathcal{H}_t^\tau$ . Since  $\mathcal{H}_t^\tau$  is closed,  $|\Psi_{t,\infty}^{\mathbf{R}}\rangle = \lim_{k \rightarrow \infty} |\Psi_{t,k}^{\mathbf{R}}\rangle \in \mathcal{H}_t^\tau$ .  $\square$

We use the following lemma to reduce the space to dimension one in later proofs.

**Lemma 24.** *Let  $\mathbf{R}$  be a sequence of (qubit) excitation rotations. Denote the simple undirected graph formed by index pairs of (qubit) single excitations in  $\mathbf{R}$  by  $G$  as in Theorem 5. Suppose*

1.  $G$  is connected.
2. For all  $|\Phi\rangle \in \mathcal{S}_{2,(a,b,c)}^{\text{paired}}$  where at least two of  $a, b, c$  is non-zero,  $|\Phi\rangle \in \left(M \cap \mathcal{H}_2^{\text{paired}} \cap \bigcap_{\tau \in \mathfrak{S}_4} \mathcal{H}_2^\tau\right)^\perp$ .

Then,

$$|\Psi_{2,\infty}^{\mathbf{R}}\rangle = \frac{1}{\binom{n}{n_e}^2 + 2\binom{n}{n_e}} \sum_{l=0}^m (|\Psi_{(l,0,0)}\rangle + |\Psi_{(0,l,0)}\rangle + |\Psi_{(0,0,l)}\rangle), \quad (97)$$

where  $|\Psi_{(a,b,c)}\rangle := \sum_{|\Phi\rangle \in \mathcal{S}_{2,(a,b,c)}^{\text{paired}}} |\Phi\rangle$ ,  $m := \min\{n_e, n - n_e\}$ .

*Proof.* Since  $G$  is connected (1<sup>st</sup> condition), vectors in  $M \cap \mathcal{H}_2^{\text{paired}}$  admits decomposition in configuration basis (Corollary 21). Say,  $\sum_{a,b,c} c(a,b,c) |\Phi'_{(a,b,c)}\rangle$  with  $|\Phi'_{(a,b,c)}\rangle = \sum_{|\Phi\rangle \in \mathcal{S}_{2,(a,b,c)}^{\text{paired}}} \pm |\Phi\rangle$ . Moreover, by the 2<sup>nd</sup> condition,  $c(a,b,c) = 0$  if two of  $a, b, c$  is non-zero. We prove (1)  $|\Phi'_{(l,0,0)}\rangle = |\Phi_{(l,0,0)}\rangle = \sum_{|\Phi\rangle \in \mathcal{S}_{2,(l,0,0)}^{\text{paired}}} |\Phi\rangle$ , and likewise for configurations  $(0, l, 0)$  and  $(0, 0, l)$ , (2)  $\dim\left(M \cap \mathcal{H}_2^{\text{paired}} \cap \bigcap_{\tau \in \mathfrak{S}_{2t}} \mathcal{H}_2^\tau\right) \leq 1$ , (3) the coefficients of  $\{|\Phi_{(l,0,0)}\rangle, |\Phi_{(0,l,0)}\rangle, |\Phi_{(0,0,l)}\rangle\}_l$  in  $|\Psi_{2,\infty}^{\mathbf{R}}\rangle$  are exactly those provided in Supplementary Equation (97).

- (1) We prove that  $|\Phi\rangle - S_{uv}|\Phi\rangle \in \left(M \cap \mathcal{H}_2^{\text{paired}}\right)^\perp \cap \mathcal{H}_2^{\text{paired}}$ , for any  $|\Phi\rangle \in \mathcal{S}_{2,(l,0,0)}^{\text{paired}}$  (and similarly for  $\mathcal{S}_{2,(0,l,0)}^{\text{paired}}$  or  $\mathcal{S}_{2,(0,0,l)}^{\text{paired}}$ ) and  $(u, v) \in E$ . After that, one can argue in the same way as in Corollary 21 to complete the proof. Suppose  $u < v$ . By the definition of  $G$ , either  $A_{uv}$  or  $A_{uv}^{\text{qubit}}$  is contained in  $\mathbf{R}$ .

- If  $R_j = A_{uv}^{\text{qubit}}$ , by Lemma 20 (Item 2)  $|\Phi\rangle - (-1)^{\Phi_u \odot \Phi_v} S_{uv} |\Phi\rangle \in \left(M_j \cap \mathcal{H}_2^{\text{paired}}\right)^\perp \cap \mathcal{H}_2^{\text{paired}}$ . Since  $\text{conf}(|\Phi\rangle) = (l, 0, 0)$ , we have  $\Phi_u, \Phi_v \in \{|I_{ab}\rangle | a, b \in \mathbb{F}_2\}$ . Hence,  $(-1)^{\Phi_u \odot \Phi_v} = 1$ , and  $|\Phi\rangle - S_{uv} |\Phi\rangle = |\Phi\rangle - (-1)^{\Phi_u \odot \Phi_v} S_{uv} |\Phi\rangle \in \left(M_j \cap \mathcal{H}_2^{\text{paired}}\right)^\perp \cap \mathcal{H}_2^{\text{paired}} \subseteq \left(M \cap \mathcal{H}_2^{\text{paired}}\right)^\perp \cap \mathcal{H}_2^{\text{paired}}$ .
- If  $R_j = A_{uv}$ , by Lemma 20 (Item 1)  $|\Phi\rangle - (-1)^{(\Phi_u \oplus \mathbf{z}) \odot (\Phi_v \oplus \mathbf{z})} S_{uv} |\Phi\rangle \in \left(M_j \cap \mathcal{H}_2^{\text{paired}}\right)^\perp \cap \mathcal{H}_2^{\text{paired}}$ , where  $\mathbf{z} = \bigoplus_{a \in (u,v)} \Phi_a$ . Since  $\text{conf}(|\Phi\rangle) = (l, 0, 0)$ , we have  $\Phi_u, \Phi_v, \mathbf{z} \in \{|I_{ab}\rangle | a, b \in \mathbb{F}_2\}$ . Hence,  $(-1)^{(\Phi_u \oplus \mathbf{z}) \odot (\Phi_v \oplus \mathbf{z})} = 1$ . The remainder is similar to the previous case.

- (2) Fix a vector  $|\Psi\rangle \in M \cap \mathcal{H}_2^{\text{paired}} \cap \bigcap_{\tau \in \mathfrak{S}_{2t}} \mathcal{H}_2^\tau$ . We have proved that  $|\Psi\rangle \in \text{span}\{|\Phi_{(l,0,0)}\rangle, |\Phi_{(0,l,0)}\rangle, |\Phi_{(0,0,l)}\rangle\}_l$ . Denote by  $c(a, b, c)$  the coefficient of  $|\Phi_{(a,b,c)}\rangle$  in  $|\Psi\rangle$ , where at most one of  $a, b, c$  is non-zero. Define  $c(a, b, c) = 0$  if at least two of  $a, b, c$  are non-zero. We prove that (2.1)  $c(a, b, c) = c(a+1, b, c) + c(a, b+1, c) + c(a, b, c+1)$ , (2.2)  $c(1, 0, 0) = c(0, 1, 0) = c(0, 0, 1)$ . If so, it must be  $|\Psi\rangle \propto \sum_{l=0}^m (|\Phi_{(l,0,0)}\rangle + |\Phi_{(0,l,0)}\rangle + |\Phi_{(0,0,l)}\rangle)$ . Hence,  $\dim\left(M \cap \mathcal{H}_2^{\text{paired}} \cap \bigcap_{\tau \in \mathfrak{S}_{2t}} \mathcal{H}_2^\tau\right) \leq 1$ .

- (2.1) Fix  $(u, v) \in E$ . Suppose  $|\Phi\rangle \in \mathcal{S}_{2,(a,b,c)}^{\text{paired}}, |\Phi_u\rangle = |I_{00}\rangle, |\Phi_v\rangle = |I_{11}\rangle$ . We need to prove that  $|\Phi\rangle - F_{uv}^{12} |\Phi\rangle - F_{uv}^{13} |\Phi\rangle - F_{uv}^{23} |\Phi\rangle$  is orthogonal to  $|\Psi\rangle$ , since the configuration of  $F_{uv}^{12} |\Phi\rangle, F_{uv}^{13} |\Phi\rangle, F_{uv}^{23} |\Phi\rangle$  is  $(a+1, b, c), (a, b+1, c), (a, b, c+1)$  respectively, and hence  $(|\Phi\rangle - F_{uv}^{12} |\Phi\rangle - F_{uv}^{13} |\Phi\rangle - F_{uv}^{23} |\Phi\rangle)^\dagger |\Psi\rangle = c(a, b, c) - c(a+1, b, c) - c(a, b+1, c) - c(a, b, c+1)$ . If two of  $a, b, c$  are non-zero, then  $c(a, b, c) = c(a+1, b, c) = c(a, b+1, c) = c(a, b, c+1) = 0$  and the equality holds trivially. Assume without loss of generality that  $a \geq 0, b = c = 0$ . Once more by definition of  $G$ , either  $A_{uv}$  or  $A_{uv}^{\text{qubit}}$  is contained in  $\mathbf{R}$ .

- If  $R_j = A_{uv}^{\text{qubit}}$ , by Lemma 20 (Item 2)  $|\Phi\rangle - F_{uv}^{12}|\Phi\rangle - F_{uv}^{13}|\Phi\rangle - F_{uv}^{23}|\Phi\rangle \in (M_j \cap \mathcal{H}_2^{\text{paired}})^\perp \cap \mathcal{H}_2^{\text{paired}} \subseteq M^\perp$ .
  - If  $R_j = A_{uv}$ , by Lemma 20 (Item 1)  $|\Phi\rangle - (-1)^{z_1+z_2}F_{uv}^{12}|\Phi\rangle - (-1)^{z_1+z_3}F_{uv}^{13}|\Phi\rangle - (-1)^{z_2+z_3}F_{uv}^{23}|\Phi\rangle \in (M_j \cap \mathcal{H}_2^{\text{paired}})^\perp \cap \mathcal{H}_2^{\text{paired}} \subseteq M^\perp$ , where  $\mathbf{z} = \bigoplus_{a \in (u,v)} \Phi_a$ . Since  $\text{conf}(|\Phi\rangle) = (l, 0, 0)$ , we have  $\mathbf{z} \in \{|I_{ab}\rangle | a, b \in \mathbb{F}_2\}$ . Thus,  $(-1)^{z_1+z_2} = 1$ , while  $(-1)^{z_1+z_3}, (-1)^{z_2+z_3} = \pm 1$ . By the 2<sup>nd</sup> condition,  $F_{uv}^{13}|\Phi\rangle, F_{uv}^{23}|\Phi\rangle \in M^\perp$ , since the configuration of  $F_{uv}^{13}|\Phi\rangle$  is  $(a, b+1, c)$  and  $a, b+1 > 0$ , and likewise for  $F_{uv}^{23}|\Phi\rangle$ . Hence,  $|\Phi\rangle - F_{uv}^{12}|\Phi\rangle - F_{uv}^{13}|\Phi\rangle - F_{uv}^{23}|\Phi\rangle \in M^\perp$ .
- (2.2) Fix a vector  $|\Phi\rangle \in \mathcal{S}_{2,(1,0,0)}^{\text{paired}}$  and two swaps  $\tau_1 = (1\ 3), \tau_2 = (1\ 4)$ . Let  $|\Phi^1\rangle := (S_{\tau_1}^b)^{\otimes n}|\Phi\rangle, |\Phi^2\rangle := (S_{\tau_2}^b)^{\otimes n}|\Phi\rangle$ . It is easy to check that the configuration of  $|\Phi^1\rangle, |\Phi^2\rangle$  is  $(0, 1, 0), (0, 0, 1)$  respectively. By Definition 12,  $|\Phi\rangle - |\Phi^1\rangle \in (\mathcal{H}_2^{\tau_1})^\perp$  and  $|\Phi\rangle - |\Phi^2\rangle \in (\mathcal{H}_2^{\tau_2})^\perp$ . Finally, since  $|\Psi\rangle \in \mathcal{H}_2^{\tau_1} \cap \mathcal{H}_2^{\tau_2}$ , we have  $0 = (|\Phi\rangle - |\Phi^1\rangle)^\dagger |\Psi\rangle = c(1, 0, 0) - c(0, 1, 0)$  and  $0 = (|\Phi\rangle - |\Phi^2\rangle)^\dagger |\Psi\rangle = c(1, 0, 0) - c(0, 0, 1)$ .
- (3) Since  $|\Psi_{2,\infty}^{\mathbf{R}}\rangle \in M \cap \mathcal{H}_2^{\text{paired}} \cap \bigcap_{\tau \in \mathfrak{S}_{2t}} \mathcal{H}_2^\tau$ , there exists constant  $c$  such that  $|\Psi_{2,\infty}^{\mathbf{R}}\rangle = c \sum_{l=0}^m (|\Phi_{(l,0,0)}\rangle + |\Phi_{(0,l,0)}\rangle + |\Phi_{(0,0,l)}\rangle)$ . Recall that  $\langle \mathbb{1}^{\otimes 2t} | \Psi_{2,\infty}^{\mathbf{R}} \rangle = 1$ , thus

$$\begin{aligned}
1 &= \langle \mathbb{1}^{\otimes 2t} | \Psi_{2,\infty}^{\mathbf{R}} \rangle = \left( \sum_{l=0}^m |\Phi_{(l,0,0)}\rangle \right)^\dagger |\Psi_{2,\infty}^{\mathbf{R}}\rangle \\
&= c \sum_{l=0}^m \binom{n}{l, l, n_e - l, n - n_e - l} + 2c \binom{n}{n_e} = \left( \binom{n}{n_e}^2 + 2 \binom{n}{n_e} \right) c.
\end{aligned} \tag{98}$$

Solving the equation yields the desired coefficients.  $\square$

## Supplementary Note 9: Average of cost is zero

In this section, we will prove that the cost function of alternated dUCC ansatzes is unbiased, i.e.,  $\mathbb{E}[C(\boldsymbol{\theta}; U_k^{\mathbf{R}}, H_{\text{el}})] = 0$ , where  $H_{\text{el}}$  is an electronic structure Hamiltonian. We also sketch a failed attack towards the variance of the cost function, which serves as an illustration of techniques used in the proof of main results.

**Theorem 25** (Unbiased cost function). *Let  $C(\boldsymbol{\theta}; U_k^{\mathbf{R}}, H_{\text{el}})$  be a cost function defined in Supplementary Equation (33), where  $U_k^{\mathbf{R}}(\boldsymbol{\theta})$  is an alternated (qubit) dUCC ansatzes defined in Supplementary Equation (36), and  $H_{\text{el}}$  is an electronic structure Hamiltonian defined in Supplementary Equation (35). We have  $\mathbb{E}_{\boldsymbol{\theta}}[C(\boldsymbol{\theta}; U_k^{\mathbf{R}}, H_{\text{el}})] = 0$ .*

*Proof.* By Proposition 10,  $|\hat{a}_p^\dagger \hat{a}_q + h.c.\rangle$  and  $|\hat{a}_p^\dagger \hat{a}_q^\dagger \hat{a}_r \hat{a}_s + h.c.\rangle$  lie in  $(\mathcal{H}_1^{\text{even}})^\perp$ , and by Corollary 16,  $|\Psi_{1,k}^{\mathbf{R}}\rangle \in \mathcal{H}_1^{\text{even}}$ . Hence,

$$\mathbb{E}[C] = \langle H_{\text{el}} | \Psi_{1,k}^{\mathbf{R}} \rangle = \sum_{pq} h_{pq} \langle \hat{a}_p^\dagger \hat{a}_q + h.c. | \Psi_{1,k}^{\mathbf{R}} \rangle + \sum_{pqrs} g_{pqrs} \langle \hat{a}_p^\dagger \hat{a}_q^\dagger \hat{a}_r \hat{a}_s + h.c. | \Psi_{1,k}^{\mathbf{R}} \rangle = 0. \tag{99}$$

$\square$

As a corollary, to calculate the variance of the cost, it suffices to calculate the 2<sup>nd</sup> moment, since

$$\text{Var}(C) = \mathbb{E}[C^2] - \mathbb{E}[C]^2 = \mathbb{E}[C^2]. \tag{100}$$

Now we sketch a failed attack towards the variance of the cost. The reader can safely skip this part. It would be great if we can give a nontrivial bound of the 2<sup>nd</sup> moment of the cost function using only 1<sup>st</sup> moments, for example utilizing the following inequality:

$$\mathbb{E}[C(\boldsymbol{\theta}; U_k^{\mathbf{R}}, O)^2] \leq \mathbb{E}[C(\boldsymbol{\theta}; U_k^{\mathbf{R}}, O^2)], \quad k \in \mathbb{N}_+ \cup \{\infty\}. \tag{101}$$

Unfortunately, this is not the case, at least not for Supplementary Equation (101). The derivation is sketched below and may serve as an example of the techniques used in the proof of main results.

Suppose we wish to bound  $\lim_{k \rightarrow \infty} \mathbb{E} [C(\boldsymbol{\theta}; U_k^{\mathbf{R}}, O)^2]$  by calculating  $\lim_{k \rightarrow \infty} \mathbb{E} [C(\boldsymbol{\theta}; U_k^{\mathbf{R}}, O^2)]$ . For simplicity, we consider the case  $O = \hat{a}_p^\dagger \hat{a}_q + h.c.$ , since it is straightforward to generalize to other cases. We further assume that the index pairs of (qubit) single excitations in  $\mathbf{R}$  form a connected graph, i.e., there exists a connected simple graph  $G = (V, E)$ , such that  $V = [n]$  and  $\mathbf{R}$  contains  $A_{uv}$  (or  $A_{uv}^{\text{qubit}}$ ) for all  $(u, v) \in E$ . The importance of this assumption will be made clear below.

Recall that  $\lim_{k \rightarrow \infty} \mathbb{E} [C(\boldsymbol{\theta}; U_k^{\mathbf{R}}, O^2)] = \lim_{k \rightarrow \infty} \langle O^2 | \left( \prod_{j=1}^{|\mathbf{R}|} \mathbb{E} [R_j^{\otimes 1,1}] \right)^k | \psi_0 \rangle^{\otimes 2} = \langle O^2 | \Psi_{1,\infty}^{\mathbf{R}} \rangle$  (Lemma 9 and Definition 6). Since  $|\psi_0\rangle^{\otimes 2} \in \mathcal{H}_1^{\text{even}}$  (Proposition 10) and  $\mathcal{H}_1^{\text{even}}$  is invariant under  $\mathbb{E} [R_j^{\otimes 1,1}]$  for all  $j$  (Corollary 16), we can restrict ourselves in the subspace  $\mathcal{H}_1^{\text{even}}$ . Fix an  $R_j \in \mathbf{R}$ , and suppose  $R_j(\theta) = \exp(\theta(\hat{\tau} - \hat{\tau}^\dagger))$ , where  $\hat{\tau} = \hat{a}_{p_1}^\dagger \dots \hat{a}_{p_r}^\dagger \hat{a}_{p_{r+1}} \dots \hat{a}_{p_{2r}}$  (or the corresponding qubit version). By Lemma 11 (Items 3 and 4), for any  $|\Phi\rangle \in \mathcal{S}_1^{\text{even}}$ ,

$$\begin{aligned} & \mathbb{E} [R_j^{\otimes 1,1}] |\Phi\rangle \\ &= \begin{cases} \frac{1}{2} |\Phi\rangle + \frac{1}{2} S_{(p_1 \ p_{r+1}) \dots (p_r \ p_{2r})} |\Phi\rangle, & \text{if } \Phi_{p_1} = \dots = \Phi_{p_r} = \bar{\Phi}_{p_{r+1}} = \dots = \bar{\Phi}_{p_{2r}}, \\ |\Phi\rangle, & \text{otherwise.} \end{cases} \end{aligned} \quad (102)$$

Notice that  $\mathbb{E} [R_j^{\otimes 1,1}]$  preserves the number of  $|00\rangle$  and  $|11\rangle$  in  $|\Phi\rangle$ , due to particle number symmetry. In particular, if  $R_j = A_{uv}$  (or  $A_{uv}^{\text{qubit}}$ ) for any  $(u, v) \in E$ , and  $|\Phi\rangle, |\Phi'\rangle \in \mathcal{S}_1^{\text{even}}$  differ by  $S_{uv}$ , the equality  $\mathbb{E} [R_j^{\otimes 1,1}] |\Psi_{1,\infty}^{\mathbf{R}}\rangle = |\Psi_{1,\infty}^{\mathbf{R}}\rangle$  implies that  $\langle \Phi | \Psi_{1,\infty}^{\mathbf{R}} \rangle = \langle \Phi' | \Psi_{1,\infty}^{\mathbf{R}} \rangle$ . The connectivity of  $G$  and the particle number symmetry thus indicates

$$|\Psi_{1,\infty}^{\mathbf{R}}\rangle \propto \sum_{\substack{|\Phi\rangle \in \mathcal{S}_1^{\text{even}}, \\ \#|11\rangle \text{ in } |\Phi\rangle \text{ is } n_e}} |\Phi\rangle. \quad (103)$$

The coefficient in (Supplementary Equation (103)) must be  $\binom{n}{n_e}^{-1}$  by the equality  $\langle \mathbb{1}_{2^n} | \Psi_{1,\infty}^{\mathbf{R}} \rangle = 1$ . Lastly, since  $O = \hat{a}_p^\dagger \hat{a}_q + h.c.$ ,

$$|O^2\rangle = |N_p + N_q - N_p N_q\rangle = \left( |00\rangle_p |11\rangle_q + |11\rangle_p |00\rangle_q \right) \otimes \bigotimes_{a \neq p,q} (|00\rangle + |11\rangle)_a. \quad (104)$$

And therefore,

$$\mathbb{E} [C(\boldsymbol{\theta}; U_\infty^{\mathbf{R}}, O^2)] = \langle O^2 | \Psi_{1,\infty}^{\mathbf{R}} \rangle = 2 \binom{n-2}{n_e-1} \binom{n}{n_e}^{-1} = \frac{2n_e(n-n_e)}{n(n-1)}. \quad (105)$$

Such an upper bound is at least  $1/\text{poly}(n)$ , and is roughly  $1/2$  when  $n_e = n/2$ , definitely not enough to argue for an exponential decay, which is a sufficient condition for BP.

## Supplementary Note 10: Proof of main result: Case 1

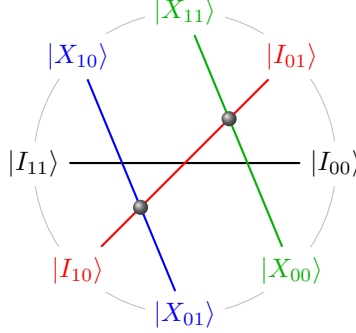
In this section, we prove the polynomial concentration of cost function for alternated dUCC ansätze containing only single excitation rotations, with mild connectivity assumption (Theorem 5 (Item 1)). Examples of such ansätze include  $k$ -BRA,  $k$ -UCCS and  $k$ -UCCGS.

**Definition 13** (Crossing number of paired state). *Let  $|\Phi\rangle \in \mathcal{S}_2^{\text{paired}}$ . Draw a graph of  $n$  vertices according to  $|\Phi\rangle$  as follows:*

1. Place the  $n$  sites of  $|\Phi\rangle$  in order on a circle. Color  $|I_{01}\rangle, |I_{10}\rangle$  by red,  $|X_{00}\rangle, |X_{11}\rangle$  by green, and  $|X_{01}\rangle, |X_{10}\rangle$  by blue. Do not color  $|I_{00}\rangle, |I_{11}\rangle$ .
2. Draw an edge inside the circle between any two sites of the same color, and color it with this same color. Make sure no three edges cross at the same point.

The crossing number of  $|\Phi\rangle$ , denoted by  $\text{cr}(|\Phi\rangle)$ , is defined to be the minimal number of crossing points of edges in color red and green, or green and blue, or red and blue. Alternatively, suppose site  $i$  is colored by  $c(i) \in \{\perp, R, G, B\}$  as above,

$$\text{cr}(|\Phi\rangle) := \#\left\{(i_1, i_2, i_3, i_4) \mid \begin{array}{l} 0 \leq i_1 < i_2 < i_3 < i_4 \leq n, c(i_1) \neq c(i_2), \\ c(i_1) = c(i_3) \neq \perp, c(i_2) = c(i_4) \neq \perp \end{array}\right\}. \quad (106)$$



**Supplementary Figure 5** Illustration of Definition 13. The crossing number of this paired state is 2, with the corresponding crossing points marked by gray balls. Notice that there are 3 crossing points not counted into the crossing number, since the horizontal edge is not colored.

For example, the crossing number of the paired state in Supplementary Equation (78) is 2 (Supplementary Figure 5). We need the following properties of crossing numbers in the proof.

**Lemma 26** (Properties of crossing numbers). *Let  $|\Phi\rangle \in \mathcal{S}_2^{\text{paired}}$ ,  $1 \leq u < v \leq n$ ,  $\mathbf{z} := \bigoplus_{a \in (u,v)} \Phi_a$ . The following properties of crossing numbers hold.*

1.  $\text{cr}(S_{uv}|\Phi\rangle) - \text{cr}(|\Phi\rangle) \equiv (\Phi_u \oplus \mathbf{z}) \odot (\Phi_v \oplus \mathbf{z}) \pmod{2}$ .
2. If  $|\Phi_u\rangle = |I_{00}\rangle$ ,  $|\Phi_v\rangle = |I_{11}\rangle$ , then

$$\begin{aligned} \text{cr}(|\Phi\rangle) &\equiv z_1 + z_2 + \text{cr}(F_{uv}^{12}|\Phi\rangle) \equiv z_1 + z_3 + \text{cr}(F_{uv}^{13}|\Phi\rangle) \\ &\equiv z_2 + z_3 + \text{cr}(F_{uv}^{23}|\Phi\rangle) \pmod{2}. \end{aligned} \quad (107)$$

*Proof.* Item 1. — The key observation here is that by swapping two neighboring sites  $j, j+1$  of  $|\Phi\rangle$ , the parity of crossing number will change by  $\Phi_j \odot \Phi_{j+1}$ . Indeed, if one of  $\Phi_j$  or  $\Phi_{j+1}$  is not colored or are both in the same color, then  $\Phi_j \odot \Phi_{j+1} \equiv 0$ , and swapping  $\Phi_j$  with  $\Phi_{j+1}$  will not change the crossing number. And if  $\Phi_j$  and  $\Phi_{j+1}$  are in different colors, then  $\Phi_j \odot \Phi_{j+1} \equiv 1$ , and swapping  $\Phi_j$  with  $\Phi_{j+1}$  will change the parity of crossing number since there are even-number of red, green or blue sites and thus the degrees of  $\Phi_j$  and  $\Phi_{j+1}$  are both odd. Consider the paired state sequence  $(|\Phi^{(t)}\rangle)_{1 \leq t \leq T}$  where  $T = 2v - 2u - 1$  and

$$|\Phi^{(t)}\rangle = \begin{cases} |\Phi\rangle, & t = 0, \\ S_{u+t-1, u+t}|\Phi^{(t-1)}\rangle, & 1 \leq t \leq v-u, \\ S_{2v-u-t-1, 2v-u-t}|\Phi^{(t-1)}\rangle, & v-u < t \leq T. \end{cases} \quad (108)$$

Notice that  $|\Phi^{(T)}\rangle = S_{uv}|\Phi\rangle$ . By the observation above,

$$\text{cr}(|\Phi^{(t)}\rangle) - \text{cr}(|\Phi^{(t-1)}\rangle) \equiv \begin{cases} \Phi_u \odot \Phi_{u+t}, & 0 < t \leq v-u, \\ \Phi_v \odot \Phi_{2v-u-t}, & v-u < t \leq T. \end{cases} \quad (109)$$

Thus,

$$\text{cr}(S_{uv}|\Phi\rangle) - \text{cr}(|\Phi\rangle) = \sum_{t=1}^T \left( \text{cr}(|\Phi^{(t)}\rangle) - \text{cr}(|\Phi^{(t-1)}\rangle) \right) \equiv (\Phi_u \oplus \mathbf{z}) \odot (\Phi_v \oplus \mathbf{z}). \quad (110)$$

The last equation uses the fact that  $\mathbf{z} \odot \mathbf{z} \equiv 0$ .

Item 2. — Let  $|\Phi^z\rangle = |\Phi\rangle$ ,  $|\Phi^a\rangle = F_{uv}^{12}|\Phi\rangle$ ,  $|\Phi^b\rangle = F_{uv}^{13}|\Phi\rangle$ ,  $|\Phi^c\rangle = F_{uv}^{23}|\Phi\rangle$ . Notice that Supplementary Equation (107) is equivalent to

$$\Phi_u^z \odot \mathbf{z} + \text{cr}(|\Phi^z\rangle) \equiv \Phi_u^a \odot \mathbf{z} + \text{cr}(|\Phi^a\rangle) \equiv \Phi_u^b \odot \mathbf{z} + \text{cr}(|\Phi^b\rangle) \equiv \Phi_u^c \odot \mathbf{z} + \text{cr}(|\Phi^c\rangle) \pmod{2}. \quad (111)$$

- If  $u + 1 = v$ , then  $\mathbf{z} = 0$ . By changing  $|\Phi^z\rangle$  to  $|\Phi^a\rangle$  (or  $|\Phi^b\rangle, |\Phi^c\rangle$ ), site  $u$  and  $v$  will both be colored by red (or green, blue), and the number of crossing points increased will be even. Hence,

$$\text{cr}(|\Phi^z\rangle) \equiv \text{cr}(|\Phi^a\rangle) \equiv \text{cr}(|\Phi^b\rangle) \equiv \text{cr}(|\Phi^c\rangle) \pmod{2}, \quad (112)$$

and Supplementary Equation (111) follows.

- If  $u + 1 < v$ , then by Supplementary Equation (110),

$$\text{cr}(S_{u,v-1}|\Phi^x\rangle) \equiv \text{cr}(|\Phi^x\rangle) + \Phi_u^x \odot \mathbf{z} + \mathbf{z} \odot \Phi_{v-1}^x, \quad \forall x \in \{z, a, b, c\}. \quad (113)$$

Similar to Supplementary Equation (112),

$$\text{cr}(S_{u,v-1}|\Phi^z\rangle) \equiv \text{cr}(S_{u,v-1}|\Phi^a\rangle) \equiv \text{cr}(S_{u,v-1}|\Phi^b\rangle) \equiv \text{cr}(S_{u,v-1}|\Phi^c\rangle) \pmod{2}. \quad (114)$$

Finally, notice that  $\Phi_{v-1}^z = \Phi_{v-1}^a = \Phi_{v-1}^b = \Phi_{v-1}^c$ . Combined with Supplementary Equations (113) and (114) we have proved Supplementary Equation (111).  $\square$

**Lemma 27.** *Let  $G = (V, E)$  be a connected graph with  $|V| = n$  vertices. Suppose  $\mathbf{R}$  contains a subsequence of single excitation rotations  $(A_{uv})_{(u,v) \in E}$ . Let  $M$  be the intersection space of  $\mathbf{R}$  defined in Corollary 13 at  $t = 2$ . For any  $|\Phi\rangle, |\Phi'\rangle \in \mathcal{S}_{2,(a,b,c)}^{\text{paired}}$ ,  $(-1)^{\text{cr}(|\Phi\rangle)}|\Phi\rangle - (-1)^{\text{cr}(|\Phi'\rangle)}|\Phi'\rangle \in M^\perp$ .*

*Proof.* The proof is similar to that of Corollary 21, but more specific.

- Suppose  $|\Phi'\rangle = S_{uv}|\Phi\rangle$  for some  $(u, v) \in E$  and  $u < v$ . By assumption, there exist some  $R_j \in \mathbf{R}$  such that  $R_j = A_{uv}$ . Thus, by Lemma 20 (Item 1),  $|\Phi\rangle - (-1)^{(\Phi_u \oplus \mathbf{z}) \odot (\Phi_v \oplus \mathbf{z})}|\Phi'\rangle \in (M_j \cap \mathcal{H}_2^{\text{paired}})^\perp \cap \mathcal{H}_2^{\text{paired}}$ , where  $\mathbf{z} := \bigoplus_{a \in (u,v)} \Phi_a$ . By Lemma 14,  $(M_j \cap \mathcal{H}_2^{\text{paired}})^\perp \cap \mathcal{H}_2^{\text{paired}} \subseteq M^\perp$ . And by Lemma 26,  $(\Phi_u \oplus \mathbf{z}) \odot (\Phi_v \oplus \mathbf{z}) \equiv \text{cr}(|\Phi'\rangle) - \text{cr}(|\Phi\rangle) \pmod{2}$ . Hence,  $(-1)^{\text{cr}(|\Phi\rangle)}|\Phi\rangle - (-1)^{\text{cr}(|\Phi'\rangle)}|\Phi'\rangle \in M^\perp$ .
- Otherwise,  $|\Phi'\rangle = S_\pi|\Phi\rangle$  for some  $\pi \in \mathfrak{S}_n$ . The permutation  $\pi$  can be decomposed into a product of swaps, and by the fact that  $G$  is connected, each swap can, in turn, be decomposed into a product of swaps on edges (pick an arbitrary path connecting  $(u, v)$  in  $G$ , the swap  $(u v)$  can be decomposed into a product of swaps along the path). Hence, there exists  $T \in \mathbb{N}$  and a sequence of edges  $(u_t, v_t)_{1 \leq t \leq T} \subseteq E$ , such that  $\pi = \prod_{t=1}^T (u_t v_t)$ . Let  $|\Phi^{(t)}\rangle = \prod_{i=1}^t S_{u_i v_i}|\Phi\rangle$ , we have  $|\Phi^{(0)}\rangle = |\Phi\rangle$ ,  $|\Phi^{(T)}\rangle = |\Phi'\rangle$  and  $|\Phi^{(t)}\rangle = S_{u_t v_t}|\Phi^{(t-1)}\rangle$  for  $1 < t \leq T$ . By the previous case,  $(-1)^{\text{cr}(|\Phi^{(t-1)}\rangle)}|\Phi^{(t-1)}\rangle - (-1)^{\text{cr}(|\Phi^{(t)}\rangle)}|\Phi^{(t)}\rangle \in M^\perp$  for  $1 < t \leq T$ . The sum of these  $T - 1$  vectors yields  $(-1)^{\text{cr}(|\Phi\rangle)}|\Phi\rangle - (-1)^{\text{cr}(|\Phi'\rangle)}|\Phi'\rangle$ , which is also a member of  $M^\perp$ .  $\square$

**Theorem 28.** *Let  $G = (V, E)$  be a connected graph with  $|V| = n$  vertices,  $\mathbf{R}$  be a sequence of single excitation rotations  $(A_{uv})_{(u,v) \in E}$ . Define  $m := \min\{n_e, n - n_e\}$ . The  $(\mathbf{R}, 2, \infty)$ -moment vector is*

$$|\Psi_{2,\infty}^{\mathbf{R}}\rangle = \frac{\binom{n+4}{2}}{\binom{n}{n_e} \binom{n+4}{n_e+2}} \sum_{\substack{a,b,c \geq 0, \\ a+b+c \leq m}} \frac{|\Psi_{(a,b,c)}\rangle}{\binom{a+b+c+2}{2} \binom{a+b+c}{a,b,c}}, \quad (115)$$

where  $|\Psi_{(a,b,c)}\rangle := \sum_{|\Phi\rangle \in \mathcal{S}_{2,(a,b,c)}^{\text{paired}}} (-1)^{\text{cr}(|\Phi\rangle)}|\Phi\rangle$ .

*Proof.* Denote the right-hand side of Supplementary Equation (115) by  $|\Psi^*\rangle$ . Use the notations  $M, M_j$  from Corollary 13. Since  $|\Psi_{2,\infty}^{\mathbf{R}}\rangle = P_M |\psi_0\rangle^{\otimes 4}$ , in order to prove  $|\Psi_{2,\infty}^{\mathbf{R}}\rangle = |\Psi^*\rangle$ , it suffices to prove that (1)  $|\Psi^*\rangle \in M$  and (2)  $|\Psi^*\rangle - |\psi_0\rangle^{\otimes 4} \in M^\perp$ .

(1) Obviously,  $|\Psi^*\rangle \in \mathcal{H}_2^{\text{paired}}$ . We prove that  $|\Psi^*\rangle$  is orthogonal to  $(M_j \cap \mathcal{H}_2^{\text{paired}})^\perp \cap \mathcal{H}_2^{\text{paired}}$ , for each  $R_j \in \mathbf{R}$ . If so, we have  $|\Psi^*\rangle \in M$  by Lemma 14. Recall the spanning set of  $(M_j \cap \mathcal{H}_2^{\text{paired}})^\perp \cap \mathcal{H}_2^{\text{paired}}$  characterized in Lemma 20 (Item 1). Suppose  $R_j = A_{uv}$ . For any  $|\Phi\rangle \in \mathcal{S}_{2,(a,b,c)}^{\text{paired}}$ , let  $\mathbf{z} = \bigoplus_{a \in (u,v)} \Phi_a$ . We check the following two cases.

- $|\Psi^*\rangle$  is orthogonal to  $|\Phi\rangle - (-1)^{(\Phi_u \oplus \mathbf{z}) \odot (\Phi_v \oplus \mathbf{z})} \mathcal{S}_{uv} |\Phi\rangle$ . In fact, the overlap between these two vectors is proportional to  $(-1)^{\text{cr}(|\Phi\rangle)} - (-1)^{(\Phi_u \oplus \mathbf{z}) \odot (\Phi_v \oplus \mathbf{z}) + \text{cr}(\mathcal{S}_{uv} |\Phi\rangle)}$ , which is 0 by Lemma 26 (Item 1).
- $|\Psi^*\rangle$  is orthogonal to  $|\Phi\rangle - (-1)^{z_1+z_2} F_{uv}^{12} |\Phi\rangle - (-1)^{z_1+z_3} F_{uv}^{13} |\Phi\rangle - (-1)^{z_2+z_3} F_{uv}^{23} |\Phi\rangle$ . In fact, the overlap between these two vectors is proportional to

$$\begin{aligned} & \frac{(-1)^{\text{cr}(|\Phi\rangle)}}{\binom{k+2}{2} \binom{k}{a,b,c}} - \frac{(-1)^{z_1+z_2+\text{cr}(|F_{uv}^{12}\Phi\rangle)}}{\binom{k+3}{2} \binom{k+1}{a+1,b,c}} \\ & - \frac{(-1)^{z_1+z_3+\text{cr}(|F_{uv}^{13}\Phi\rangle)}}{\binom{k+3}{2} \binom{k+1}{a,b+1,c}} - \frac{(-1)^{z_2+z_3+\text{cr}(|F_{uv}^{23}\Phi\rangle)}}{\binom{k+3}{2} \binom{k+1}{a,b,c+1}}. \end{aligned} \quad (116)$$

Here we define  $k := a+b+c$ . By Lemma 26 (Item 2), the numerators in the four fractions in Supplementary Equation (116) are the same. Factoring out the four identical numerators, it can be proved that Supplementary Equation (116) equals 0 for any integer  $a, b, c$  using combinatorial arguments.

(2) Next, we prove  $|\Psi^*\rangle - |\psi_0\rangle^{\otimes 4} \in M^\perp$ , by expressing  $|\Psi^*\rangle - |\psi_0\rangle^{\otimes 4}$  as a linear combination of vectors in  $(M \cap \mathcal{H}_2^{\text{paired}})^\perp \cap \mathcal{H}_2^{\text{paired}} \subseteq M^\perp$ . Recalls that the union of the spanning sets of each  $(M_j \cap \mathcal{H}_2^{\text{paired}})^\perp \cap \mathcal{H}_2^{\text{paired}}$  (characterized in Lemma 20 (Item 1)) spans  $(M \cap \mathcal{H}_2^{\text{paired}})^\perp \cap \mathcal{H}_2^{\text{paired}}$ .

- For any  $|\Phi\rangle \in \mathcal{S}_{2,(0,0,0)}^{\text{paired}}$ , by Lemma 27, we have

$$|\Phi\rangle - |\psi_0\rangle^{\otimes 4} \in M^\perp. \quad (117)$$

- For  $|\Phi^z\rangle \in \mathcal{S}_{2,(a,b,c)}^{\text{paired}}$ ,  $|\Phi^a\rangle \in \mathcal{S}_{2,(a+1,b,c)}^{\text{paired}}$ ,  $|\Phi^b\rangle \in \mathcal{S}_{2,(a,b+1,c)}^{\text{paired}}$ ,  $|\Phi^c\rangle \in \mathcal{S}_{2,(a,b,c+1)}^{\text{paired}}$ , by Lemma 20, Lemma 26 (Item 2), and Lemma 27, we have

$$\begin{aligned} & (-1)^{\text{cr}(|\Phi^z\rangle)} |\Phi^z\rangle - (-1)^{\text{cr}(|\Phi^a\rangle)} |\Phi^a\rangle \\ & - (-1)^{\text{cr}(|\Phi^b\rangle)} |\Phi^b\rangle - (-1)^{\text{cr}(|\Phi^c\rangle)} |\Phi^c\rangle \in M^\perp. \end{aligned} \quad (118)$$

We show that there exists functions  $w, s : \mathbb{N}^3 \rightarrow \mathbb{R}$ , such that

$$\begin{aligned} |\Psi^*\rangle - |\psi_0\rangle^{\otimes 4} &= \frac{1}{s(0,0,0)} \sum_{(117)} (|\Phi\rangle - |\psi_0\rangle^{\otimes 4}) \\ & - \sum_{a,b,c} w(a,b,c) \sum_{(118)} \left( (-1)^{\text{cr}(|\Phi^z\rangle)} |\Phi^z\rangle - (-1)^{\text{cr}(|\Phi^a\rangle)} |\Phi^a\rangle \right. \\ & \quad \left. - (-1)^{\text{cr}(|\Phi^b\rangle)} |\Phi^b\rangle - (-1)^{\text{cr}(|\Phi^c\rangle)} |\Phi^c\rangle \right). \end{aligned} \quad (119)$$

Here the under script indicates that the summation is taken over vectors in Supplementary Equations (117) and (118). Let  $D := \frac{\binom{n+4}{2}}{\binom{n}{n_e} \binom{n+4}{n_e+2}}$ . Let  $s(a,b,c)$  be the number of different paired states with configuration  $(a,b,c)$ :

$$s(a,b,c) := \frac{n!}{(n - n_e - a - b - c)(n_e - a - b - c)!(a!b!c!)^2}, \quad (120)$$

and define

$$w(a,b,c) := \frac{a!b!c!}{s(a+1,b,c)s(a,b+1,c)s(a,b,c+1)} f(a+b+c), \quad (121)$$

where

$$f(k) := \begin{cases} \frac{1}{\binom{n}{n_e}} - D, & k = 0, \\ \frac{k}{(n-n_e-k+1)(n_e-k+1)} f(k-1) - \frac{D}{\binom{k+2}{2} k!}, & k \geq 1. \end{cases} \quad (122)$$

Comparing the coefficients of vectors on both sides of Supplementary Equation (119), we have to prove the following linear equations.

$$\begin{aligned} D &= \frac{1 - s(0, 0, 0)}{s(0, 0, 0)} - w(0, 0, 0)s(1, 0, 0)s(0, 1, 0)s(0, 0, 1), \quad (123) \\ \frac{D}{\binom{k+2}{2} \binom{k}{a, b, c}} &= -w(a, b, c)s(a+1, b, c)s(a, b+1, c)s(a, b, c+1) \\ &\quad + w(a-1, b, c)s(a-1, b, c)s(a-1, b+1, c)s(a-1, b, c+1) \\ &\quad + w(a, b-1, c)s(a, b-1, c)s(a+1, b-1, c)s(a, b-1, c+1) \\ &\quad + w(a, b, c-1)s(a, b, c-1)s(a+1, b, c-1)s(a, b+1, c-1). \quad (124) \end{aligned}$$

Here we define  $k := a + b + c$ , and  $w(a, b, c) = s(a, b, c) = 0$  if at least one of  $a, b, c < 0$ . Supplementary Equation (123) follows from definition. It can be verified that the right-hand side of Supplementary Equation (124) equals

$$a!b!c! \left( -f(k) + \frac{k}{(n-n_e-k+1)(n_e-k+1)} f(k-1) \right), \quad (125)$$

which equals the left-hand side by definition.  $\square$

Notice that the moment vector  $|\Psi_{2, \infty}^{\mathbf{R}}\rangle$  in Theorem 28 does not depend on the structure of  $G$  except the connectivity. As an immediate corollary, the  $(\mathbf{R}, 2, \infty)$ -moment vectors of  $k$ -BRA,  $k$ -UCCS, and  $k$ -UCCGS are the same, since the underlying graphs  $G$ , which are a path, a complete bipartite graph, and a complete graph respectively, are all connected.

**Corollary 29.** *Let  $\mathbf{R}$  be defined in Theorem 28.*

$$|\Psi_{2, \infty}^{\text{BRA}}\rangle = |\Psi_{2, \infty}^{\text{UCCS}}\rangle = |\Psi_{2, \infty}^{\text{UCCGS}}\rangle = |\Psi_{2, \infty}^{\mathbf{R}}\rangle. \quad (126)$$

With  $|\Psi_{2, \infty}^{\mathbf{R}}\rangle$  characterized, we can calculate the 2<sup>nd</sup> moment of the cost function for any observables in the  $k \rightarrow \infty$  limit. The first case of the main result is stated formally as the following corollary.

**Corollary 30** (Main result, Case 1). *Let  $\mathbf{R}$  be defined in Theorem 28,  $C(\boldsymbol{\theta}; U_k^{\mathbf{R}}, H_{\text{el}})$  be the cost function defined in Supplementary Equation (33). Here the observable  $H_{\text{el}}$  is an electronic structure Hamiltonian defined in Supplementary Equation (35), with coefficients  $\mathbf{h} = (h_{pq})_{p>q}$ ,  $\mathbf{g} = (g_{pqrs})_{p>q>r>s}$ . We have*

$$\lim_{k \rightarrow \infty} \text{Var}(C(\boldsymbol{\theta}; U_k^{\mathbf{R}}, H_{\text{el}})) = \|\mathbf{h}\|_2^2 \frac{4n_e(n-n_e)}{n(n-1)(n+2)} + \|\mathbf{g}\|_2^2 \frac{2 \binom{n_e}{2} \binom{n-n_e}{2}}{45 \binom{n+2}{6}}. \quad (127)$$

*Proof.* Recall that

$$\begin{aligned} \text{Var}(C(\boldsymbol{\theta}; U_k^{\mathbf{R}}, H_{\text{el}})) &= \mathbb{E}[C(\boldsymbol{\theta}; U_k^{\mathbf{R}}, H_{\text{el}})^2] \\ &= (\langle H_{\text{el}} | \Psi_{2, \infty}^{\mathbf{R}} \rangle)^{\otimes 2} = \sum_{p>q} h_{pq}^2 (\langle \hat{a}_p^\dagger \hat{a}_q + h.c. |)^{\otimes 2} |\Psi_{2, \infty}^{\mathbf{R}}\rangle \\ &\quad + \sum_{p>q>r>s} g_{pqrs}^2 (\langle \hat{a}_p^\dagger \hat{a}_q^\dagger \hat{a}_r \hat{a}_s + h.c. |)^{\otimes 2} |\Psi_{2, \infty}^{\mathbf{R}}\rangle + \text{cross terms}. \quad (128) \end{aligned}$$

The contribution of cross terms is zero. To see that, take  $(\langle O_1 | \otimes \langle O_2 |) |\Psi_{2, \infty}^{\mathbf{R}}\rangle$  with  $O_1 = \hat{a}_p^\dagger \hat{a}_q + h.c.$ ,  $O_2 = \hat{a}_p^\dagger \hat{a}_r + h.c.$  ( $q \neq r$ ) as an example. Notice that  $P := \prod_{i=1}^n (\frac{1}{2} \mathbb{1}_{2^n}^{\otimes 2i} + \frac{1}{2} Z_i^{\otimes 2i})$  is the orthogonal projection onto  $\mathcal{H}_i^{\text{even}}$ . However,



$$\begin{aligned}
P(|O_1\rangle \otimes |O_2\rangle) &= P(O_1 \otimes \mathbb{1}_{2^n} \otimes O_2 \otimes \mathbb{1}_{2^n}) \sum_{j,j' \in [2^n]} |j, j, j', j'\rangle \\
&= \left( \prod_{i \in [n] \setminus \{q\}} \left( \frac{1}{2} \mathbb{1}_{2^n}^{\otimes 4} + \frac{1}{2} Z_i^{\otimes 4} \right) \right) (O_1 \otimes \mathbb{1}_{2^n} \otimes O_2 \otimes \mathbb{1}_{2^n}) \\
&\quad \underbrace{\left( \frac{1}{2} \mathbb{1}_{2^n}^{\otimes 4} - \frac{1}{2} Z_q^{\otimes 4} \right) \sum_{j,j' \in [2^n]} |j, j, j', j'\rangle}_{=0} = 0. \quad (129)
\end{aligned}$$

Hence,  $|O_1\rangle \otimes |O_2\rangle \in (\mathcal{H}_t^{\text{even}})^\perp$ . Consequently,  $(\langle O_1| \otimes \langle O_2|) |\Psi_{2,\infty}^{\mathbf{R}}\rangle = 0$  since  $|\Psi_{2,\infty}^{\mathbf{R}}\rangle \in \mathcal{H}_t^{\text{even}}$ . The same argument can be extended to when one or both of  $O_1, O_2$  are double excitation Hermitians, except for the tricky case where both  $O_1, O_2$  are double excitation Hermitians and the sets of indices are the same. For example, when  $O_1 = \hat{a}_1^\dagger \hat{a}_2^\dagger \hat{a}_3 \hat{a}_4 + h.c.$ ,  $O_2 = \hat{a}_1^\dagger \hat{a}_3^\dagger \hat{a}_2 \hat{a}_4 + h.c.$ ,  $(\langle O_1| \otimes \langle O_2|) |\Psi_{2,\infty}^{\mathbf{R}}\rangle$  may not be 0. However, we have assumed that terms like  $\hat{a}_1^\dagger \hat{a}_3^\dagger \hat{a}_2 \hat{a}_4 + h.c.$  do not appear in  $H_{\text{el}}$  to rule out the non-zero cases since they are not essential.

Finally, by Theorem 28 and Proposition 17,

$$(\langle \hat{a}_p^\dagger \hat{a}_q + h.c. |)^{\otimes 2} |\Psi_{2,\infty}^{\mathbf{R}}\rangle = \frac{4 \binom{n+4}{2}}{\binom{n}{n_e} \binom{n+4}{n_e+2}} \sum_{a=0}^{m-1} \frac{\binom{n-2}{2a} \binom{2a}{a} \binom{n-2-2a}{n_e-1-a}}{\binom{a+3}{2} \binom{a+1}{1}} \quad (130)$$

$$= \frac{4n_e(n-n_e)}{n(n-1)(n+2)}, \quad (131)$$

$$(\langle \hat{a}_p^\dagger \hat{a}_q \hat{a}_r \hat{a}_s + h.c. |)^{\otimes 2} |\Psi_{2,\infty}^{\mathbf{R}}\rangle = \frac{4 \binom{n+4}{2}}{\binom{n}{n_e} \binom{n+4}{n_e+2}} \sum_{a=0}^{m-2} \frac{\binom{n-4}{2a} \binom{2a}{a} \binom{n-4-2a}{n_e-2-a}}{\binom{a+4}{2} \binom{a+2}{2}} \quad (132)$$

$$= \frac{2 \binom{n_e}{2} \binom{n-n_e}{2}}{45 \binom{n+2}{6}}. \quad (133)$$

Here  $m := \min(n_e, n - n_e)$ . □

Notice that  $\lim_{k \rightarrow \infty} \text{Var}(C) = 1/\text{poly}(n)$  if  $h_{pq}, g_{pqrs} \in O(1)$ .

## Supplementary Note 11: Proof of main result: Case 2

In this section, we prove the polynomial/exponential concentration of the cost function for alternated dUCC ansätze containing only qubit single excitation rotations, with a mild connectivity assumption (Theorem 5 (Item 3)). Examples of such ansätze include  $k$ -qubit-UCCS and  $k$ -qubit-UCCGS.

**Theorem 31.** *Let  $G = (V, E)$  be a connected graph with  $|V| = n$  vertices,  $\mathbf{R}$  a sequence of qubit single excitation rotations  $(A_{uv}^{\text{qubit}})_{(u,v) \in E}$ . Define  $m := \min\{n_e, n - n_e\}$ . Depending on the structure of  $G$ , the moment vector  $|\Psi_{2,\infty}^{\mathbf{R}}\rangle$  admits one of the following forms.*

1. *If  $G$  is a path or a ring, then  $|\Psi_{2,\infty}^{\mathbf{R}}\rangle = S_\pi |\Psi_{2,\infty}^{\text{BRA}}\rangle$  with  $\pi \in \mathfrak{S}_n$  and  $(\pi(i), \pi(i+1)) \in E$  for all  $i \in [n-1]$ .*
2. *If  $n = 2n_e$ ,  $G$  is bipartite, and both parts of  $G$  have an even size (i.e., let  $V_1 \cup V_2$  be the unique partition of vertices such that both  $V_1$  and  $V_2$  are independent sets,  $|V_1|$  and  $|V_2|$  are both even), then  $|\Psi_{2,\infty}^{\mathbf{R}}\rangle$  can be written in the form of Supplementary Equation (96), with*

$$c(a, b, c) = \begin{cases} D, & \text{if } a = b = c = 0, \\ \frac{D}{3}, & \text{if exactly one of } a, b, c \text{ is nonzero, and } a + b + c < n_e, \\ \frac{\binom{n}{n_e} - 2}{\binom{n}{n_e} + 2} \cdot \frac{D}{3}, & \text{if exactly one of } a, b, c \text{ is nonzero, and } a + b + c = n_e, \\ \frac{2}{\binom{n}{n_e} + 2} \cdot \frac{D}{3}, & \text{if exactly two of } a, b, c \text{ is nonzero, and } a + b + c = n_e, \\ 0, & \text{otherwise.} \end{cases} \quad (134)$$

And for  $|\Phi\rangle \in \mathcal{S}_{2,(a,b,c)}^{\text{paired}}$ ,

$$\begin{aligned} & \text{sign}(|\Phi\rangle) \\ &= \begin{cases} -(-1)^{\sum_{p<q \in V_1} \Phi_p \odot \Phi_q}, & \text{if exactly two of } a, b, c \text{ is nonzero, and } a + b + c = n_e, \\ 1, & \text{otherwise.} \end{cases} \end{aligned} \quad (135)$$

Here we define  $D := \frac{3\binom{n}{n_e} + 6}{\binom{n}{n_e}^3 + 4\binom{n}{n_e}^2}$ .

3. Otherwise,  $|\Psi_{2,\infty}^{\mathbf{R}}\rangle$  is given in Supplementary Equation (97).

As an immediate corollary, we can determine the  $(\mathbf{R}, 2, \infty)$ -moment vector of  $k$ -qubit-UCCS and  $k$ -qubit-UCCGS, where the underlying graph  $G$  is a complete bipartite graph and a complete graph, respectively.

**Corollary 32.**  $|\Psi_{2,\infty}^{\text{qUCCS}}\rangle$  is determined by Theorem 31 (2), and  $|\Psi_{2,\infty}^{\text{qUCCGS}}\rangle$  is determined by Theorem 31 (3).

With  $|\Psi_{2,\infty}^{\mathbf{R}}\rangle$  characterized, we can calculate the 2<sup>nd</sup> moment of the cost function for any observables in the  $k \rightarrow \infty$  limit. Case 2 of the main result is stated formally as the following corollary.

**Corollary 33** (Main result, Case 2). Let  $\mathbf{R}, G$  be defined in Theorem 31, and  $C(\boldsymbol{\theta}; U_k^{\mathbf{R}}, H_{\text{el}})$  be the cost function defined in Supplementary Equation (33). Here the observable  $H_{\text{el}}$  is an electronic structure Hamiltonian defined in Supplementary Equation (35), with coefficients  $\mathbf{h} = (h_{pq})_{p>q}$ ,  $\mathbf{g} = (g_{pqrs})_{p>q>r>s}$ .

1. If  $G$  is a path or a ring, then  $\lim_{k \rightarrow \infty} \text{Var}(C)$  is the same as in Corollary 30.
2. If  $n = 2n_e$ ,  $G$  is bipartite, and both parts of  $G$  have an even size, then,

$$\begin{aligned} \lim_{k \rightarrow \infty} \text{Var}(C(\boldsymbol{\theta}; U_k^{\mathbf{R}}, H_{\text{el}})) &= \sum_{p>q} h_{pq}^2 \frac{4\binom{n-2}{n_e-1} \left[ \binom{n}{n_e} + 2(1 - (-1)^{[q \leq n_e < p] + p - q}) \right]}{\binom{n}{n_e}^3 + 4\binom{n}{n_e}^2} \\ &+ \sum_{p>q>r>s} g_{pqrs}^2 \frac{4\binom{n-4}{n_e-2} \left[ \binom{n}{n_e} + 2(1 - (-1)^{[q \leq n_e < p \vee s \leq n_e < r] + p - q + r - s}) \right]}{\binom{n}{n_e}^3 + 4\binom{n}{n_e}^2}. \end{aligned} \quad (136)$$

Here we define  $[P] = 1$  if a proposition  $P$  is true and  $[P] = 0$  otherwise.

3. Otherwise,

$$\lim_{k \rightarrow \infty} \text{Var}(C(\boldsymbol{\theta}; U_k^{\mathbf{R}}, H_{\text{el}})) = \|\mathbf{h}\|_2^2 \frac{4\binom{n-2}{n_e-1}}{\binom{n}{n_e}^2 + 2\binom{n}{n_e}} + \|\mathbf{g}\|_2^2 \frac{4\binom{n-4}{n_e-2}}{\binom{n}{n_e}^2 + 2\binom{n}{n_e}}. \quad (137)$$

*Proof.* Similar to the proof of Corollary 30, it suffices to evaluate  $\langle \langle O |^{\otimes 2} \rangle | \Psi_{2,\infty}^{\mathbf{R}} \rangle$  for  $O = \hat{a}_p^\dagger \hat{a}_q + h.c.$  and  $O = \hat{a}_p^\dagger \hat{a}_q^\dagger \hat{a}_r \hat{a}_s + h.c.$

Item 1. Case 1 is already proved in Corollary 30.

Item 2. Let  $D = \frac{3\binom{n}{n_e} + 6}{\binom{n}{n_e}^3 + 4\binom{n}{n_e}^2}$ . By Theorem 31 and Proposition 17,

$$\begin{aligned} & \langle \langle \hat{a}_p^\dagger \hat{a}_q + h.c. | \rangle^{\otimes 2} | \Psi_{2,\infty}^{\mathbf{R}} \rangle \\ &= \binom{n-2}{n_e-1} \cdot \frac{D}{3} - (-1)^{[q \leq n_e < p] + p - q} \binom{n-2}{n_e-1} \cdot \frac{2}{\binom{n}{n_e} + 2} \frac{D}{3} \\ &= \frac{4\binom{n-2}{n_e-1} \left[ \binom{n}{n_e} + 2(1 - (-1)^{[q \leq n_e < p] + p - q}) \right]}{\binom{n}{n_e}^3 + 4\binom{n}{n_e}^2}, \end{aligned} \quad (138)$$

$$\begin{aligned}
& (\langle \hat{a}_p^\dagger \hat{a}_q^\dagger \hat{a}_r \hat{a}_s + h.c. \rangle^{\otimes 2} | \Psi_{2,\infty}^{\mathbf{R}} \rangle) \\
&= \binom{n-4}{n_e-2} \cdot \frac{D}{3} - (-1)^{[q \leq n_e < p \vee s \leq n_e < r] + p - q + r - s} \binom{n-4}{n_e-2} \cdot \frac{2}{\binom{n}{n_e} + 2} \frac{D}{3} \\
&= \frac{4 \binom{n-4}{n_e-2} \left[ \binom{n}{n_e} + 2(1 - (-1)^{[q \leq n_e < p \vee s \leq n_e < r] + p - q + r - s}) \right]}{\binom{n}{n_e}^3 + 4 \binom{n}{n_e}^2}.
\end{aligned} \tag{139}$$

Item 3. By Theorem 31 and Proposition 17,

$$(\langle \hat{a}_p^\dagger \hat{a}_q + h.c. \rangle^{\otimes 2} | \Psi_{2,\infty}^{\mathbf{R}} \rangle) = \frac{4 \binom{n-2}{n_e-1}}{\binom{n}{n_e}^2 + 2 \binom{n}{n_e}}, \tag{140}$$

$$(\langle \hat{a}_p^\dagger \hat{a}_q^\dagger \hat{a}_r \hat{a}_s + h.c. \rangle^{\otimes 2} | \Psi_{2,\infty}^{\mathbf{R}} \rangle) = \frac{4 \binom{n-4}{n_e-2}}{\binom{n}{n_e}^2 + 2 \binom{n}{n_e}}. \tag{141}$$

□

Notice that if  $n_e = \Theta(n)$ ,  $\lim_{k \rightarrow \infty} \text{Var}(C) = 1/\text{poly}(n)$  in case Item 1, and  $\lim_{k \rightarrow \infty} \text{Var}(C) = \exp(-\Theta(n))$  in case Items 2 and 3.

### 11.1 Proof of Theorem 31 (1)

*Proof of Theorem 31 (Item 1).* The basis rotation ansätze consists of single excitation rotations acting on edges of a path that connects all neighboring qubits, i.e.,  $E = \{(i, i+1) | i \in [n-1]\}$ . When acting on two neighboring qubits, single excitations are equivalent to qubit single excitations ( $\hat{a}_{i+1}^\dagger \hat{a}_i = Q_{i+1} Q_i$ ). Thus, when  $G$  is a path connecting all neighboring qubits,  $|\Psi_{2,\infty}^{\mathbf{R}}\rangle$  is exactly  $|\Psi_{2,\infty}^{\text{BRA}}\rangle$ . Suppose  $G$  is an arbitrary path. Fix one of the two corresponding permutations  $\pi \in \mathfrak{S}_n$ , such that  $(\pi(i), \pi(i+1)) \in E, \forall i \in [n-1]$ . By examining the proof of Theorem 28, it can be checked that the moment vector remains unchanged if one replaces the initial state  $|\psi_0\rangle^{\otimes 4}$  by any paired state in  $\mathcal{S}_{2,(0,0,0)}^{\text{paired}}$ . Thus,

$$\begin{aligned}
S_\pi |\Psi_{2,\infty}^{\text{BRA}}\rangle &= S_\pi \lim_{k \rightarrow \infty} \prod_{l=1}^k \prod_{i=1}^{n-1} \tilde{A}_{i,i+1} |\psi_0\rangle^{\otimes 4} = S_\pi \lim_{k \rightarrow \infty} \prod_{l=1}^k \prod_{i=1}^{n-1} \tilde{A}_{i,i+1}^{\text{qubit}} (S_\pi^{-1} |\psi_0\rangle^{\otimes 4}) \\
&= \lim_{k \rightarrow \infty} \prod_{l=1}^k \prod_{i=1}^{n-1} \tilde{A}_{\pi(i), \pi(i+1)}^{\text{qubit}} |\psi_0\rangle^{\otimes 4} = |\Psi_{2,\infty}^{\mathbf{R}}\rangle.
\end{aligned} \tag{142}$$

To extend the conclusion to rings, it suffices to show the equality for the “standard” ring, i.e.,  $E = \{(i, i+1) | i \in [n-1]\} \cup \{(1, n)\}$ , and argue for arbitrary rings similar to Supplementary Equation (142). Let  $P_{M_1} = \tilde{A}_{1n}$ ,  $P_{M_2} = \tilde{A}_{1n}^{\text{qubit}}$ . It suffices to prove that  $M_1 \cap \mathcal{H}_2^{\text{paired}} = M_2 \cap \mathcal{H}_2^{\text{paired}}$ . If so, one can replace  $\tilde{A}_{1n}^{\text{qubit}}$  by  $\tilde{A}_{1n}$  without changing  $\mathbb{E}[C^2]$ . Since  $\tilde{A}_{i,i+1}^{\text{qubit}}$  can also be replaced by  $\tilde{A}_{i,i+1}$  for  $i \in [n-1]$ , one concludes that  $|\Psi_{2,\infty}^{\mathbf{R}}\rangle = |\Psi_{2,\infty}^{\text{BRA}}\rangle$  according to Theorem 28. Equivalently, we prove that the spanning sets are the same for  $(M_1 \cap \mathcal{H}_2^{\text{paired}})^\perp \cap \mathcal{H}_2^{\text{paired}}$  and  $(M_2 \cap \mathcal{H}_2^{\text{paired}})^\perp \cap \mathcal{H}_2^{\text{paired}}$ . By comparing Item 1 and Item 2 in Lemma 20, we need to prove for any  $|\Phi\rangle \in \mathcal{S}_2^{\text{paired}}$  with  $\mathbf{z} := \bigoplus_{1 < i < n} \Phi_i$ , that (1)  $(\Phi_1 \oplus \mathbf{z}) \odot (\Phi_n \oplus \mathbf{z}) \equiv \Phi_1 \odot \Phi_n \pmod{2}$ , (2) if  $|\Phi_1\rangle = |I_{00}\rangle, |\Phi_n\rangle = |I_{11}\rangle$ , then  $z_1 + z_2 \equiv z_1 + z_3 \equiv z_2 + z_3 \pmod{2}$ .

(1) Since  $|\Phi\rangle$  is a paired state, we have  $|\mathbf{z} \oplus \Phi_1 \oplus \Phi_n\rangle \in \{|I_{00}\rangle, |I_{11}\rangle\}$ . Hence,

$$\Phi_1 \odot \Phi_n \equiv (\Phi_1 \oplus (\mathbf{z} \oplus \Phi_1 \oplus \Phi_n)) \odot (\Phi_n \oplus (\mathbf{z} \oplus \Phi_1 \oplus \Phi_n)) \equiv (\Phi_1 \oplus \mathbf{z}) \odot (\Phi_n \oplus \mathbf{z}) \pmod{2}. \tag{143}$$

(2) Since  $|\Phi\rangle$  is a paired state, and  $|\Phi_1\rangle = |I_{00}\rangle, |\Phi_n\rangle = |I_{11}\rangle$ , we have  $|\mathbf{z}\rangle \in \{|I_{00}\rangle, |I_{11}\rangle\}$ . Hence,  $z_1 + z_2 \equiv z_1 + z_3 \equiv z_2 + z_3 \pmod{2}$ .

□

## 11.2 Proof of Theorem 31 (2)

**Lemma 34.** *Let  $G, \text{sign}, c$  be defined in Theorem 31 (Item 2). Suppose  $(u, v)$  is an edge of  $G$ . For any  $|\Phi\rangle \in \mathcal{S}_{2,(a,b,c)}^{\text{paired}}$ , if  $c(a, b, c) \neq 0$ , then  $\text{sign}(S_{uv}|\Phi\rangle) = (-1)^{\Phi_u \odot \Phi_v} \text{sign}(|\Phi\rangle)$ .*

*Proof.* Let  $|\Phi'\rangle = S_{uv}|\Phi\rangle$ . Recall that  $G$  is a bipartite graph, and the two parts  $V_1, V_2$  of  $G$  are both even. Assume without loss of generality that  $u \in V_1, v \in V_2$ . By definition,  $\text{sign}(|\Phi\rangle) / \text{sign}(|\Phi'\rangle) = (-1)^{(\Phi_u \oplus \Phi_v) \odot \bigoplus_{w \in V_1 \setminus \{v\}} \Phi_w}$ . We prove by comparing  $\text{sign}(|\Phi\rangle) / \text{sign}(|\Phi'\rangle)$  and  $(-1)^{\Phi_u \odot \Phi_v}$ .

- If  $\Phi_u = \bar{\Phi}_v$  or  $\Phi_u = \Phi_v$ , then  $\Phi_u \oplus \Phi_v \in \{|I_{00}\rangle, |I_{11}\rangle\}$ . Hence,  $\text{sign}(|\Phi\rangle) / \text{sign}(|\Phi'\rangle) = 1$ . Meanwhile,  $(-1)^{\Phi_u \odot \Phi_v} = 1$ .
- If one of  $\Phi_u, \Phi_v$  is  $|I_{00}\rangle$  or  $|I_{11}\rangle$ , then by the definition of  $c(a, b, c)$ , at most one of  $a, b, c$  is non-zero. In such case, we have  $\Phi_p \odot \Phi_q \equiv 0 \pmod{2}$  for any  $p, q \in V$ . Hence,  $\text{sign}(|\Phi\rangle) / \text{sign}(|\Phi'\rangle) = 1$ . Meanwhile,  $(-1)^{\Phi_u \odot \Phi_v} = 1$ .
- Otherwise, it must be the case that exactly two of  $a, b, c$  are non-zero, and  $\Phi_u \notin \{\Phi_v, \bar{\Phi}_v\}$ . We have  $\text{sign}(|\Phi\rangle) / \text{sign}(|\Phi'\rangle) = -1$ , since  $\bigoplus_{w \in V_1 \setminus u} \Phi_w$  must be one of  $\Phi_u, \bar{\Phi}_u, \Phi_v, \bar{\Phi}_v$ , by the fact that  $|V_1|$  is even. Meanwhile,  $(-1)^{\Phi_u \odot \Phi_v} = -1$ .

□

**Lemma 35.** *Let  $G, \text{sign}, c$  be defined in Theorem 31 (Item 2). Suppose  $(u, v)$  is an edge of  $G$ . For any  $|\Phi^z\rangle \in \mathcal{S}_{2,(a,b,c)}^{\text{paired}}$ , with  $|\Phi_u^z\rangle = |I_{00}\rangle, |\Phi_v^z\rangle = |I_{11}\rangle$ , let  $|\Phi^a\rangle = F_{uv}^{12}|\Phi^z\rangle, |\Phi^b\rangle = F_{uv}^{13}|\Phi^z\rangle, |\Phi^c\rangle = F_{uv}^{23}|\Phi^z\rangle$ . We have*

$$\begin{aligned} \text{sign}(|\Phi^z\rangle) c(a, b, c) &= \text{sign}(|\Phi^a\rangle) c(a+1, b, c) \\ &\quad + \text{sign}(|\Phi^b\rangle) c(a, b+1, c) + \text{sign}(|\Phi^c\rangle) c(a, b, c+1). \end{aligned} \quad (144)$$

*Proof.* We prove this by evaluating the values of  $\text{sign}$  and  $c$  in Supplementary Equation (144).

- If  $a = b = c = 0$ , the signs of  $|\Phi^z\rangle, |\Phi^a\rangle, |\Phi^b\rangle, |\Phi^c\rangle$  are all 1, and Supplementary Equation (144) follows from the equality  $D = \frac{D}{3} + \frac{D}{3} + \frac{D}{3}$ .
- If exactly one of  $a, b, c$  is non-zero, and  $a + b + c < n_e - 1$ , the signs of  $|\Phi^z\rangle, |\Phi^a\rangle, |\Phi^b\rangle, |\Phi^c\rangle$  are all 1, and Supplementary Equation (144) follows from the equality  $\frac{D}{3} = \frac{D}{3} + 0 + 0$ .
- If exactly one of  $a, b, c$  is non-zero, and  $a + b + c = n_e - 1$ , the signs of  $|\Phi^z\rangle, |\Phi^a\rangle, |\Phi^b\rangle, |\Phi^c\rangle$  are all 1. To see that, we may assume without loss of generality that  $u \in V_1$  and  $v \in V_2$ , and  $a = n_e - 1$ . By definition,  $\text{sign}(|\Phi^z\rangle) = \text{sign}(|\Phi^a\rangle) = 1$ , and

$$\text{sign}(|\Phi^b\rangle) = -(-1)^{\sum_{p < q \in V_1} \Phi_p^b \odot \Phi_q^b} = -(-1)^{\Phi_u^b \odot \bigoplus_{w \in V_1 \setminus u} \Phi_w^b} = 1, \quad (145)$$

since  $|\Phi_v^b\rangle \in \{|X_{00}\rangle, |X_{11}\rangle\}$  and  $|\Phi_w^b\rangle \in \{|I_{01}\rangle, |I_{10}\rangle\}$  for  $w \in V_1 \setminus \{v\}$ , and  $|V_1|$  is even. Similarly,  $\text{sign}(|\Phi^c\rangle) = 1$ . Supplementary Equation (144) follows from the equality

$$\frac{D}{3} = \frac{2}{\binom{n}{n_e} + 2} \cdot \frac{D}{3} + \frac{2}{\binom{n}{n_e} + 2} \cdot \frac{D}{3} + \frac{\binom{n}{n_e} - 2}{\binom{n}{n_e} + 2} \cdot \frac{D}{3}. \quad (146)$$

- Otherwise, we may assume that exactly two of  $a, b, c$  are non-zero, and  $a + b + c = n_e - 1$ , since in other cases the coefficients of  $|\Phi^z\rangle, |\Phi^a\rangle, |\Phi^b\rangle, |\Phi^c\rangle$  are all zero. Assume without loss of generality that  $c = 0, v \in V_1$ , and  $u \in V_2$ . By definition,

$$\text{sign}(|\Phi^a\rangle) / \text{sign}(|\Phi^b\rangle) = (-1)^{(\Phi_u^a \oplus \Phi_v^b) \odot \bigoplus_{w \in V_1 \setminus \{v\}} \Phi_w^a} = -1, \quad (147)$$

since  $|\Phi_v^a\rangle \in \{|I_{01}\rangle, |I_{10}\rangle\}$ ,  $|\Phi_v^b\rangle \in \{|X_{00}\rangle, |X_{11}\rangle\}$ ,  $|\Phi_w^a\rangle \in \{|I_{01}\rangle, |I_{10}\rangle, |X_{00}\rangle, |X_{11}\rangle\}$  for  $w \in V_1 \setminus \{v\}$ , and  $|V_1|$  is even. Supplementary Equation (144) follows from the equality

$$0 = \frac{2}{\binom{n}{n_e} + 2} \cdot \frac{D}{3} - \frac{2}{\binom{n}{n_e} + 2} \cdot \frac{D}{3} + 0. \quad (148)$$

□

**Lemma 36.** Let  $G = (V, E)$  be a simple, connected graph with  $|V| = n$  vertices and  $\max_{v \in V} \deg(v) \geq 3$ . Suppose  $\mathbf{R}$  contains a subsequence of qubit single excitation rotations  $(A_{uv}^{\text{qubit}})_{(u,v) \in E}$ . Let  $M$  be the intersection space of  $\mathbf{R}$  defined in Corollary 13 at  $t = 2$ . For any  $|\Phi\rangle \in \mathcal{S}_{2,(a,b,c)}^{\text{paired}}$ , if one of the following two cases happens, then  $|\Phi\rangle \in M^\perp$ .

1. Two of  $a, b, c$  are non-zero and  $2(a + b + c) < n$ .
2. All of  $a, b, c$  are non-zero.

*Proof.* Fix a vertex  $v \in V$  such that  $\deg(v) \geq 3$ , and pick  $u_1, u_2, u_3$  from the neighborhood of  $v$ . Then  $v, u_1, u_2, u_3$  form a star motif centered at  $v$ .

(1) Assume without loss of generality that  $a, b > 0$ . Since  $2(a + b + c) < n$ , there is at least one  $|I_{00}\rangle$  or  $|I_{11}\rangle$  in  $|\Phi\rangle$ . We may assume that

$$|\Phi_v\rangle = |I_{01}\rangle, |\Phi_{u_1}\rangle \in \{|I_{00}\rangle, |I_{11}\rangle\}, |\Phi_{u_2}\rangle = |X_{00}\rangle, |\Phi_{u_3}\rangle = |X_{11}\rangle. \quad (149)$$

This is because by Corollary 21, once we prove  $|\Phi\rangle \in M^\perp$ , we can argue that  $|\Phi'\rangle \in M^\perp$  for any  $|\Phi'\rangle \in \mathcal{S}_{2,(a,b,c)}^{\text{paired}}$ . Consider the vector sequence  $|\Phi^{(0)}\rangle = |\Phi\rangle$ , and

$$|\Phi^{(1)}\rangle = S_{vu_1} |\Phi\rangle, \quad |\Phi^{(2)}\rangle = S_{vu_2} |\Phi^{(1)}\rangle, \quad |\Phi^{(3)}\rangle = S_{vu_1} |\Phi^{(2)}\rangle, \quad (150)$$

$$|\Phi^{(4)}\rangle = S_{vu_3} |\Phi^{(3)}\rangle, \quad |\Phi^{(5)}\rangle = S_{vu_2} |\Phi^{(4)}\rangle, \quad |\Phi^{(6)}\rangle = S_{vu_1} |\Phi^{(5)}\rangle, \quad (151)$$

$$|\Phi^{(7)}\rangle = S_{vu_2} |\Phi^{(6)}\rangle, \quad |\Phi^{(8)}\rangle = S_{vu_3} |\Phi^{(7)}\rangle. \quad (152)$$

It can be verified that  $|\Phi^{(8)}\rangle = |\Phi\rangle$ . By Lemma 20 (Item 2), the following vectors lie in  $(M \cap \mathcal{H}_2^{\text{paired}})^\perp \cap \mathcal{H}_2^{\text{paired}} \subseteq M^\perp$ .

$$|\Phi^{(0)}\rangle - |\Phi^{(1)}\rangle, \quad |\Phi^{(1)}\rangle - |\Phi^{(2)}\rangle, \quad |\Phi^{(2)}\rangle + |\Phi^{(3)}\rangle, \quad |\Phi^{(3)}\rangle + |\Phi^{(4)}\rangle, \quad (153)$$

$$|\Phi^{(4)}\rangle - |\Phi^{(5)}\rangle, \quad |\Phi^{(5)}\rangle - |\Phi^{(6)}\rangle, \quad |\Phi^{(6)}\rangle - |\Phi^{(7)}\rangle, \quad |\Phi^{(7)}\rangle + |\Phi^{(8)}\rangle. \quad (154)$$

Combining these vectors to eliminate  $|\Phi^{(1)}\rangle, |\Phi^{(2)}\rangle, \dots, |\Phi^{(7)}\rangle$ , we get  $|\Phi\rangle \in M^\perp$ , since  $|\Phi^{(0)}\rangle = |\Phi^{(8)}\rangle = |\Phi\rangle$ .

(2) Similarly, assume that

$$|\Phi_v\rangle = |I_{01}\rangle, |\Phi_{u_1}\rangle = |X_{01}\rangle, |\Phi_{u_2}\rangle = |X_{00}\rangle, |\Phi_{u_3}\rangle = |X_{11}\rangle. \quad (155)$$

Consider the vector sequence in Supplementary Equations (150) to (152). By Lemma 20 (Item 2), the following vectors lie in  $(M \cap \mathcal{H}_2^{\text{paired}})^\perp \cap \mathcal{H}_2^{\text{paired}} \subseteq M^\perp$ .

$$|\Phi^{(0)}\rangle + |\Phi^{(1)}\rangle, \quad |\Phi^{(1)}\rangle + |\Phi^{(2)}\rangle, \quad |\Phi^{(2)}\rangle + |\Phi^{(3)}\rangle, \quad |\Phi^{(3)}\rangle + |\Phi^{(4)}\rangle, \quad (156)$$

$$|\Phi^{(4)}\rangle + |\Phi^{(5)}\rangle, \quad |\Phi^{(5)}\rangle + |\Phi^{(6)}\rangle, \quad |\Phi^{(6)}\rangle - |\Phi^{(7)}\rangle, \quad |\Phi^{(7)}\rangle + |\Phi^{(8)}\rangle. \quad (157)$$

Combining these vectors to eliminate  $|\Phi^{(1)}\rangle, |\Phi^{(2)}\rangle, \dots, |\Phi^{(7)}\rangle$ , we get  $|\Phi\rangle \in M^\perp$ , since  $|\Phi^{(0)}\rangle = |\Phi^{(8)}\rangle = |\Phi\rangle$ .  $\square$

**Lemma 37.** Same conditions as Theorem 31 (Item 2). For  $|\Phi\rangle, |\Phi'\rangle \in \mathcal{S}_2^{\text{paired}}$ , if  $\text{conf}(|\Phi\rangle) = \text{conf}(|\Phi'\rangle)$ , then  $\text{sign}(|\Phi\rangle)|\Phi\rangle - \text{sign}(|\Phi'\rangle)|\Phi'\rangle \in M^\perp$ .

*Proof.* Suppose  $\text{conf}(|\Phi\rangle) = (a, b, c)$ . If  $(a, b, c)$  satisfies the conditions in Lemma 36, then  $|\Phi\rangle, |\Phi'\rangle \in M^\perp$ , hence  $(-1)^{\text{sign}(|\Phi\rangle)}|\Phi\rangle - (-1)^{\text{sign}(|\Phi'\rangle)}|\Phi'\rangle \in M^\perp$ . Otherwise,  $c(a, b, c) \neq 0$  by definition in Supplementary Equation (134). The rest of the proof is similar to that of Lemma 27, using Lemma 20 (Item 2), Lemma 34 and connectivity of  $G$ .  $\square$

**Lemma 38.** Same condition as Theorem 31 (Item 2). For any  $|\Phi\rangle \in \mathcal{S}_{2,(a,b,c)}^{\text{paired}}, |\Phi'\rangle \in \mathcal{S}_{2,(a',b',c')}^{\text{paired}}$ , if one of the following 3 cases happens, we have  $\text{sign}(|\Phi\rangle)|\Phi\rangle - \text{sign}(|\Phi'\rangle)|\Phi'\rangle \in M^\perp$ .

1.  $a + b = a' + b' = n_e$  and  $a, b, a', b' > 0$ .
2.  $a + c = a' + c' = n_e$  and  $a, c, a', c' > 0$ .
3.  $b + c = b' + c' = n_e$  and  $b, c, b', c' > 0$ .

*Proof.* We prove the first case since the other 2 cases are similar. It suffices to prove that for any  $0 < l < n_e - 1$ , if  $a = l + 1, b = n_e - a, a' = l, b' = n_e - a'$ , then  $\text{sign}(|\Phi\rangle)|\Phi\rangle - \text{sign}(|\Phi'\rangle)|\Phi'\rangle \in M^\perp$ . Furthermore, we may assume that there exists  $(u, v) \in E$  and  $|\Phi^z\rangle \in \mathcal{S}_{2,(l,n_e-l-1,0)}^{\text{paired}}$  such that  $|\Phi\rangle = F_{uv}^{12}|\Phi^z\rangle, |\Phi'\rangle = F_{uv}^{13}|\Phi^z\rangle$ , since one can then use Lemma 37 to argue for general cases. By definition of  $G$ , there exists  $R_j \in \mathbf{R}$  such that  $R_j = A_{uv}^{\text{qubit}}$ . By Lemma 20 (Item 2) and Lemma 14,  $|\Phi^z\rangle - |\Phi\rangle - |\Phi'\rangle - F_{uv}^{23}|\Phi^z\rangle \in \left(M_j \cap \mathcal{H}_2^{\text{paired}}\right)^\perp \cap \mathcal{H}_2^{\text{paired}} \subseteq M^\perp$ . Since  $\text{conf}(|\Phi^z\rangle) = (l, n_e - l - 1, 0), \text{conf}(F_{uv}^{23}|\Phi^z\rangle) = (l, n_e - l - 1, 1)$ , we have  $|\Phi^z\rangle, F_{uv}^{23}|\Phi^z\rangle \in M^\perp$  according to Lemma 36. Hence,  $|\Phi\rangle + |\Phi'\rangle \in M^\perp$ . It remains to show that  $\text{sign}(|\Phi\rangle)/\text{sign}(|\Phi'\rangle) = -1$ , which has been proved in Supplementary Equation (147).  $\square$

*Proof of Theorem 31 (Item 2).* Denote the state specified in Supplementary Equations (134) to (135) by  $|\Psi^*\rangle$ . Use the notations  $M, M_j$  from Corollary 13. We proceed similarly to the proof of Theorem 28 by showing that (1)  $|\Psi^*\rangle \in M$  and (2)  $|\Psi^*\rangle - |\psi_0\rangle^{\otimes 4} \in M^\perp$ .

- (1) Obviously,  $|\Psi^*\rangle \in \mathcal{H}_2^{\text{paired}}$ . We prove that  $|\Psi^*\rangle$  is orthogonal to  $\left(M_j \cap \mathcal{H}_2^{\text{paired}}\right)^\perp \cap \mathcal{H}_2^{\text{paired}}$ , for each  $R_j \in \mathbf{R}$ . If so, we have  $|\Psi^*\rangle \in M$  by Lemma 14. Recall the spanning set of  $\left(M_j \cap \mathcal{H}_2^{\text{paired}}\right)^\perp \cap \mathcal{H}_2^{\text{paired}}$  characterized in Lemma 20 (Item 2). Suppose  $R_j = A_{uv}^{\text{qubit}}$ . For any  $|\Phi\rangle \in \mathcal{S}_{2,(a,b,c)}^{\text{paired}}$ , we check the following two cases.

- $|\Psi^*\rangle$  is orthogonal to  $|\Phi\rangle - (-1)^{\Phi_u \odot \Phi_v} S_{uv} |\Phi\rangle$ . In fact, the overlap between these two vectors is proportional to  $\text{sign}(|\Phi\rangle) - (-1)^{\Phi_u \odot \Phi_v} \text{sign}(S_{uv} |\Phi\rangle)$ , which is 0 by Lemma 34.
- $|\Psi^*\rangle$  is orthogonal to  $|\Phi\rangle - F_{uv}^{12}|\Phi\rangle - F_{uv}^{13}|\Phi\rangle - F_{uv}^{23}|\Phi\rangle$ . In fact, the overlap between these two vectors is proportional to  $\text{sign}(|\Phi\rangle) c(a, b, c) - \text{sign}(F_{uv}^{12}|\Phi\rangle) c(a + 1, b, c) - \text{sign}(F_{uv}^{13}|\Phi\rangle) c(a, b + 1, c) - \text{sign}(F_{uv}^{23}|\Phi\rangle) c(a, b, c + 1)$ , which is 0 by Lemma 35.

- (2) Next, we prove  $|\Psi^*\rangle - |\psi_0\rangle^{\otimes 4} \in M^\perp$ , by expressing  $|\Psi^*\rangle - |\psi_0\rangle^{\otimes 4}$  as a linear combination of vectors in  $\left(M \cap \mathcal{H}_2^{\text{paired}}\right)^\perp \cap \mathcal{H}_2^{\text{paired}} \subseteq M^\perp$ . Recalls that the union of the spanning sets of each  $\left(M_j \cap \mathcal{H}_2^{\text{paired}}\right)^\perp \cap \mathcal{H}_2^{\text{paired}}$  (characterized in Lemma 20 (Item 2)) spans  $\left(M \cap \mathcal{H}_2^{\text{paired}}\right)^\perp \cap \mathcal{H}_2^{\text{paired}}$ .

- For any  $|\Phi\rangle \in \mathcal{S}_{2,(0,0,0)}^{\text{paired}}$ , by Lemma 37,

$$|\Phi\rangle - |\psi_0\rangle^{\otimes 4} \in M^\perp. \quad (158)$$

- For any  $|\Phi^z\rangle \in \mathcal{S}_{2,(0,0,0)}^{\text{paired}}, |\Phi^a\rangle \in \mathcal{S}_{2,(1,0,0)}^{\text{paired}}, |\Phi^b\rangle \in \mathcal{S}_{2,(0,1,0)}^{\text{paired}}, |\Phi^c\rangle \in \mathcal{S}_{2,(0,0,1)}^{\text{paired}}$ , by Lemma 20 (Item 2) and Lemma 37,

$$|\Phi^z\rangle - |\Phi^a\rangle - |\Phi^b\rangle - |\Phi^c\rangle \in M^\perp. \quad (159)$$

- For any  $|\Phi^{a'}\rangle \in \mathcal{S}_{2,(l,0,0)}^{\text{paired}}, |\Phi^{a''}\rangle \in \mathcal{S}_{2,(l+1,0,0)}^{\text{paired}}$  with  $1 \leq l \leq n_e - 2$ , by Lemma 20 (Item 2), Lemma 36 and Lemma 37,

$$|\Phi^{a'}\rangle - |\Phi^{a''}\rangle \in M^\perp. \quad (160)$$

And similarly by replace  $a$  by  $b, c$  (and the corresponding configurations), we have

$$|\Phi^{b'}\rangle - |\Phi^{b''}\rangle \in M^\perp, \quad (161)$$

$$|\Phi^{c'}\rangle - |\Phi^{c''}\rangle \in M^\perp. \quad (162)$$

- For any  $|\Phi^{az}\rangle \in \mathcal{S}_{2,(n_e-1,0,0)}^{\text{paired}}, |\Phi^{aa}\rangle \in \mathcal{S}_{2,(n_e,0,0)}^{\text{paired}}, |\Phi^{ab}\rangle \in \mathcal{S}_{2,(l,n_e-l,0)}^{\text{paired}}, |\Phi^{ac}\rangle \in \mathcal{S}_{2,(l,0,n_e-l)}^{\text{paired}}$  with  $0 < l < n_e$ , by Lemma 20 (Item 2), Lemma 37 and Lemma 38,

$$|\Phi^{az}\rangle - |\Phi^{aa}\rangle - \text{sign}(|\Phi^{ab}\rangle)|\Phi^{ab}\rangle - \text{sign}(|\Phi^{ac}\rangle)|\Phi^{ac}\rangle. \quad (163)$$

And similarly by replacing  $a, b, c$  (and the corresponding configurations), we have

$$|\Phi^{bz}\rangle - |\Phi^{bb}\rangle - \text{sign}(|\Phi^{ab}\rangle) |\Phi^{ab}\rangle - \text{sign}(|\Phi^{bc}\rangle) |\Phi^{bc}\rangle, \quad (164)$$

$$|\Phi^{cz}\rangle - |\Phi^{cc}\rangle - \text{sign}(|\Phi^{ac}\rangle) |\Phi^{ac}\rangle - \text{sign}(|\Phi^{bc}\rangle) |\Phi^{bc}\rangle. \quad (165)$$

We prove that there exists functions  $s, w : \mathbb{N} \rightarrow \mathbb{R}$ , such that

$$\begin{aligned} & |\Psi^*\rangle - |\psi_0\rangle^{\otimes 4} \\ &= \frac{1}{s(0)} \sum_{(158)} (|\Phi\rangle - |\psi_0\rangle^{\otimes 4}) \\ &- w(0) \sum_{(159)} (|\Phi^z\rangle - |\Phi^a\rangle - |\Phi^b\rangle - |\Phi^c\rangle) \\ &- \sum_{l=1}^{n_e-2} w(l) \left( \sum_{(160)} (|\Phi^{a'}\rangle - |\Phi^{a''}\rangle) \right. \\ &\quad \left. + \sum_{(161)} (|\Phi^{b'}\rangle - |\Phi^{b''}\rangle) + \sum_{(162)} (|\Phi^{c'}\rangle - |\Phi^{c''}\rangle) \right) \\ &- w(n_e-1) \sum_{(163)} (|\Phi^{az}\rangle - |\Phi^{aa}\rangle - \text{sign}(|\Phi^{ab}\rangle) |\Phi^{ab}\rangle - \text{sign}(|\Phi^{ac}\rangle) |\Phi^{ac}\rangle) \\ &- w(n_e-1) \sum_{(164)} (|\Phi^{bz}\rangle - |\Phi^{bb}\rangle - \text{sign}(|\Phi^{ab}\rangle) |\Phi^{ab}\rangle - \text{sign}(|\Phi^{bc}\rangle) |\Phi^{bc}\rangle) \\ &- w(n_e-1) \sum_{(165)} (|\Phi^{cz}\rangle - |\Phi^{cc}\rangle - \text{sign}(|\Phi^{ac}\rangle) |\Phi^{ac}\rangle - \text{sign}(|\Phi^{bc}\rangle) |\Phi^{bc}\rangle). \end{aligned} \quad (166)$$

Here, the subscripts indicate that the summation is taken over vectors in Supplementary Equations (158) to (165).

Abusing the notation  $s(\cdot, \cdot, \cdot)$  in the proof of Theorem 28, we define  $s(l) := s(l, 0, 0)$ .  $w(\cdot)$  is defined recursively as follows:

$$w(l) = \begin{cases} s(1)^{-3} (s(0)^{-1} - D), & l = 0, \\ s(2)^{-1} (s(0)s(1)^2 w(0) - \frac{D}{3}), & l = 1, \\ s(l+1)^{-1} (s(l-1)w(l-1) - \frac{D}{3}), & 2 \leq l \leq n_e - 2, \\ \frac{1}{6s(n_e-1)s(n_e)} \cdot \frac{2}{\binom{n_e}{n_e}+2} \cdot \frac{3}{\binom{n_e}{n_e}^2-2\binom{n_e}{n_e}} \cdot \frac{D}{3}, & l = n_e - 1. \end{cases} \quad (167)$$

By comparing coefficients of vectors on both sides of Supplementary Equation (166), we have to prove the following linear equations:

$$D = \frac{1}{s(0)} - s(1)^3 w(0), \quad (168)$$

$$\frac{D}{3} = s(0)s(1)^2 w(0) - s(2)w(1), \quad (169)$$

$$\frac{D}{3} = s(l-1)w(l-1) - s(l+1)w(l), \quad (2 \leq l \leq n_e - 2), \quad (170)$$

$$\frac{D}{3} = s(n_e-2)w(n_e-2) - \left( \sum_{i=1}^{n_e-1} s(i, n_e-i, 0) \right)^2 s(n_e)w(n_e-1), \quad (171)$$

$$\frac{2}{\binom{n_e}{n_e}+2} \cdot \frac{D}{3} = 6s(n_e-1)s(n_e)w(n_e-1), \quad (172)$$

$$\frac{\binom{n_e}{n_e}-2}{\binom{n_e}{n_e}+2} \cdot \frac{D}{3} = \left( \sum_{i=1}^{n_e-1} s(i, n_e-i, 0) \right)^2 s(n_e-1)w(n_e-1). \quad (173)$$

Notice that Supplementary Equations (168) to (170) and (172) holds by definition, and one can check that Supplementary Equation (173) also holds. To prove Supplementary Equation (171), we multiply  $s(l)$  on both sides of Supplementary Equation (170) to get

$$s(l-1)s(l)w(l-1) - s(l)s(l+1)w(l) = \frac{D}{3}s(l), \quad 2 \leq l \leq n_e - 2. \quad (174)$$

Thus,

$$s(1)s(2)w(1) - s(n_e - 2)s(n_e - 1)w(n_e - 2) = \frac{D}{3} \sum_{l=2}^{n_e-2} s(l). \quad (175)$$

And Supplementary Equation (171) follows.  $\square$

### 11.3 Proof of Theorem 31 (3)

*Proof of Theorem 31 (3).* It suffices to prove that if  $|\Phi\rangle \in \mathcal{S}_{2,(a,b,c)}^{\text{paired}}$  and at least two of  $a, b, c$  is non-zero, then  $|\Phi\rangle \in \left(M \cap \mathcal{H}_2^{\text{paired}} \cap \bigcap_{\tau \in \mathfrak{S}_4} \mathcal{H}_2^\tau\right)^\perp$ . The rest follows immediately from Lemma 24. Since we did not fall into case 1 or 2, it must be  $\max_{v \in V} \deg v \geq 3$ , and

- (1)  $n \neq 2n_e$ ,
- (2) or  $G$  contains an odd ring as a subgraph, and the size of the ring is smaller than  $n$ ,
- (3) or  $G$  is bipartite, but one part of  $G$  has an odd size.

We prove that  $|\Phi\rangle \in M^\perp$  in the first 2 cases, and  $|\Phi\rangle \in \left(M \cap \mathcal{H}_2^{\text{paired}} \cap \bigcap_{\tau \in \mathfrak{S}_4} \mathcal{H}_2^\tau\right)^\perp$  in the 3<sup>rd</sup> case. It suffices to prove the case where exactly two of  $a, b, c$  are non-zero and  $2(a+b+c) = n$ , since otherwise  $|\Phi\rangle \in M^\perp$  according to Lemma 36. Assume without loss of generality that  $a, b > 0$  and  $2(a+b) = n$ .

- (1) If  $n \neq 2n_e$ , then  $a+b+c \leq \min(n_e, n-n_e) < \frac{n}{2}$ . Hence,  $|\Phi\rangle \in M^\perp$  by Lemma 36.
- (2) Suppose  $G$  contains a ring  $G' = (V', E')$  as subgraph, where  $V' = \{v_1, \dots, v_r\}, E' = \{(v_i, v_{i+1}) | i \in [r-1]\} \cup \{(v_1, v_r)\}$ , and  $3 \leq r \leq n$  is an odd number. Assume without loss of generality that  $|\Phi_{v_1}\rangle = |I_{01}\rangle, |\Phi_{v_r}\rangle = |X_{00}\rangle$ . Consider the vector sequence  $(|\Phi^{(t)}\rangle)_{0 \leq t \leq T}$  where  $T = 2r - 2$  such that

$$|\Phi^{(t)}\rangle = \begin{cases} |\Phi\rangle, & t = 0, \\ S_{t,t+1} |\Phi^{(t-1)}\rangle, & 1 \leq t < r, \\ S_{2r-t-2, 2r-t-1} |\Phi^{(t-1)}\rangle, & r \leq t < T, \\ S_{1r} |\Phi^{(t-1)}\rangle, & t = T. \end{cases} \quad (176)$$

It is easy to see that  $|\Phi^{(T)}\rangle = |\Phi\rangle$ . Construct a vector  $|\Phi^{(t)}\rangle \pm |\Phi^{(t+1)}\rangle \in M^\perp$  for each  $0 \leq t < T - 1$  according to Lemma 20 (Item 2), one can argue that  $|\Phi\rangle \in M^\perp$ .

- (3) Suppose the two parts of  $G$  are  $V_1, V_2$ , and  $|V_1|$  is odd. We first show that for any  $|\Phi\rangle \in \mathcal{S}_{2,(a,b,c)}^{\text{paired}}, |\Phi'\rangle \in \mathcal{S}_{2,(a',b',c')}^{\text{paired}}$ , if  $2(a+b) = 2(a'+b') = n$  and  $a, b, a', b' > 0$ , then

$$(-1)^{n_a(|\Phi\rangle; V_1)} |\Phi\rangle - (-1)^{n_a(|\Phi'\rangle; V_1)} |\Phi'\rangle \in M^\perp. \quad (177)$$

Here we define  $n_a(|\Phi\rangle; V_1) := n_{01}^I(|\Phi\rangle; V_1) + n_{10}^I(|\Phi\rangle; V_1)$ . The proof is similar to Lemma 37 and Lemma 38, hence we only provide a proof sketch.

- Supplementary Equation (177) holds if  $a = a'$ . — For any edge  $(u, v)$ , there exists  $R_j \in \mathbf{R}$  such that  $R_j = A_{pq}^{\text{qubit}}$ . By Lemma 20 (Item 2) and Lemma 14, we have  $|\Phi\rangle - (-1)^{\Phi_u \odot \Phi_v} S_{uv} |\Phi\rangle \in \left(M \cap \mathcal{H}_2^{\text{paired}}\right)^\perp \cap \mathcal{H}_2^{\text{paired}} \subseteq M^\perp$ . On the other hand, one checks that  $n_a(|\Phi\rangle; V_1) - n_a(S_{uv} |\Phi\rangle; V_1) \equiv \Phi_u \odot \Phi_v \pmod{2}$ . Hence, Supplementary Equation (177) holds if  $|\Phi'\rangle = S_{uv} |\Phi\rangle$ . The connectivity of  $G$  then implies that Supplementary Equation (177) holds if  $\text{conf}(|\Phi\rangle) = \text{conf}(|\Phi'\rangle) = (a, b, 0)$ .
- Supplementary Equation (177) holds if  $a = a' + 1$ . — We may assume that there exists  $(u, v) \in E$  and  $|\Phi^z\rangle \in \mathcal{S}_{2,(a',b,0)}^{\text{paired}}$  such that  $|\Phi\rangle = F_{uv}^{12} |\Phi^z\rangle, |\Phi'\rangle = F_{uv}^{13} |\Phi^z\rangle$ . By Lemma 20



(Item 2) and Lemma 14, we have  $|\Phi^z\rangle - |\Phi\rangle - |\Phi'\rangle - F_{uv}^{23}|\Phi^z\rangle \in \left(M \cap \mathcal{H}_2^{\text{paired}}\right)^\perp \cap \mathcal{H}_2^{\text{paired}} \subseteq M^\perp$ . By Lemma 36,  $|\Phi^z\rangle, F_{uv}^{23}|\Phi^z\rangle \in M^\perp$ . Hence,  $|\Phi\rangle + |\Phi'\rangle \in M^\perp$ . On the other hand,  $n_a(|\Phi\rangle; V_1) - n_a(|\Phi'\rangle; V_1) = 1$ . Hence, Supplementary Equation (177) holds.

Remark that when  $|V_1|$  is even,  $-(-1)^{n_a(|\Phi\rangle; V_1)}$  coincides with  $\text{sign}(|\Phi\rangle)$  defined in Supplementary Equation (135), while when  $|V_1|$  is odd  $\text{sign}(|\Phi\rangle)$  is always -1.

Next, we show that  $|\Phi\rangle \in M^\perp + (\mathcal{H}_2^\tau)^\perp$  with  $\tau = (1\ 4)$ , which completes the proof. Let  $|\Phi'\rangle = (S_\tau^b)^{\otimes n}|\Phi\rangle$ . It is straightforward to check that  $\text{conf}(|\Phi'\rangle) = (b, a, 0)$  and  $n_a(|\Phi\rangle; V_1) + n_a(|\Phi'\rangle; V_1) = |V_1| \equiv 1 \pmod{2}$ . Hence, by Supplementary Equation (177) we have  $|\Phi\rangle + |\Phi'\rangle \in M^\perp$ . On the other hand, by definition of  $\mathcal{H}_2^\tau$  we have  $|\Phi\rangle - |\Phi'\rangle \in (\mathcal{H}_2^\tau)^\perp$ . Thus,  $|\Phi\rangle \in M^\perp + (\mathcal{H}_2^\tau)^\perp$ .  $\square$

## Supplementary Note 12: Proof of main result: Case 3 and 4

In this section, we prove the exponential concentration of the cost function for alternated dUCC ansätze containing both single and double (qubit) excitation rotations, with a mild connectivity assumption (Theorem 5 (Items 2 and 4)). Examples of such ansätze include  $k$ -UCCSD,  $k$ -UCCGSD,  $k$ -UpCCGSD,  $k$ -qubit-UCCSD and  $k$ -qubit-UCCGSD.

**Theorem 39.** *Let  $G = (V, E)$  be a connected graph with  $|V| = n$  vertices,  $\mathbf{R}$  be a sequence of single excitation rotations  $(A_{uv})_{(u,v) \in E}$  concatenated with at least one double excitation rotation  $B_{pqrs}$ . We have  $|\Psi_{2,\infty}^{\mathbf{R}}\rangle = |\Psi_{2,\infty}^{\text{qUCCGS}}\rangle$ .*

*Proof.* It suffices to prove that if  $|\Phi\rangle \in \mathcal{S}_{2,(a,b,c)}^{\text{paired}}$  and at least two of  $a, b, c$  are non-zero, then  $|\Phi\rangle \in M^\perp$ . The theorem then follows immediately from Lemma 24. Assume without loss of generality that  $a, b > 0, p > q > r > s$ , and

$$|\Phi_p\rangle = |I_{01}\rangle, \quad |\Phi_q\rangle = |X_{00}\rangle, \quad |\Phi_r\rangle = |I_{10}\rangle, \quad |\Phi_s\rangle = |X_{11}\rangle. \quad (178)$$

Denote  $\mathbf{z}_1 = \bigoplus_{a \in (s,r)} \Phi_a, \mathbf{z}_2 = \bigoplus_{a \in (r,q)} \Phi_a, \mathbf{z}_3 = \bigoplus_{a \in (q,p)} \Phi_a$ . Consider the following state sequence:

$$|\Phi^{(0)}\rangle = |\Phi\rangle, \quad |\Phi^{(1)}\rangle = S_{sp}S_{rq}|\Phi\rangle, \quad |\Phi^{(2)}\rangle = S_{rq}|\Phi^{(1)}\rangle, \quad |\Phi^{(3)}\rangle = S_{sp}|\Phi^{(2)}\rangle. \quad (179)$$

Obviously  $|\Phi^{(3)}\rangle = |\Phi\rangle$ . By Lemma 20 (Item 3),

$$|\Phi^{(0)}\rangle - (-1)^{(\Phi_p \oplus \mathbf{z}_1 \oplus \mathbf{z}_3) \odot (\Phi_q \oplus \mathbf{z}_1 \oplus \mathbf{z}_3)} |\Phi^{(1)}\rangle \in \left(M \cap \mathcal{H}_2^{\text{paired}}\right)^\perp \cap \mathcal{H}_2^{\text{paired}} \subseteq M^\perp. \quad (180)$$

By Lemma 27,

$$|\Phi^{(1)}\rangle - (-1)^{(\Phi_q \oplus \mathbf{z}_2) \odot (\Phi_r \oplus \mathbf{z}_2)} |\Phi^{(2)}\rangle \in M^\perp, \quad (181)$$

$$|\Phi^{(2)}\rangle - (-1)^{(\Phi_p \oplus \mathbf{z}_1 \oplus \mathbf{z}_2 \oplus \mathbf{z}_3 \oplus \Phi_q \oplus \Phi_r) \odot (\Phi_s \oplus \mathbf{z}_1 \oplus \mathbf{z}_2 \oplus \mathbf{z}_3 \oplus \Phi_q \oplus \Phi_r)} |\Phi^{(3)}\rangle \in M^\perp. \quad (182)$$

Combining Supplementary Equations (180) to (182) to eliminate  $|\Phi^{(1)}\rangle, |\Phi^{(2)}\rangle$  we get  $|\Phi\rangle \in M^\perp$ , since  $|\Phi^{(0)}\rangle = |\Phi^{(3)}\rangle = |\Phi\rangle$ .  $\square$

For alternated qubit dUCC ansätze, we make mild assumptions about the topology  $G$  as well as the position of qubit double excitation rotations.

**Theorem 40.** *Let  $G = (V, E)$  be a connected graph with  $|V| = n$  vertices and  $\max_{v \in V} \deg(v) \geq 3$ ,  $\mathbf{R}$  be a sequence of qubit single excitation rotations  $(A_{uv}^{\text{qubit}})_{(u,v) \in E}$  concatenated with at least one qubit double excitation rotation  $B_{pqrs}^{\text{qubit}}$ . Assume, only when  $n = 2n_e$  and  $G$  is a bipartite graph with two non-empty even parts  $V = V_1 \cup V_2$ , that  $|V_1 \cap \{p, q, r, s\}| = 2$ . We have  $|\Psi_{2,\infty}^{\mathbf{R}}\rangle = |\Psi_{2,\infty}^{\text{qUCCGS}}\rangle$ .*

*Proof.* If  $n \neq 2n_e$  or  $G$  is not a bipartite graph with two non-empty even parts, then  $\dim M = 1$  (Theorem 31 (Item 3)), and it must be  $|\Psi_{2,\infty}^{\mathbf{R}}\rangle = |\Psi_{2,\infty}^{\text{qUCCGS}}\rangle$ . Otherwise, we show that if  $|\Phi\rangle \in \mathcal{S}_{2,(a,b,c)}^{\text{paired}}$  and at least two of  $a, b, c$  is non-zero, then  $|\Phi\rangle \in M^\perp$ . The theorem then follows immediately from Lemma 24. Similar to the proof of Theorem 39, we assume Supplementary Equation (178), and consider the paired state sequence Supplementary Equation (179). By Lemma 20 (Item 4),

$$|\Phi^{(0)}\rangle + |\Phi^{(1)}\rangle \in \left(M \cap \mathcal{H}_2^{\text{paired}}\right)^\perp \cap \mathcal{H}_2^{\text{paired}} \subseteq M^\perp. \quad (183)$$

By Lemma 37,

$$|\Phi^{(1)}\rangle + |\Phi^{(2)}\rangle, |\Phi^{(2)}\rangle + |\Phi^{(3)}\rangle \in M^\perp. \quad (184)$$

Combining Supplementary Equations (183) and (184) to eliminate  $|\Phi^{(1)}\rangle, |\Phi^{(2)}\rangle$  we get  $|\Phi\rangle \in M^\perp$ , since  $|\Phi^{(0)}\rangle = |\Phi^{(3)}\rangle = |\Phi\rangle$ .  $\square$

As an immediate corollary, the moment vectors of the 2<sup>nd</sup> moment at infinity step of  $k$ -UCCSD,  $k$ -UCCGSD,  $k$ -UpCCGSD,  $k$ -qubit-UCCSD, and  $k$ -qubit-UCCGSD are the same.

**Corollary 41.** *We have*

$$|\Psi_{2,\infty}^{\text{UCCSD}}\rangle = |\Psi_{2,\infty}^{\text{UCCGSD}}\rangle = |\Psi_{2,\infty}^{\text{UpCCGSD}}\rangle = |\Psi_{2,\infty}^{\text{qUCCSD}}\rangle = |\Psi_{2,\infty}^{\text{qUCCGSD}}\rangle = |\Psi_{2,\infty}^{\text{qUCCGS}}\rangle. \quad (185)$$

With the moment vector of the 2<sup>nd</sup> moment characterized, we can calculate the 2<sup>nd</sup> moment of the cost function for any observables. Cases 3 and 4 of the main result are stated formally as the following corollary.

**Corollary 42** (Main result, Cases 3 and 4). *Let  $\mathbf{R}$  be defined in Theorems 39 and 40, and  $C(\Theta; U_k^{\mathbf{R}}, H_{\text{el}})$  be the cost function defined in Supplementary Equation (33), where  $H_{\text{el}}$  is an electronic structure Hamiltonian defined in Supplementary Equation (35).  $\lim_{k \rightarrow \infty} \text{Var}(C)$  is the same as in Corollary 33 (Item 3).*

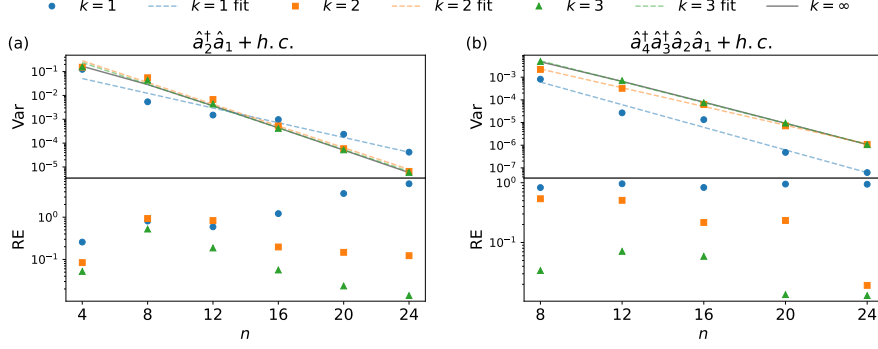
Notice that  $\lim_{k \rightarrow \infty} \text{Var}(C) = \exp(-\Theta(n))$ .

## Supplementary Note 13: More numerical results

To support this conjecture, we further investigate how the variance of the cost function for  $k$ -UCCSD changes with increasing  $n$  when  $k$  is small. In Supplementary Figure 6, we plot the scaling of the cost variance for  $k$ -UCCSD, with respect to  $n \in \{4, 8, \dots, 24\}$  when  $k \in \{1, 2, 3, \infty\}$ . Like in main text Figure 2, we only display the results for two fixed observables  $\hat{a}_2^\dagger \hat{a}_1 + h.c.$  and  $\hat{a}_4^\dagger \hat{a}_3^\dagger \hat{a}_2 \hat{a}_1 + h.c.$ , and the estimated data points with an exponential function  $a \exp(b \cdot n)$ . Unlike the main text Figure 2, the number of electrons is set to  $n_e = n/4$ . It can be seen that the observation of main text Figure 2 also holds for Supplementary Figure 6, indicating that our conclusions for  $k$ -UCCSD are not affected by the number of electrons  $n_e$ .

## Supplementary References

- [1] Preskill, J. Quantum computing in the NISQ era and beyond. *Quantum* **2**, 79 (2018).
- [2] Feynman, R. P., Leighton, R. B., Sands, M. *et al.* *The Feynman lectures on physics* Vol. 1 (Addison-Wesley Reading, MA, 1971).
- [3] Peruzzo, A. *et al.* A variational eigenvalue solver on a photonic quantum processor. *Nature communications* **5**, 4213 (2014).
- [4] Kandala, A. *et al.* Hardware-efficient variational quantum eigensolver for small molecules and quantum magnets. *nature* **549**, 242–246 (2017).
- [5] O’Malley, P. J. *et al.* Scalable quantum simulation of molecular energies. *Physical Review X* **6**, 031007 (2016).



**Supplementary Figure 6** Scaling of the cost variance and relative error to asymptotic variance for  $k$ -UCCSD when  $n_e = n/4$ . Here we present the cost variance (Var) and the relative error to asymptotic variance (RE) for the  $k$  alternations of unitary coupled cluster with singles and doubles ( $k$ -UCCSD) ansatz measured by (a)  $\hat{a}_2^\dagger \hat{a}_1 + h.c.$  and (b)  $\hat{a}_4^\dagger \hat{a}_3^\dagger \hat{a}_2 \hat{a}_1 + h.c.$ . The abbreviation “h.c.” stands for “Hermitian conjugate”. The number of qubit is  $n \in \{4, 8, \dots, 24\}$ , with the number of electrons given by  $n_e = n/4$ . For each observable, the illustrated variances for  $k = 1, 2, 3$  are estimated from 6000 random samples at each  $n$  value, and are represented by blue circles, orange squares, and green triangles, respectively. The variances for  $k = 1, 2, 3$  are fitted using the function  $a \exp(b \cdot n)$ , with the resulting fitting curves shown as blue, orange, and green dashed lines. The computed asymptotic variances ( $k \rightarrow \infty$ ) are depicted as gray solid curves. In the lower half of each panel, we display the relative error of the variances at  $k = 1, 2, 3$  compared to the asymptotic variances, also represented by blue circles, orange squares, and green triangles. The error bars, estimated as  $\sqrt{2/(6000 - 1)} \cdot \text{Var}$ , are not shown as they are smaller than the data points.

- [6] Nam, Y. *et al.* Ground-state energy estimation of the water molecule on a trapped-ion quantum computer. *npj Quantum Information* **6**, 33 (2020).
- [7] Colless, J. I. *et al.* Computation of molecular spectra on a quantum processor with an error-resilient algorithm. *Physical Review X* **8**, 011021 (2018).
- [8] Holmes, Z., Sharma, K., Cerezo, M. & Coles, P. J. Connecting ansatz expressibility to gradient magnitudes and barren plateaus. *PRX Quantum* **3**, 010313 (2022).
- [9] Cerezo, M. & Coles, P. J. Higher order derivatives of quantum neural networks with barren plateaus. *Quantum Science and Technology* **6**, 035006 (2021).
- [10] Arrasmith, A., Cerezo, M., Czarnik, P., Cincio, L. & Coles, P. J. Effect of barren plateaus on gradient-free optimization. *Quantum* **5**, 558 (2021).
- [11] Sack, S. H., Medina, R. A., Michailidis, A. A., Kueng, R. & Serbyn, M. Avoiding barren plateaus using classical shadows. *PRX Quantum* **3**, 020365 (2022).
- [12] Grant, E., Wossnig, L., Ostaszewski, M. & Benedetti, M. An initialization strategy for addressing barren plateaus in parametrized quantum circuits. *Quantum* **3**, 214 (2019).
- [13] Zhang, K., Liu, L., Hsieh, M.-H. & Tao, D. Escaping from the barren plateau via gaussian initializations in deep variational quantum circuits. *Advances in Neural Information Processing Systems* **35**, 18612–18627 (2022).
- [14] Friedrich, L. & Maziero, J. Avoiding barren plateaus with classical deep neural networks. *Physical Review A* **106**, 042433 (2022).
- [15] Binkowski, L., Koßmann, G., Osborne, T. J., Schwonnek, R. & Ziegler, T. From barren plateaus through fertile valleys: Conic extensions of parameterised quantum circuits. *arXiv preprint arXiv:2310.04255* (2023).
- [16] Volkoff, T. & Coles, P. J. Large gradients via correlation in random parameterized quantum circuits. *Quantum Science and Technology* **6**, 025008 (2021).
- [17] Verdon, G. *et al.* Learning to learn with quantum neural networks via classical neural networks. *arXiv preprint arXiv:1907.05415* (2019).

- [18] Skolik, A., McClean, J. R., Mohseni, M., Smagt, P. V. D. & Leib, M. Layerwise learning for quantum neural networks. *Quantum Machine Intelligence* **3**, 1–11 (2021).
- [19] Mastropietro, D., Korpas, G., Kungurtsev, V. & Marecek, J. Fleming-viot helps speed up variational quantum algorithms in the presence of barren plateaus. *arXiv preprint arXiv:2311.18090* (2023).
- [20] Fedorov, D. A., Peng, B., Govind, N. & Alexeev, Y. VQE method: a short survey and recent developments. *Materials Theory* **6**, 2 (2022).
- [21] Barkoutsos, P. K. *et al.* Quantum algorithms for electronic structure calculations: Particle-hole hamiltonian and optimized wave-function expansions. *Physical Review A* **98**, 022322 (2018).
- [22] Wecker, D., Hastings, M. B. & Troyer, M. Progress towards practical quantum variational algorithms. *Physical Review A* **92**, 042303 (2015).
- [23] Szabo, A. & Ostlund, N. S. *Modern quantum chemistry: introduction to advanced electronic structure theory* (Courier Corporation, 2012).
- [24] Taube, A. G. & Bartlett, R. J. New perspectives on unitary coupled-cluster theory. *International journal of quantum chemistry* **106**, 3393–3401 (2006).
- [25] Lee, J., Huggins, W. J., Head-Gordon, M. & Whaley, K. B. Generalized unitary coupled cluster wave functions for quantum computation. *Journal of chemical theory and computation* **15**, 311–324 (2018).
- [26] McClean, J. R., Boixo, S., Smelyanskiy, V. N., Babbush, R. & Neven, H. Barren plateaus in quantum neural network training landscapes. *Nature communications* **9**, 4812 (2018).
- [27] Larocca, M. *et al.* Diagnosing barren plateaus with tools from quantum optimal control. *Quantum* **6**, 824 (2022).
- [28] Cerezo, M. *et al.* Variational quantum algorithms. *Nature Reviews Physics* **3**, 625–644 (2021).
- [29] Evangelista, F. A., Chan, G. K.-L. & Scuseria, G. E. Exact parameterization of fermionic wave functions via unitary coupled cluster theory. *The Journal of Chemical Physics* **151**, 244112 (2019). URL <https://doi.org/10.1063/1.5133059>.
- [30] Quantum, G. A. *et al.* Hartree-fock on a superconducting qubit quantum computer. *Science* **369**, 1084–1089 (2020).
- [31] Arrasmith, A., Holmes, Z., Cerezo, M. & Coles, P. J. Equivalence of quantum barren plateaus to cost concentration and narrow gorges. *Quantum Science and Technology* **7**, 045015 (2022).
- [32] Tang, H. L. *et al.* qubit-adapt-vqe: An adaptive algorithm for constructing hardware-efficient ansätze on a quantum processor. *PRX Quantum* **2**, 020310 (2021).
- [33] Thouless, D. J. Stability conditions and nuclear rotations in the hartree-fock theory. *Nuclear Physics* **21**, 225–232 (1960).
- [34] McArdle, S., Endo, S., Aspuru-Guzik, A., Benjamin, S. C. & Yuan, X. Quantum computational chemistry. *Reviews of Modern Physics* **92**, 015003 (2020).
- [35] Ragone, M. *et al.* A lie algebraic theory of barren plateaus for deep parameterized quantum circuits. *Nature Communications* **15**, 7172 (2024). URL <https://doi.org/10.1038/s41467-024-49909-3>.
- [36] Fontana, E. *et al.* Characterizing barren plateaus in quantum ansätze with the adjoint representation. *Nature Communications* **15**, 7171 (2024). URL <https://doi.org/10.1038/s41467-024-49910-w>.

- [37] Diaz, N., García-Martín, D., Kazi, S., Larocca, M. & Cerezo, M. Showcasing a barren plateau theory beyond the dynamical lie algebra. *arXiv preprint arXiv:2310.11505* (2023).
- [38] Grimsley, H. R., Claudino, D., Economou, S. E., Barnes, E. & Mayhall, N. J. Is the trotterized uccsd ansatz chemically well-defined? *Journal of chemical theory and computation* **16**, 1–6 (2019).
- [39] Dallaire-Demers, P.-L., Romero, J., Veis, L., Sim, S. & Aspuru-Guzik, A. Low-depth circuit ansatz for preparing correlated fermionic states on a quantum computer. *Quantum Science and Technology* **4**, 045005 (2019).
- [40] Miao, Q. & Barthel, T. Equivalence of cost concentration and gradient vanishing for quantum circuits: an elementary proof in the riemannian formulation. *Quantum Science and Technology* **9**, 045039 (2024). URL <https://dx.doi.org/10.1088/2058-9565/ad6fca>.
- [41] Napp, J. Quantifying the barren plateau phenomenon for a model of unstructured variational ansatz. *arXiv preprint arXiv:2203.06174* (2022).
- [42] Jozsa, R. & Miyake, A. Matchgates and classical simulation of quantum circuits. *Proceedings of the Royal Society A: Mathematical, Physical and Engineering Sciences* **464**, 3089–3106 (2008).
- [43] Cerezo, M. *et al.* Does provable absence of barren plateaus imply classical simulability? or, why we need to rethink variational quantum computing. *arXiv preprint arXiv:2312.09121* (2023).
- [44] Collins, B. & Matsumoto, S. On some properties of orthogonal weingarten functions. *Journal of Mathematical Physics* **50**, 113516 (2009). URL <https://doi.org/10.1063/1.3251304>.
- [45] Monbroussou, L., Landman, J., Grilo, A. B., Kukla, R. & Kashefi, E. Trainability and expressivity of hamming-weight preserving quantum circuits for machine learning. *arXiv preprint arXiv:2309.15547* (2023).
- [46] Halperin, I. The product of projection operators. *Acta Sci. Math.(Szeged)* **23**, 96–99 (1962).
- [47] National Institute of Science and Technology. Computational chemistry comparison and benchmark database. URL <https://cccbdb.nist.gov/>.
- [48] Park, C.-Y. & Killoran, N. Hamiltonian variational ansatz without barren plateaus. *Quantum* **8**, 1239 (2024).
- [49] Grimsley, H. R., Barron, G. S., Barnes, E., Economou, S. E. & Mayhall, N. J. Adaptive, problem-tailored variational quantum eigensolver mitigates rough parameter landscapes and barren plateaus. *npj Quantum Information* **9**, 19 (2023).
- [50] Cerezo, M., Sone, A., Volkoff, T., Cincio, L. & Coles, P. J. Cost function dependent barren plateaus in shallow parametrized quantum circuits. *Nature communications* **12**, 1791 (2021).
- [51] Farhi, E., Goldstone, J. & Gutmann, S. A quantum approximate optimization algorithm. *arXiv preprint arXiv:1411.4028* (2014).
- [52] Pesah, A. *et al.* Absence of barren plateaus in quantum convolutional neural networks. *Physical Review X* **11**, 041011 (2021).
- [53] Zhao, C. & Gao, X.-S. Analyzing the barren plateau phenomenon in training quantum neural networks with the ZX-calculus. *Quantum* **5**, 466 (2021).
- [54] Liu, Z., Yu, L.-W., Duan, L.-M. & Deng, D.-L. Presence and absence of barren plateaus in tensor-network based machine learning. *Physical Review Letters* **129**, 270501 (2022).
- [55] Martín, E. C., Plekhanov, K. & Lubasch, M. Barren plateaus in quantum tensor network optimization. *Quantum* **7**, 974 (2023).

- [56] Jacot, A., Gabriel, F. & Hongler, C. Neural tangent kernel: Convergence and generalization in neural networks. *Advances in neural information processing systems* **31** (2018).
- [57] Mao, R. Data and code for "Towards determining the presence of barren plateaus in some chemically inspired variational quantum algorithms" (2024). URL <https://doi.org/10.5281/zenodo.13359192>.